

**TREATING PERIODONTAL DISEASE THROUGH THE RECRUITMENT AND  
EXPANSION OF ENDOGENOUS REGULATORY T CELLS**

by

**Andrew J. Glowacki**

Bachelor of Science in Chemical Engineering, Iowa State University of Science and  
Technology, 2008

Submitted to the Graduate Faculty of  
Swanson School of Engineering in partial fulfillment  
of the requirements for the degree of  
Ph.D. in Chemical Engineering

University of Pittsburgh

2015

UNIVERSITY OF PITTSBURGH  
SWANSON SCHOOL OF ENGINEERING

This dissertation was presented

by

Andrew J. Glowacki

It was defended on

October 29, 2015

and approved by

Charles Sfeir, Ph.D., D.D.S., Associate Professor, Department of Oral Biology, Periodontics  
and Bioengineering

Eric J. Beckman, Ph.D., George M. Bevier Distinguished Service Professor, Department of  
Chemical and Petroleum Engineering and Bioengineering

Sarah L. Gaffen, Ph.D., Professor, Division of Rheumatology and Clinical Immunology and  
Immunology

Ipsita Banerjee, Ph. D., Associate Professor, Department of Chemical and Petroleum  
Engineering and Bioengineering

Dissertation Director: Steven R. Little, Ph.D., William Kepler Whiteford Professor,  
Department of Chemical and Petroleum Engineering, Bioengineering, Pharmaceutical  
Sciences, Ophthalmology and Immunology

Copyright © by Andrew J. Glowacki

2015

# **TREATING PERIODONTAL DISEASE THROUGH THE RECRUITMENT AND EXPANSION OF ENDOGENOUS REGULATORY T CELLS**

Andrew J. Glowacki, PhD

University of Pittsburgh, 2015

Periodontal disease, also known as gum disease, affects an estimated 64 million Americans and is the leading cause of tooth loss. Current clinical therapies focus on the removal of invasive oral bacteria that initiate the disease through scaling and root planing and administration of antibiotics. However, it is now understood that tissue destruction in periodontal disease is carried out by an exacerbated inflammatory immune response. Furthermore, recent literature suggests that the severe forms of the disease may be characterized by a decrease in the presence of a subset of cells responsible for directing immune regulation, Regulatory T cells (Tregs). To address the underlying immune dysfunction, we have developed acellular approaches, utilizing translatable bioerodible microspheres composed of poly(lactide-co-glycolide) capable releasing factors that can recruit endogenous Tregs and induce local Tregs in the periodontium for the treatment of periodontal disease. Specifically, we have developed microspheres that release the Treg-associated C-C motif chemokine 22 (CCL22) and vasoactive intestinal peptide (VIP) for the local recruitment of endogenous Tregs *in vivo* and prevention of alveolar bone resorption. Furthermore, CCL22 microspheres led to a reduction in the expression of damaging inflammatory mediators and conversely, led to an upregulation of anti-inflammatory molecules that could potentially lead to tissue regeneration. Secondly, we demonstrate that CCL22 microspheres are capable of being

administered using standard clinical techniques to effectively treat ligature-induced periodontitis in beagle dogs. CCL22 microspheres reduce clinical scores of inflammation including periodontal probing depths and bleeding on probing as well as reduced tooth supporting alveolar bone resorption in dogs. Finally, we describe an alternative strategy to bolster Treg population in situ, through the local expansion of Tregs by PLGA microspheres releasing a combination of transforming growth factor beta (TGF- $\beta$ ), rapamycin (Rapa) and interleukin 2 (IL-2). Administration of TGF- $\beta$ , Rapa, IL-2 microspheres in a mouse model for periodontal disease significantly reduced the primary outcome of periodontal disease, alveolar bone resorption. Taken together, controlled release formulations that harness the body's sophisticated immunoregulatory cells provide an easy-to-use, off-the-shelf therapeutic modality for treating inflammatory periodontal disease and may become the next clinical standard treatment.

## TABLE OF CONTENTS

|  |            |
|--|------------|
| <b>ACKNOWLEDGMENTS .....</b>   | <b>XIX</b> |
| <b>1.0 INTRODUCTION.....</b>   | <b>1</b>   |
| <b>1.1 STRATEGIES TO DIRECT THE ENRICHMENT, EXPANSION, AND RECRUITMENT OF ENDOGENOUS REGULATORY CELLS FOR THE TREATMENT OF DISEASE .....</b> | <b>1</b>   |
| <b>1.1.1 Loss of tissue homeostasis and regulation leads to disease.....</b>   | <b>1</b>   |
| <b>1.1.2 Homeostasis and disease .....</b>   | <b>2</b>   |
| <b>1.1.3 Other immune regulators, mesenchymal stem cells as mediators of homeostasis .....</b>   | <b>4</b>   |
| <b>1.1.4 Regulatory T cells as mediators of homeostasis .....</b>  | <b>6</b>   |
| <b>1.1.5 Limitations of cell therapies .....</b>   | <b>7</b>   |
| <b>1.1.6 Harnessing the potential of the body’s own endogenous regulators .....</b>  | <b>8</b>   |
| <b>1.1.7 Regulatory T cells as regulators of regeneration .....</b>  | <b>9</b>   |
| <b>1.1.8 Engineering techniques for harnessing endogenous mesenchymal stem cells .....</b>   | <b>11</b>  |
| <b>1.1.9 Future vision for engineering treatments for harnessing endogenous regulators for disease .....</b>                                 | <b>15</b>  |
| <b>1.2 STRATEGIES TO RECRUIT AND EXPAND ENDOGENOUS REGULATORY CELLS FOR THE TREATMENT OF PERIODONTAL DISEASE .....</b>                       | <b>15</b>  |
| <b>1.3 PERIODONTAL DISEASE .....</b>   | <b>18</b>  |
| <b>1.3.1 Prevalence and implications of periodontal disease.....</b>   | <b>18</b>  |
| <b>1.3.2 Current clinical treatments for periodontal disease .....</b>   | <b>19</b>  |
| <b>1.3.3 Current clinically available host modulators .....</b>  | <b>21</b>  |

|        |   |           |
|--------|---|-----------|
| 1.3.4  | Immune reaction, chemokines, and the attraction of lymphocytes to the periodontium .....  | 21        |
| 1.3.5  | Complications associated with the inhibition or blocking of inflammation .<br>.....   | 22        |
| 1.3.6  | How the body naturally regulates inflammation .....   | 23        |
| 1.3.7  | A biomimetic, engineered approach to promote immune regulation in periodontal disease.....  | 24        |
| 1.3.8  | Hypothesis: increasing the presence of regulatory T cells in the periodontal tissues using Treg-recruiting or Treg-expanding microspheres may attenuate periodontal disease symptoms and promote tissue regeneration<br>..... | 27        |
| 2.0    | <b>CONTROLLED RELEASE OF CCL22 FOR THE RECRUITMENT OF TREGS AND TREATMENT OF PERIODONTAL DISEASE IN A MICE MODEL.....</b>   | <b>28</b> |
| 2.1    | <b>INTRODUCTION .....</b>   | <b>28</b> |
| 2.2    | <b>METHODS.....</b>   | <b>30</b> |
| 2.2.1  | Microsphere preparation .....   | 30        |
| 2.2.2  | Microsphere characterization .....  | 32        |
| 2.2.3  | CCL22 microsphere administration in mice .....  | 33        |
| 2.2.4  | Periodontal disease induction in mice .....   | 35        |
| 2.2.5  | Bacteria cultures.....  | 36        |
| 2.2.6  | Mouse anti-GITR treatment for Treg inhibition .....   | 37        |
| 2.2.7  | Assessment of periodontal disease induced bone loss in mice.....  | 38        |
| 2.2.8  | Assessment of inflammatory cell infiltrate in mice .....  | 38        |
| 2.2.9  | mRNA extraction from mouse maxilla .....  | 39        |
| 2.2.10 | DNA extraction from mouse maxilla.....  | 39        |
| 2.2.11 | Extraction of gingiva proteins from mice .....  | 39        |

|        |  |           |
|--------|--|-----------|
| 2.2.12 | <b>Histological sectioning and immunohistochemical staining of mouse maxilla</b>   | <b>40</b> |
| 2.2.13 | <b>Statistical analyses</b>  | <b>40</b> |
| 2.3    | <b>RESULTS</b>   | <b>41</b> |
| 2.3.1  | <b>Characterization of rmCCL22 PLGA microspheres</b>   | <b>41</b> |
| 2.3.2  | <b>CCL22 microspheres significantly reduce alveolar bone resorption in mice models for periodontitis</b>   | <b>49</b> |
| 2.3.3  | <b>CCL22 microspheres reduce the inflammatory infiltrate in mice, without altering bacterial levels</b>  | <b>52</b> |
| 2.3.4  | <b>CCL22 microspheres recruit regulatory T cells to the periodontium of mice, gingival mRNA expression and protein quantification</b>                              | <b>54</b> |
| 2.3.5  | <b>Histological assessment of Tregs presence and reduced osteoclast in the periodontium of mice treated with CCL22 microspheres</b>                                | <b>56</b> |
| 2.3.6  | <b>Anti-GITR inhibition of Tregs reverses the therapeutic effect of CCL22 microsphere treatments</b>   | <b>59</b> |
| 2.3.7  | <b>Exploratory PCR array to identify the molecular mechanisms of Treg recruiting CCL22 microsphere treatments</b>  | <b>62</b> |
| 2.3.8  | <b>Quantitative mRNA analysis of key markers to elucidate the molecular mechanisms of Treg recruitment by CCL22 microspheres in a mouse model of periodontitis</b> | <b>65</b> |
| 2.4    | <b>DISCUSSION</b>  | <b>67</b> |
| 3.0    | <b>CONTROLLED RELEASE OF CCL22 FROM PLGA MICROSPHERES FOR THE TREATMENT OF PERIODONTAL DISEASE IN A DOG MODEL</b>  | <b>70</b> |
| 3.1    | <b>INTRODUCTION</b>  | <b>70</b> |
| 3.1.1  | <b>Advantages and disadvantages of rodent models for periodontal disease</b>   | <b>70</b> |
| 3.1.2  | <b>Advantages and disadvantages of non-human primates for experimental periodontal disease models</b>  | <b>73</b> |
| 3.1.3  | <b>Advantages and disadvantages of dog models for periodontitis</b>  | <b>74</b> |

|       |   |           |
|-------|---|-----------|
| 3.1.4 | CCL22 microspheres for the treatment of periodontitis in the ligature induced dog model of periodontitis .....  | 74        |
| 3.2   | METHODS.....  | 75        |
| 3.2.1 | Microsphere preparation .....   | 75        |
| 3.2.2 | Microsphere characterization .....  | 76        |
| 3.2.3 | Recombinant human CCL22 microsphere administration in dogs.....   | 76        |
| 3.2.4 | Periodontal disease induction in beagle dogs .....  | 77        |
| 3.2.5 | Assessment of periodontal disease in dogs, alveolar bone loss and clinical scores .....   | 78        |
| 3.2.6 | Statistical analyses.....   | 79        |
| 3.3   | RESULTS.....  | 79        |
| 3.3.1 | Characterization of rhCCL22 PLGA microspheres.....  | 79        |
| 3.3.2 | rhCCL22 microspheres reduce the clinical scores of periodontal disease and inflammation in ligature induced dog periodontitis .....                           | 81        |
| 3.3.3 | rhCCL22 microspheres prevent alveolar bone loss in dogs.....  | 84        |
| 3.4   | DISCUSSION.....   | 89        |
| 4.0   | <b>CONTROLLED RELEASE OF VASOACTIVE INTESTINAL PEPTIDE (VIP) FOR THE RECRUITMENT OF TREGS AND TREATMENT OF EXPERIMENTAL PERIODONTAL DISEASE IN MICE .....</b> | <b>92</b> |
| 4.1   | INTRODUCTION .....  | 92        |
| 4.1.1 | Introduction to vasoactive intestinal peptide and periodontal disease .....   | 92        |
| 4.2   | METHODS.....  | 94        |
| 4.2.1 | Vasoactive intestinal peptide (VIP) microsphere preparation .....   | 94        |
| 4.2.2 | VIP microsphere characterization.....   | 95        |
| 4.2.3 | VIP microsphere <i>in vitro</i> release assays .....  | 95        |
| 4.2.4 | Primary mouse dendritic cell isolation.....   | 96        |

|        |  |     |
|--------|--|-----|
| 4.2.5  | Primary mouse dendritic cell cultures with VIP.....  | 97  |
| 4.2.6  | Measuring CCL22 production by VIP treated DCs .....  | 98  |
| 4.2.7  | Primary mouse CD4+ T cell isolation and chemotaxis.....  | 99  |
| 4.2.8  | Murine periodontal disease induction.....  | 100 |
| 4.2.9  | Bacteria cell culture .....  | 100 |
| 4.2.10 | Assessment of periodontal disease-induced bone loss in mice .....  | 101 |
| 4.3    | RESULTS.....   | 101 |
| 4.3.1  | VIP microsphere characterization.....  | 101 |
| 4.3.2  | VIP in vitro release from PLGA microspheres .....  | 103 |
| 4.3.3  | VIP microspheres induce CCL22 production by dendritic cells .....  | 105 |
| 4.3.4  | VIP microsphere-treated dendritic cells recruit CD4 <sup>+</sup> FoxP3 <sup>+</sup> regulatory T cells <i>in vitro</i> ..... | 107 |
| 4.3.5  | Vasoactive intestinal peptide PLGA microspheres reduce alveolar bone loss in murine periodontitis .....                      | 109 |
| 4.4    | DISCUSSION.....  | 110 |
| 5.0    | ENGINEERING LOCAL TREG-INDUCING MICROSPHERES FOR THE TREATMENT OF PERIODONTAL DISEASE IN A MOUSE MODEL.....                  | 114 |
| 5.1    | INTRODUCTION .....   | 114 |
| 5.2    | METHODS.....   | 116 |
| 5.2.1  | Treg inducing microsphere fabrication .....  | 116 |
| 5.2.2  | Characterization of Treg inducing microsphere formulations.....  | 119 |
| 5.2.3  | Treg inducing microsphere administration in mice.....  | 120 |
| 5.2.4  | Periodontal disease induction in mice .....  | 120 |
| 5.2.5  | Bacteria cultures.....   | 121 |

|         |  |     |
|---------|--|-----|
| 5.2.6   | Assessment of periodontal disease induced bone loss in mice.....                                 | 122 |
| 5.2.7   | Statistical analyses.....  | 123 |
| 5.3     | RESULTS.....   | 123 |
| 5.3.1   | Characterization of Treg inducing PLGA microspheres .....  | 123 |
| 5.3.2   | Controlled release of TGF- $\beta$ , IL-2, and Rapamycin from PLGA microspheres.....             | 125 |
| 5.3.3   | Treg inducing microspheres prevent alveolar bone loss in experimental murine periodontitis ..... | 127 |
| 5.4     | DISCUSSION.....  | 129 |
| 6.0     | FUTURE WORK.....   | 132 |
| 6.1     | DEVELOPING CCL22 RELEASING MICROSPHERES FOR CLINICAL USE .....                                   | 132 |
| 6.1.1   | Navigating FDA regulation for the development of CCL22 microspheres .. ..                        | 132 |
| 6.1.1.1 | IND Chemistry, Manufacturing and Control for CCL22 releasing microspheres .....                  | 133 |
| 6.1.1.2 | IND Toxicology and Pharmacology of CCL22 releasing microspheres .....                            | 133 |
| 6.1.1.3 | IND Clinical Protocol design for CCL22 releasing microspheres                                    | 134 |
| 6.2     | FUTURE INVESTIGATIONS USING TREG-INDUCING MICROPARTICLE FORMULATIONS.....                        | 134 |
| 6.2.1   | Future work for Vasoactive Intestinal Peptide (VIP) releasing microspheres .....                 | 135 |
| 6.2.2   | Future work for TFG- $\beta$ and rapamycin microsphere formulations .....                        | 136 |
|         | BIBLIOGRAPHY.....  | 138 |

## LIST OF FIGURES

|  |    |
|--|----|
| Figure 1: Synthetic strategies to recruit and enhance Tregs for the amelioration of disease, restoration of homeostasis, and promotion of tissue regeneration <sup>59</sup> .....  | 11 |
| Figure 2: How MSCs migrate to sites of disease or injury and potential modes of regulating immune cells <sup>59</sup> .....  | 12 |
| Figure 3: Synthetic engineering strategies to expand and chemoattract endogenous MSCs and Tregs <sup>59</sup> .....  | 14 |
| Figure 4: Periodontal disease structure and progression. Healthy periodontal tissue is characterized by pink gingivae, absence of plaque and high alveolar bone levels. Gingivitis is characterized by inflammation of the gums (gingiva) and the presence of bacterial biofilms or plaques, however tissue destruction has not occurred or is mild. Disease is categorized as periodontitis once significant tissue damage has occurred, typically displaying periodontal pocket depths of 3 mm or more. Deep pockets, typically greater than 6 mm are categorized as severe or advanced periodontitis. Cementoenamel junction (CEJ) is static architecture of the tooth root often used as a referenced for tissue destruction when performing clinical attachment loss measurements. The alveolar bone crest (ABC) signifies the peak height of the tooth supporting bone, typically clinically measured using dental X-rays..... | 17 |
| Figure 5: Clinical therapies for periodontitis, scaling and root planing and local antibiotics. ....   | 20 |
| Figure 6: Clinical treatment, periodontal open flap surgery.....   | 20 |
| Figure 7: Fabrication of PLGA microspheres encapsulating aqueous protein.....  | 31 |
| Figure 8: <i>In vitro</i> releasate sampling from PLGA microspheres.....   | 32 |
| Figure 9: CCL22 microsphere administration route in mice.....  | 34 |
| Figure 10: CCL22 microsphere treatment experimental schedule in <i>Actinobacillus actinomycetemcomitans</i> infected Black/6 mice.....   | 34 |
| Figure 11: CCL22 microsphere treatment timeline in <i>Porphyromonas gingivalis</i> infected BALB/cJ mice.....  | 35 |
| Figure 12: Surface morphology of non-porous rmCCL22 microspheres (scanning electron micrographs).....  | 42 |
| Figure 13: Volume average size distributions for rmCCL22 microspheres.....   | 43 |

|  |    |
|--|----|
| Figure 14: <i>In vitro</i> cumulative release of recombinant mouse CCL22 from non-porous PLGA microspheres. ....   | 44 |
| Figure 15: Combination of non-porous rmCCL22 PLGA microsphere formulations for long-lasting constant release. ....   | 46 |
| Figure 16: Comparison of porous, rmCCL22 PLGA microspheres and non-porous rm CCL22 PLGA microspheres.....  | 47 |
| Figure 17: Characterization of porous rmCCL22 microspheres, microsphere size distribution and cumulative <i>in vitro</i> release <sup>46</sup> . ....  | 48 |
| Figure 18: CCL22 microspheres prevent alveolar bone loss in <i>Actinobacillus actinomycetemcomitans</i> infected C57 black/6 mice <sup>45</sup> . (A) Representative stereoscope images of defleshed maxilla from C57BL/6J mice infected with <i>Actinobacillus actinomycetemcomitans</i> ( <i>Aa</i> ) 30 days after inoculation. Results of treatment with blank (unloaded) PLGA microspheres (top), and CCL22 microspheres (bottom), injected into maxillary gingiva on days -1, 10 and 20 relative to the first <i>Aa</i> inoculation, scale bar 0.5 mm. (B) Area measurement between the cemento-enamel junction (CEJ) and alveolar bone crest (ABC) on the buccal root surface, untreated mice were infected but did not receive microspheres, no <i>Aa</i> served as uninfected controls. N = 5-8 mice. **P < 0.05 determined by One-Way ANOVA followed by Bonferroni's multiple comparisons test, untreated, CCL22 and Blank groups were statistically different from no <i>Aa</i> infection. .... | 50 |
| Figure 19: CCL22 microspheres prevent alveolar bone resorption in <i>Porphyromonas gingivalis</i> experimental BALB/cJ mouse model. BALB/cJ mice colonized with <i>Porphyromonas gingivalis</i> treated with CCL22 microspheres injected in the maxillary gingiva at days -1, 20, 40 showed significant reduction in alveolar bone loss and increased presence of regulatory T cells in the periodontium 60 days after initial colonization. Uninfected mice (no <i>Pg</i> ) and infected Untreated mice served as controls for CCL22 microsphere treated mice, (CCL22). (A) Representative microscope images of defleshed maxilla, scale bar for CCL22 0.5mm, scale bar for Untreated and no <i>Pg</i> 1mm. (B) Quantification of alveolar bone resorption represented by the area between the cemento-enamel junction (CEJ) and alveolar bone crest (ABC) in square microns. ** P<0.05 determined by ANOVA followed by Tukey HSD post hoc multiple comparison test <sup>45</sup> .....                   | 51 |
| Figure 20: CCL22 microsphere treatment led to a reduction in total inflammatory cells in the mouse gingiva, without affecting the levels of <i>Actinobacillus actinomycetemcomitans</i> bacteria found within the periodontium. (A) Inflammatory cell counts in the periodontal tissue following treatments (B) the PCR expression of <i>Aa</i> -specific bacterial 16s ribosomal DNA in the periodontal tissue normalized by palatal tissue weight following treatment, taken from C57BL/6J mice infected with <i>Actinobacillus actinomycetemcomitans</i> ( <i>Aa</i> ) 30 days after inoculation. N = 5-8 mice. (C) Overall bacterial counts were quantified by measuring the 16s ribosomal DNA in the periodontal tissue of mice 30 days after initial inoculation, normalized by palatal tissue weight. No statistical differences were detected among the groups. (D) Serum collected post-mortem 30 days after <i>Aa</i> colonization was   |    |

analyzed for inflammatory marker C-reactive protein. Untreated, CCL22 and Blank treated mice had statistically higher levels of serum CRP than no *Aa* uninfected controls. No differences were detectable among the infected animals. \*\*P < 0.05 determined by One-Way ANOVA followed by Bonferroni's multiple comparisons test, untreated, CCL22 and Blank groups were statistically different from no *Aa* infection<sup>45</sup>. ..... 53

Figure 21: CCL22 microspheres recruited regulatory T cells (Tregs) to the periodontium of mice. Periodontal tissues were resected from C57BL/6J mice infected with *Actinobacillus actinomycetemcomitans* (*Aa*) 30 days after inoculation, microspheres were injected into maxillary gingiva on days -1, 10 and 20 relative to the first *Aa* inoculation. CCL22 microsphere treated mice, blank (unloaded) microsphere and untreated mice served as infected experimental and control groups, uninfected no *Aa* mice served as positive controls. (A) mRNA expression of *Foxp3*, *Il10*, *Tgfβ*, *Il4*, *Ccl22* and *Ctla4* in periodontal tissue as measured by quantitative PCR. The mRNA expression levels were compared by the value of  $2^{(-\Delta Ct)} - 1$ , as compared to  $\beta$ -actin reference. (B) IL-10, TGF- $\beta$ , and CTLA-4 protein levels in periodontal tissues as determined by ELISA from digested periodontal tissues of mice. N = 5 mice. \*\*P < 0.05 determined by One-Way ANOVA followed by Bonferroni's multiple comparisons test, untreated, CCL22 and Blank groups were statistically different from no *Aa*<sup>45</sup>. ..... 55

Figure 22: Histological evidence of Treg recruitment to CCL22 microspheres in mice. BALB/cJ mice colonized with *Porphyromonas gingivalis* treated with CCL22 microspheres injected in the maxillary gingiva at days -1, 20, 40 showed significant reduction in alveolar bone loss and increased presence of regulatory T cells in the periodontium 60 days after initial colonization. Uninfected mice (no *Pg*) and infected Untreated mice served as controls for CCL22 microsphere treated mice, (CCL22). (A-B) Representative immunohistochemistry images of CCL22 microsphere treated mouse maxilla. Sections were stained with H&E (A-B), and immunohistochemistry was performed with anti-mouse FOXP3 antibody (C). FOXP3 positive cells were observed in periodontal tissue (arrows), FOXP3+ cells were only detectable in sections from CCL22 treated mice. Scale bar = A: 1,000 $\mu$ m, B, C: 100 $\mu$ m. *T*: tooth, *G*: gingiva, and *B*: alveolar bone<sup>45</sup>. ..... 57

Figure 23: Histological TRAP staining, CCL22 microsphere treated mice show reduced expression of osteoclast (TRAP) activity. BALB/cJ mice colonized with *Porphyromonas gingivalis* treated with CCL22 microspheres injected in the maxillary gingiva at days -1, 20, 40 showed significant reduction TRAP staining. Representative images from age match controlled mice, CCL22 microsphere treated mice and untreated, infected mice, Scale bar (red), 50  $\mu$ m. .... 59

Figure 24: Anti-GITR inhibition of Tregs reverses the therapeutic effect of CCL22 microspheres in mice. Systemic blockage of Tregs was performed by i.p. injection of anti-GITR antibodies in C57BL/6J mice infected with *Actinobacillus actinomycetemcomitans* (*Aa*), disease indicators were measured after 30 days. CCL22 microsphere injected mice, CCL22 microsphere + anti-GITR, and untreated mice served as infected experimental and control groups, uninfected no *Aa* mice served as positive controls, microspheres were delivered on days -1, 10 and 20 relative to the first *Aa* inoculation. (A) Alveolar bone loss as determined

by the measuring the area between cementoenamel junction (CEJ) to the alveolar bone crest (ABC) of resected, de-fleshed maxilla. (B) The number of inflammatory cells in the periodontal tissues was determined after digesting the periodontal tissues. (C) IL-10 and TGF- $\beta$  protein levels in digested palatal tissues determined by ELISA. N = 5 mice. \*\*P < 0.05 determined by One-Way ANOVA followed by Bonferroni's multiple comparisons test, untreated, CCL22 and CCL22 + ant-GITR were statistically different from no *Aa*<sup>45</sup>.  
 ..... 61

Figure 25: Exploratory PCR array identifying the molecular mechanisms of Treg recruitment by CCL22 microsphere treatment in mice. The Treg-recruiting formulation enhanced the expression of osteogenic, regenerative and anti-inflammatory markers in the periodontium. The expression mRNA in the periodontal tissue of mice 30 days after *Actinobacillus actinomycetemcomitans* (*Aa*) inoculation was analyzed using a custom-designed, exploratory PCR array. Samples were collected from periodontal tissue of C57BL/6J mice that were: infected with *Aa* without treatment (Untreated control, solid bars) and also infected with *Aa* and injected with CCL22 releasing microspheres (CCL22, unfilled bars), microspheres were delivered on days -1, 10 and 20 relative to the first *Aa* inoculation. The threshold for upregulation (more than 5 fold increase) and down regulation (less than 0.5 fold decrease) in CCL22 treated group compared to the control untreated group was indicated with lines<sup>45</sup> ..... 64

Figure 26: Quantitative PCR analysis of periodontal disease mediators in response to Treg recruiting CCL22 microspheres in mice. The Treg recruiting formulation decreased inflammatory cytokine expression and increased the expression of pro-regenerative factors. Periodontal tissues were resected from C57BL/6J mice infected with *Actinobacillus actinomycetemcomitans* (*Aa*) 30 days after inoculation. CCL22 microsphere injected mice, blank (unloaded) microsphere and untreated mice served as infected experimental and control groups, uninfected no *Aa* mice served as positive controls, microspheres were delivered on days -1, 10 and 20 relative to the first *Aa* inoculation. (A) mRNA expression of *Tnfa*, *Il1 $\beta$* , *Ifn $\gamma$* , *Il17*, *Rankl*, *Bmp7*, *Dmp1*, *Runx2*, *Colla1*, and *Opg* in periodontal tissue was analyzed by quantitative PCR. mRNA expression levels were compared by the value of  $2^{-(\Delta Ct)}$ -1 with reference to  $\beta$ -actin. (B) TNF and RANKL protein levels were measured in digested palatal tissues by ELISA. N = 5 mice. \*\*P < 0.05 determined by One-Way ANOVA followed by Bonferroni's multiple comparisons test, untreated, CCL22 and Blank groups were statistically different from no *Aa* except for the mRNA expression of BMP7, DMP1 and RUNX2<sup>45</sup> ..... 66

Figure 27: rhCCL22 treatment schedule and ligature induced periodontal disease induction in dogs.  
 ..... 77

Figure 28: Characterization of rhCCL22 PLGA microspheres for treatment of periodontal disease in the ligature induced dog model. (A) Scanning electron microscope image of poly(lactic-co-glycolic) acid microspheres encapsulating rhCCL22. (B) Cumulative fraction released from rhCCL22 microspheres determined by *in vitro* in phosphate buffered saline and measured by ELISA. (C) Volume impedance microsphere size distribution, average

particle diameter 16.6  $\mu\text{m}$  represented by red-dashed line, standard deviation  $\pm 5.8 \mu\text{m}$ <sup>45</sup>.  
..... 80

Figure 29: rhCCL22 microspheres reduced observational swelling and plaque build up in ligature induced dog periodontitis. Dogs received scaling and root planing followed by ligature placement (untreated), or followed by ligature placement and CCL22 microsphere treatment or blank (unloaded) microsphere controls, microspheres were deposited into the subgingival pocket at 0 and 4 weeks after ligature placement. Representative digital pictures as taken on the date of ligature placement (0 week) and after the 8 weeks of treatment (8 weeks, terminal endpoint) of the premolars and carnassial teeth of beagle dogs<sup>45</sup>. ..... 82

Figure 30: rhCCL22 microsphere administration prevents exacerbation of clinical probing depths and bleeding upon probing scores in dogs. Beagle dogs receiving periodontal disease inducing ligatures at week 0 were monitored for pocket depth and bleeding on probing at 6 sites per tooth (3 buccal, 3 lingual) of their second, third, fourth premolars as well as their carnassial tooth. (A) Periodontal pocket depth increase as measured at 4 weeks – 0 week and 8 week – 0 week after treatment for molar sites. (B) The percentage of bleeding sites on probing of all the probed sites at 0, 4, and 8 weeks. Dogs treated with CCL22 microspheres deposited into the periodontal pocket at times 0 and 4 weeks (CCL22) were compared to untreated (Untreated) and empty microspheres (Blank) controls. \*P<0.05, student t-test<sup>45</sup>. ..... 83

Figure 31: 3D-reconstructed microCT images of the buccal face of dog mandibles. (A) Representative 3D microCT images from mandibles of each animal on the buccal face of the left mandible post mortem, 8 weeks of ligature placement, and (B) right mandible, n = 3 animals per group. One dog was missing premolar 4 on birth (top row, third panel, (B)), therefore no ligatures were placed on this tooth and it was excluded from the study. Dogs treated with CCL22 microspheres deposited into the periodontal pocket at times 0 and 4 weeks (CCL22) were compared to untreated (Untreated) and empty microspheres (Blank) controls<sup>45</sup>. ..... 85

Figure 32: Quantification of alveolar bone loss in ligature induce dogs. MicroCT quantification of alveolar bone loss prevention in dogs treated with CCL22 microspheres. (A) Representative 3D X-ray microtomography image of beagle dog fourth premolar (P4) and first molar (M1). To quantify alveolar bone loss, 5 linear measurements of the distance between the cemento-enamel junction (CEJ) and alveolar bone crest (ABC) were taken at 0.3 mm spacing on the distal face of the P4 and M1 (quantified and shown in Fig. 6). Additionally, the CEJ to ABC distance was measured at sites spaced 0.6 mm apart along the buccal face of the P4 (14 sites) and M1 (26 sites). (B) A representative image showing the measurements of the CEJ to the ABC were performed after re-orientation of the microCT slices to align the apical roots and CEJ. (C) Linear bone loss between the CEJ and ABC along the buccal face of the left and right premolars (P4) and molars (M1) displaying the trends in alveolar bone resorption. Dogs treated with CCL22 microspheres deposited into the periodontal pocket at times 0 and 4 weeks (CCL22) were compared to untreated (Untreated) and empty microspheres (Blank) controls<sup>45</sup>. ..... 86

Figure 33: Administration of CCL22 microspheres significantly prevented alveolar bone resorption dog periodontitis. Dogs received scaling and root planing followed by ligature placement (untreated), or followed by ligature placement and CCL22 microsphere treatment or blank (unloaded) microsphere controls, microspheres were deposited into the subgingival pocket at 0 and 4 weeks after ligature placement. (A) Representative 3D images of left mandibular buccal surface of treated and control fourth premolar and carnassial teeth taken post-mortem with microCT scans. Red lines illustrate representative CEJ-ABC distances, which were measured using 2D slices of the tooth as described in Fig. S8. (B) Quantification of overall alveolar bone loss per dog determined as a summation of linear distances between the alveolar bone crest (ABC) and cemento-enamel junction (CEJ) on the buccal and distal sites of the fourth premolar (P4) and carnassial (first molar, M1). (C) Quantification of the average linear bone loss on the P4 and M1 distal and molar sites, calculated on a per tooth basis. N = 3 dogs per group. \*\*P < 0.05, determined by ANOVA followed by Tukey-HSD multiple comparisons post test<sup>45</sup>. ..... 88

Figure 34: Vasoactive intestinal peptide (VIP) may induce Tregs through multiple pathways. First, direct activation of CD4+CD25- naïve T cells to inducible Tregs, and second, activation of tolerogenic dendritic cells which then promote inducible Treg generation through activation of CD8+CD25- naïve T cells<sup>143</sup>. ..... 93

Figure 35: Vasoactive intestinal peptide loaded PLGA microspheres. VIP microspheres composed of 12.6 kDa PLGA (50:50) showed non-porous and porosity on scanning electron micrographs. Furthermore, size distributions of the microspheres revealed that the non-porous microspheres had a mean diameter of 16.9 microns, and the porous microspheres had a mean diameter of 18.9 microns. .... 103

Figure 36: Controlled release of vasoactive intestinal peptide (VIP) from PLGA microspheres. Porous microspheres were fabricated with 7.5 mmol NaCl in the first emulsion, inner aqueous phase, non-porous microspheres received no porogen. Cumulative release of VIP shown in phosphate buffered saline (PBS). ..... 104

Figure 37: CCL22 production by dendritic cells treated with VIP microspheres experimental schedule..... 105

Figure 38: CCL22 production from VIP microsphere treated murine dendritic cells. Primary mouse dendritic cells were cultured and matured with LPS, then treated with soluble VIP, or VIP microspheres, blank PLGA microspheres served as controls. Media was sampled for CCL22 production (measured by ELISA) 7 hours after LPS and VIP treatment. .... 106

Figure 39: Mature dendritic cells (DCs) treated with vasoactive intestinal peptide (VIP) released from PLGA microspheres recruit more Tregs than mature DCs or blank PLGA microsphere treated DCs. Transwell migration assay using 3 µm transwell filters, primary dendritic cells matured with LPS (or immature, no LPS normalized control) were treated with soluble VIP 2.5 x 10<sup>-8</sup> M concentration, VIP non-porous PLGA microspheres (estimated quantity comparable to 2.5 x 10<sup>-8</sup> M VIP) or blank PLGA microspheres were placed in the

bottom wells. Primary mouse CD4+ T cells were placed in the top transwell chambers, and left for 2 hours to migrate to the VIP treated dendritic cells. Cells from the bottom well were collected and analyzed using flow cytometry to quantify the number of CD4+FoxP3+ Regulatory T cells that migrated through the transwell filters..... 108

Figure 40: Vasoactive intestinal peptide microspheres reduce alveolar bone loss in an experimental mouse model of periodontal disease. (A) Representative stereoscope images of defleshed maxilla from C57BL/6J mice infected with *Actinobacillus actinomycetemcomitans* (*Aa*) 30 days after inoculation. Results of treatment with blank unloaded PLGA controls, CCL22 microsphere, and VIP microspheres injected into the maxillary gingiva at days -1, 10 and 20 relative to first *Aa* inoculation. (B) Quantification of the area between the cemento-enamel junction (CEJ) and alveolar bone crest (ABC) on the buccal tooth surface. Sham infected mice received heat killed *Actinobacillus actinomycetemcomitans* and served as positive controls. \*P < 0.05 determined by student T test..... 110

Figure 41: Single emulsion PLGA microsphere fabrication for rapamycin microspheres..... 119

Figure 42: Surface morphology of Treg inducing microspheres. Three batches of microspheres encapsulating TGF- $\beta$ , IL-2, and Rapamycin were fabricated for in situ Treg induction. Images are representative scanning electron micrographs of each microsphere formulation. Top magnification 300x, scale bar 10  $\mu$ m, bottom magnification 2000x, scale bar 10  $\mu$ m. .... 124

Figure 43: Release of TGF- $\beta$ , IL-2, and rapamycin from PLGA microspheres for the local induction of Tregs. TGF- $\beta$ , and IL-2 PLGA microspheres fabricated using a double emulsion technique. Rapamycin microspheres fabricated using a single emulsion fabrication protocol. Cumulative release of TGF- $\beta$ , IL-2 and rapamycin shown as measured in phosphate buffered saline (PBS)..... 126

Figure 44: TGF- $\beta$ , IL-2, and rapamycin Treg inducing microspheres prevent alveolar bone loss in an experimental model for periodontal disease. BALB/cJ mice colonized with *Porphyromonas gingivalis* treated with Treg inducing microspheres injected in the maxillary gingiva at days -1, 20, 40 showed significant reduction in alveolar bone loss 60 days after initial colonization. Uninfected mice age matched control mice, infected Untreated, and blank microsphere treated mice served as controls. Alveolar bone loss was quantified by the summation of 38 linear cemento-enamel junction (CEJ) to alveolar bone crest (ABC) measurements using microCT scans of resected maxilla. \*\*P<0.05 determined by ANOVA followed by Tukey HSD post hoc multiple comparison test..... 128

## ACKNOWLEDGMENTS

First and foremost, I thank Dr. Steve Little for recruiting me to the University of Pittsburgh and providing a supportive, educational and inspirational laboratory environment for me to pursue my Ph.D in. Steve has been an outstanding mentor and has sincerely helped me to develop my technical, analytical and communicative skills under his hands on guidance. I would also like to thank Dr. Charles Sfeir for providing ample mentorship and guidance over the entirety of my graduate career. I also thank our collaborator Dr. Gustavo P. Garlet (University of Sao Paulo, Bauru, Brazil) for guidance and mentorship during my thesis work, especially with regards to regulatory T cell biology and in the development of the mouse model for periodontal disease at the University of Pittsburgh. Together, under the guidance of Dr. Little, Dr. Sfeir and Dr. Garlet, I received a lot of experience writing numerous successful grant proposals to a variety of funding institutions. I thank Dr. Sarah Gaffen for always being available for discussion of immunological and periodontal model experiments, both in mice and in dogs. I thank Dr. Ipsita Banerjee for support and constructive comments through my Ph.D. I would also like to thank Dr. Eric Beckman for his unwavering and energetic support, both of my thesis endeavors and my recent entrepreneurial activities.

Furthermore, I would like to thank Dr. Sayuri Yoshizawa for all the mentorship, teaching and help she provided conducting both mouse and dog experiments over the course of my Ph.D. I thank Dr. Morgan Fedorchak for providing constant personal and professional guidance over the past few years. Additionally, I would like to thank Dr. Riccardo Gottardi for his hands on mentorship and encouragement during my thesis work. I thank Dr. Angus Thomson for the mentorship and early immunological guidance during my Ph.D. program. I would also like to thank

all members of the Little lab who have helped develop my research over the past few years. I would like to thank the NIH NIDCR and Dr. Leslie Frieden for the financial support through my F31 predoctoral fellowship. Finally, I would like to thank Dr. Balaji Narasiman from Iowa State University and all his lab members for encouraging me to pursue a Ph.D.

On a personal note, I would like to thank my family and friends for all their support over the past 29 years. I thank my parents for always believing I could do anything I set my mind to and providing support to help me achieve all of my goals. I would also like to thank my motorcycle for providing an escape vehicle to help relax after a long week in the lab. Most of all, I would like to thank my wife, Jaime, for always being supportive of me and putting up with everything I put her through. I cannot imagine how hard pursuing a Ph.D. would be without her constant encouragement and love.

## **1.0 INTRODUCTION**

### **1.1 STRATEGIES TO DIRECT THE ENRICHMENT, EXPANSION, AND RECRUITMENT OF ENDOGENOUS REGULATORY CELLS FOR THE TREATMENT OF DISEASE**

#### **1.1.1 Loss of tissue homeostasis and regulation leads to disease**

Disease and injury perturb the balance of processes associated with inflammation and tissue remodeling, resulting in positive feedback loops, exacerbation of disease and compromised tissue repair. Conversely, under homeostatic healthy conditions, these processes are tightly regulated through the expansion and/or recruitment of specific cell populations, promoting a balanced steady state. Better understanding of these regulatory processes and recent advances in biomaterials and biotechnology have prompted strategies to utilize cells for the treatment and prevention of disease through regulation of inflammation and promotion of tissue repair. Herein, the text below describes how cells that regulate these processes can be increased in prevalence at a site of disease or injury. This work also reviews several relevant cell therapy approaches as well as new strategies for directing endogenous cells capable of promoting environmental homeostasis and even the establishment of a pro-regenerative micro-environment. Collectively, these examples may

provide a blueprint for next-generation “medicine” that spurs the body’s own cells to action and replaces conventional drugs.

### **1.1.2 Homeostasis and disease**

Biological homeostasis is most commonly referred to as a balance or ‘steady state’ between two competing processes such as inflammation and immune regulation and anabolism and catabolism in tissue remodeling. In actuality, biological homeostasis is more aptly described as a dynamic equilibrium (as opposed to a true “steady state”) involving the sensing of perturbations, and in turn, processes that regulate these perturbations. Specifically, a perturbation produces a change in outcome that is then detected, inducing a corresponding regulatory activity that leads to negative feedback to restore balance. A simple analogy to this mechanism is a thermostat that measures the temperature with a sensor and, in response to the sensor’s reading, regulates heating/cooling to stabilize the environmental temperature. Notably, in a disease state or following injury, perturbations in biological process are not always properly regulated, resulting in an instability that can lead to improper healing and even tissue destruction and functional impairment.

Inflammatory signaling is a key modulator of homeostasis, which is evident, for instance, in unbalanced mucosal inflammation of the gut culminating in inflammatory bowel diseases (Crohn’s disease, ulcerative colitis)<sup>1</sup>. Even in sites conventionally thought of as immune privileged such as the eye, aberrant, unbalanced inflammation can lead to uveitis, dry eye disease and glaucoma<sup>2</sup>. Moreover, traumatic injury, which starts with tissue damage, can induce abnormal signaling pathways<sup>3</sup> and an inflammatory response that becomes a major disruptor to homeostasis<sup>4</sup>, leading to tissue degradation<sup>5</sup>, dysregulation<sup>3</sup> and failure to repair. Finally, tissue homeostasis and regulated inflammation are key to the survival of transplanted tissues and organs<sup>6</sup>.

Different therapeutic approaches have emerged over the past several decades that attempt to address inflammation and homeostatic imbalance. Anti-inflammatory drugs, such as COX-1/2 inhibitors, resolvins, glucocorticoids, and more recently small molecule anti-proliferative agents such as methotrexate, cyclosporine, tacrolimus and rapamycin have been used to inhibit inflammation in attempt to suppress inflammation during disease or tissue repair<sup>7</sup>. However, the negative side effects of such treatments that have limited specificity can potentially outweigh any benefits (e.g. steroid induced osteoporosis, impaired wound healing, thrombosis and cardiovascular disease)<sup>7</sup>.

More recently, anti-inflammatory biologics, such as TNF blockers<sup>7</sup>, have emerged as more effective and specific therapies for treating aberrant inflammation. However, biologics are still primarily administered systemically in relatively large quantities, leading to complications such as increased susceptibility to infection and cancer development<sup>7</sup>. Furthermore, the clinical efficacy of targeting specific cytokines has not yielded the robust results that were expected based on animal models, such as in Crohn's disease where one-third the patients do not respond to TNF antagonists, likely because inflammatory perturbations leading to disease are complex processes governed by many cytokine and signaling networks, (for example, in Crohn's disease the IL-12, and IL-23 cytokine pathways have a major role in the disease in addition to TNF)<sup>8,9</sup>.

In recent years, several approaches have emerged to deliver or boost the expression of anti-inflammatory cytokines and molecules, as opposed to blocking inflammatory cytokines. For example recombinant IL-10 and IL-11 have been used in phase II clinical trials for inflammatory Crohn's disease (reviewed<sup>8</sup>), however such treatments had disappointing efficacy compared to steroid treated controls possibly due to the overwhelming abundance of inflammatory mediators present in disease sites<sup>8,10</sup>.

In contrast, the mechanisms that cells use to regulate these processes *in situ* are sophisticated and dynamic, which is difficult to reproduce using current technology. One viable approach, therefore, is to somehow boost the number of cells that perform these complex regulatory functions at the site of a disease or injury. Presumably, these cells would be much more effective at naturally regulating the processes and either avoiding a disease state or restoring a local environment to a healthy state. Two cell types that hold great promise in regards to treatments of disease and the restoration of homeostasis to promote tissue regeneration are mesenchymal stem cells (MSCs) and CD4+CD25+Foxp3+ regulatory T cells (Tregs)<sup>11-14</sup>. Accordingly, MSCs and Tregs have been extensively explored for cell therapies (involving the isolation, *ex vivo* expansion, and re-administration of the cells) for a large number of applications through clinical trials<sup>11, 14, 15</sup>.

### **1.1.3 Other immune regulators, mesenchymal stem cells as mediators of homeostasis**

MSCs are commonly used in tissue engineering and regenerative medicine applications because of their well-known capacity to differentiate into multiple cell types. Their key feature of interest here, though, is their ability to migrate to a damaged tissue (homing) in response to the locally released inflammatory chemokines and, once there, to inhibit the inflammation by modulating innate and adaptive immune cells via soluble factors or cell-cell interaction<sup>16, 17</sup>. The most straightforward way to increase the numbers of MSCs in a biological environment would be to administer the desired cell type after differentiating or expanding these cells *ex vivo* (defined as a cell therapy). For instance, several clinical trials are ongoing to use MSCs injected in the central nervous system as a treatment for ischemic stroke and traumatic brain injury, being used as promoters of tissue regeneration, mediated by the MSCs produced factors<sup>18</sup>. Interestingly, infusion of MSCs into the body has been reported in numerous animal experiments and clinical trials to

treat a variety of additional conditions such as graft vs. host disease (GvHD), myocardial infarction, osteogenesis imperfecta, Type I diabetes, and Crohn's disease<sup>19, 20</sup>, but, although functional improvements of tissues were reported, only few engrafted MSCs were detected *in vivo*<sup>21, 22</sup>. These findings support the concept of MSCs achieving tissue repair not only through their *in situ* differentiation and engraftment but also by their regulatory function, promoting regeneration from other cell types and suppressing the immune response<sup>19</sup>. Moreover, it is reported that secretion of heme oxygenase-1 (HO-1) by MSCs can promote the formation of another regulatory cell type, Tregs<sup>23</sup>, which in turn suppress the pro-inflammation reaction of other immune cells as described in detail later. Thus, it is likely that these two key regulators of the body, MSCs and Tregs, are, in fact, connected to one another and perhaps even act in a cooperative fashion.

In addition to immunomodulatory cytokines, MSCs also secrete other factors to support survival of cells (trophic factors), and promote regeneration. These factors include, G-CSF, GM-CSF, SCF, LIF, CSF, IL-11, IL-6, VEGF, HGF, angiopoietin-1, EGF, KGF, and bFGF as extensively described elsewhere<sup>24</sup> and can enhance cell growth, proliferation, differentiation, extracellular matrix production, and favor cell recruitment and vascularization, all processes involved in tissue repair and regeneration<sup>14</sup>. In wound healing, both preclinical and clinical studies have shown that MSCs can accelerate wound closure by modulating the inflammatory response, promoting effective vascularization and the migration of keratinocytes, and inhibiting apoptosis<sup>11</sup>. Since MSCs are capable of displaying antifibrotic, angiogenic and regulatory properties, they are being explored to treat or prevent ongoing alloreactivity, with the first clinical trials in transplant recipients already underway<sup>25, 26</sup>.

#### 1.1.4 Regulatory T cells as mediators of homeostasis

Regulatory T-cells (or Tregs) are a heterogeneous population of CD4<sup>+</sup>, CD25<sup>+</sup>, FoxP3<sup>+</sup> T helper cells characterized by high levels of secretion of the anti-inflammatory cytokine IL-10, and TGFβ, which mediates a part of their suppressor functions<sup>12</sup>. Given their potent regulatory phenotype, the local enrichment of autologous or *ex vivo*-expanded adoptively transferred Tregs is a very desirable therapeutic approach for a multitude of immune-mediated destructive pathologies<sup>12, 13, 27</sup>.

*Ex vivo* produced Treg cells have been already explored in several clinical trials. For example, the isolation and *ex vivo* expansion of Tregs from umbilical cord blood sources was shown to reduce the incidence of acute GvHD in phase I trials for bone marrow transplantation<sup>28</sup>. The success of this trial appears to related to the Tregs ability to suppress CD4<sup>+</sup> and CD8<sup>+</sup> effector T cells also present in the hematopoietic cell transfers<sup>29</sup>. Similarly, it has been reported that the combined cell therapy of Tregs and T effector cells infused in phase I clinical trial patients receiving Human Leukocyte Antigen (HLA) mismatched bone marrow helped reconstitute the patients immune system, while preventing GvHD<sup>30</sup>. These Treg cell therapies take the place of strict systemic immunosuppression protocols that are normally given to patients receiving mismatched donor bone marrow transplants, thus greatly alleviating the risk for infection or other illness<sup>31</sup>. Treg cell therapies also have the potential to complement mesenchymal stem cell therapies. In a mouse critical size cranial defect model, the adoptive transfer of both MSCs and Tregs yielded robust wound healing and bone regeneration, whereas MSC therapy alone only resulted in only modest tissue regeneration<sup>32</sup>. In this case, it was shown that the addition of Tregs greatly diminished levels of inflammatory cytokines IFNγ and TNF that would otherwise inhibit bone regeneration likely through the expression of effector immune cells<sup>32</sup>. This corroborates the notion that Tregs and MSCs do indeed function synergistically to regulate the local

microenvironment and promote tissue healing. While several Treg based cell therapies have proven successful in the clinic, utilization of Treg therapies for broader applications of autoimmunity and immune suppression still face many obstacles.

### **1.1.5 Limitations of cell therapies**

Harnessing the full functional repertoire of cells via cell therapy has led to exciting advances in treatment of disease and injury, however there are many challenges yet to overcome. The hurdles of cell therapies are well known and have been thoroughly reviewed elsewhere<sup>11, 14, 15, 33</sup>. These can be briefly described as: 1) difficulty in establishment of cell sources capable of generating sufficient numbers of cells<sup>34, 35</sup>, 2) inability to specifically expand and separate target therapeutic cells<sup>15, 36</sup>, 3) difficulty maintaining functional capabilities of re-introduced cells due to T cell plasticity<sup>37</sup>, and 4) possible tumorigenicity<sup>38</sup>. Furthermore, when taking into account clinical therapy needs, the ability to adhere to good manufacturing practice (GMP) at every step of the process is non-trivial and poses significant limitations to the widespread use of many cell therapies.

A very promising therapeutic alternative to cell therapies may be the direct, selective recruitment of a patient's own endogenous antigen-specific tolerogenic DCs or Tregs to the desired body compartment. There they could modulate the host response to the introduction of a foreign material (bio implantation) or a transplanted organ, or they could help to establish a regenerative *milieu* after tissue damage.

### 1.1.6 Harnessing the potential of the body's own endogenous regulators

Recent advances in the understanding of the biological processes that govern inflammation and regulation of inflammation have led to development of synthetic strategies aimed at recruiting or expanding the body's own endogenous regulators in order to restore homeostasis and promote regeneration, while avoiding the complications associated with *ex vivo* cell expansion and re-administration. A large number of both synthetic and natural biomaterials have been investigated for many different applications, reviewed elsewhere<sup>39-42</sup>. However, several recent approaches have harnessed the endogenous immune regulators in attempt to restore homeostasis and promote regeneration.

One strategy that could be used to increase the prevalence of regulators at a local site is the specific recruitment of a patient's own natural, endogenous Tregs using a recombinant chemokine, CCL22. Although the chemokine receptor for CCL22 (CCR4) is expressed on a variety of different lymphocytes, it appears that it is more highly expressed on FoxP3<sup>+</sup> Treg<sup>43</sup> and CCL22 seems to be a primary chemokine that directs natural Treg homing *in vivo*<sup>44</sup>. Accordingly, controlled release of recombinant CCL22 using degradable PLGA microspheres is an effective strategy for direct site-specific recruitment natural Tregs *in vivo*<sup>45,46</sup>. These recruited endogenous Tregs were shown to also effectively reduce the severity of inflammatory periodontal disease in both mouse and dog models<sup>45</sup>. Additionally, Tregs have also been recruited in order to protect pancreatic islets and prevent autoimmune diabetes in mice, however, CCL22 production was induced by adenovirus gene delivery (encoding for CCL22) to the islets<sup>47</sup>. Recently, others have developed targeted nanoparticles for the delivery of Treg-inducing factors, specifically, using anti-CD4 tagged PLGA nanoparticles releasing leukemia inhibitory factor (LIF) capable of inducing the expansion of non-human primate Tregs *in vitro*<sup>48</sup>. Furthermore, leukemia inhibitory factor

released from PLGA nanoparticles was shown enhance  $\beta$ -islet transplantation to restore insulin production in a mouse model for diabetes (presumably through the induction of Tregs)<sup>49</sup>. Another strategy to harness endogenous Tregs for murine diabetes combined the delivery of antisense oligonucleotides directed against CD40, CD80 and CD86 from polymeric microspheres<sup>50</sup>. These combination particles encapsulating antisense oligonucleotides were capable of inducing the expansion of endogenous Tregs (potentially mediated by tolerogenic dendritic cells) and preventing type 1 diabetes in mice, furthermore, isolated Tregs from treated mice were capable of preventing t-cell mediated  $\beta$ -islet destruction in secondary mouse recipients, suggesting that the particles led to the induction of stable Treg phenotypes<sup>50</sup>.

An alternative strategy to bolster endogenous regulatory T cells is to differentiate a more prevalent population of cells (such as naïve CD4<sup>+</sup> T cells) into regulatory T-cells. To this end, it was found that the combination of TGF $\beta$ , rapamycin and IL-2 were shown to robustly convert both mouse and human naïve CD4<sup>+</sup> lymphocytes to, FoxP3<sup>+</sup> regulatory T cells *in vitro*<sup>51</sup>. If a strategy could be developed to apply this technique *in vivo*, it could represent a promising approach for generating far more induced Treg at a local site than is possible by recruiting naturally occurring Treg.

### **1.1.7 Regulatory T cells as regulators of regeneration**

Although it is well known that the strategic modulation of endogenous immune regulators, such as Tregs, can effectively mediate destructive inflammation, it is not as commonly discussed in the literature how these cells also appear to promote regeneration<sup>45</sup>. One way in which endogenous regulators may promote tissue healing and regeneration is through the release of pleiotropic cytokines such as IL-10 and TGF $\beta$ . For example, IL-10 is known to play an important role in bone

metabolism *in vivo*, accordingly IL-10-deficient mice display both decreased osteoblast generation and bone formation<sup>52</sup>. Similarly, TGF $\beta$  has been shown to play a role in promoting cell growth, differentiation and extracellular matrix, and therefore is considered an anabolic cytokine<sup>53-55</sup>. Indeed, TGF $\beta$  is known to recruit osteoblast precursors, induce their differentiation and up-regulate the expression of collagen type 1, even in disease conditions<sup>56, 57</sup>. The controlled release of CCL22 and subsequent recruitment of endogenous Tregs (as shown by local increases in FoxP3) not only decreased the severity of disease in mice, but also upregulated both IL-10 and TGF $\beta$  expression in the tissue<sup>45</sup>. In addition, a host of both hard and soft tissue pro-regenerative factors such as BMP4, BMP7, RUNX2, ALP, DMP1, COL1A1<sup>45</sup> were upregulated as well concurrently with the downregulation of factors known to be involved with both hard and soft tissue destruction<sup>45</sup>, as shown in Figure 1. Indeed, the addition of Tregs has been an emerging trend in regenerative therapies, where Tregs have been utilized for complete repair of critical size defects in mouse skulls<sup>32</sup>, and ischemic kidney repair<sup>58</sup>.

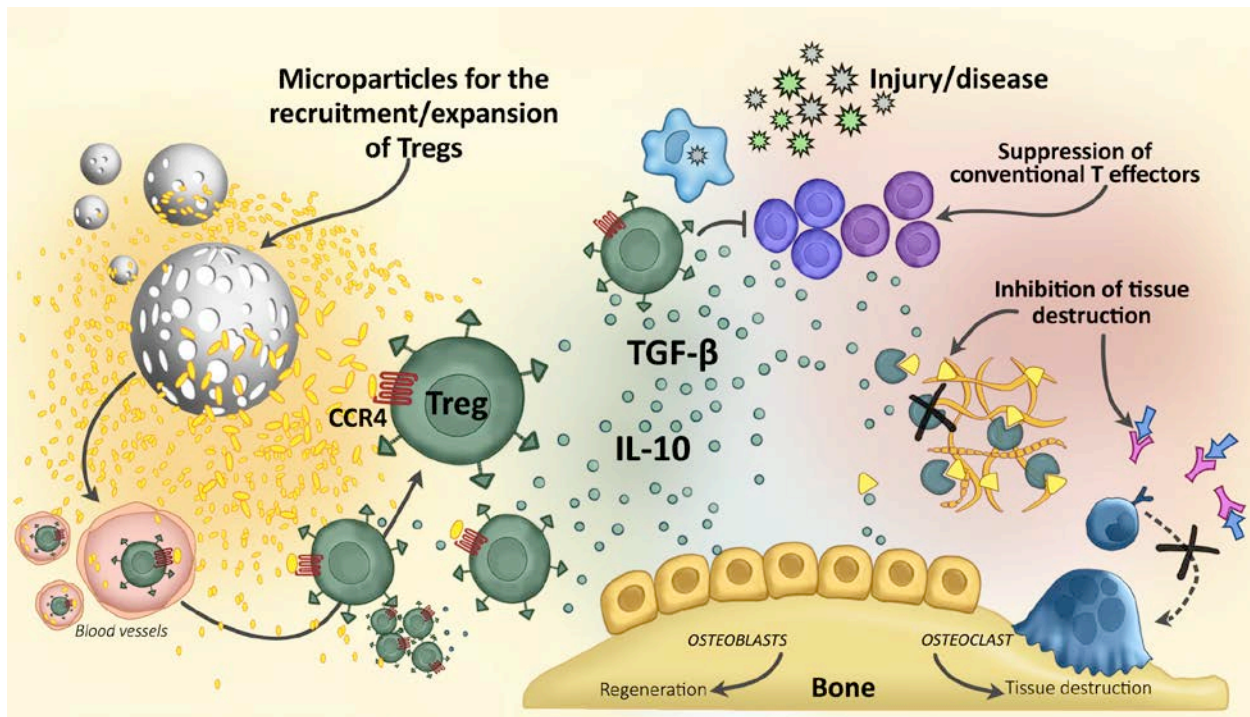


**Figure 1: Synthetic strategies to recruit and enhance Tregs for the amelioration of disease, restoration of homeostasis, and promotion of tissue regeneration<sup>59</sup>.**

### 1.1.8 Engineering techniques for harnessing endogenous mesenchymal stem cells

In theory, an analogous approach to what is discussed above could be developed by mimicking the natural mechanisms of migration of endogenous mesenchymal stem cells. For instance, MSCs migrate to the injured or inflamed site by sensing chemokines gradients and locally regulate immune reactions and promote tissue regeneration by cell-cell contact or secretion of cytokines Figure 2. A synthetically driven homing of MSCs would then theoretically promote these same functions and benefit broad area of diseases including inflammatory and degenerative diseases.

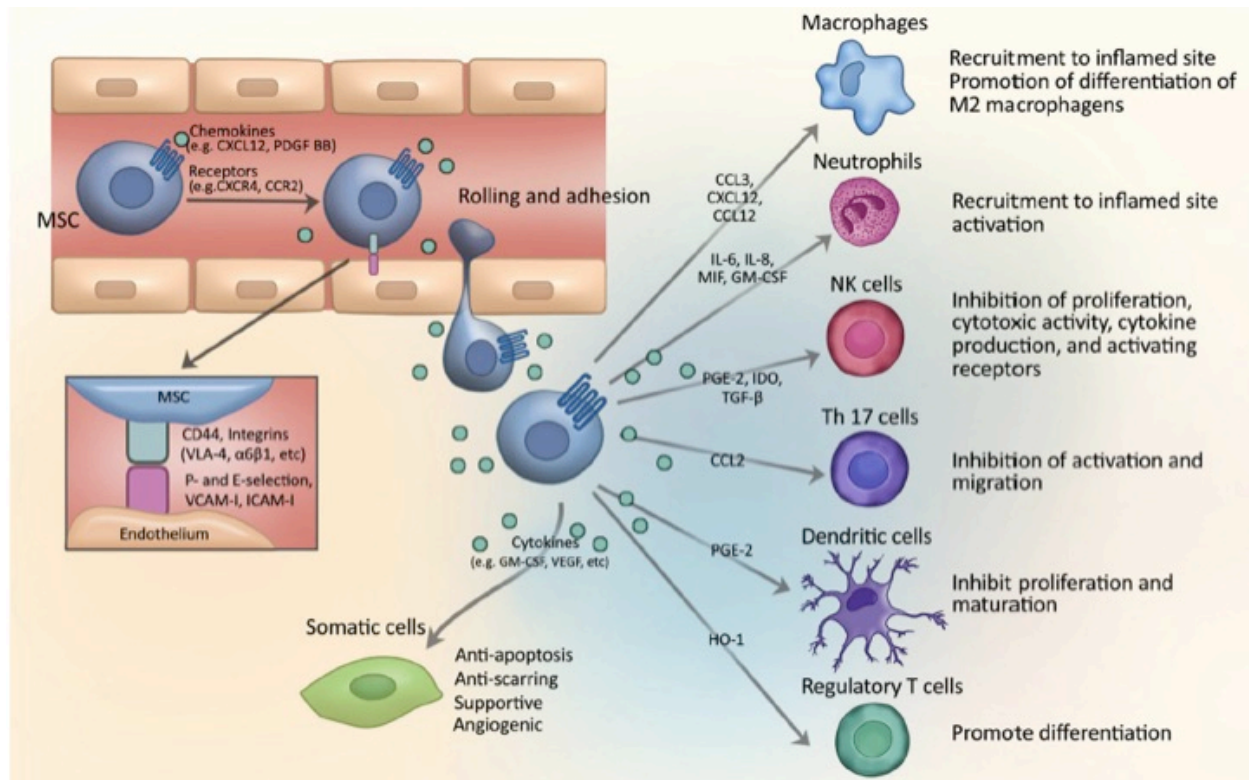


**Figure 2: How MSCs migrate to sites of disease or injury and potential modes of regulating immune cells<sup>59</sup>.**

One obvious strategy to recruit endogenous MSCs could rely on the creation of a local gradient of a chemoattractant molecule of choice to induce cells chemotaxis<sup>60</sup>. Several chemokines have been implicated to induce MSC homing<sup>61</sup>; one of the most widely used chemoattractant is stromal cell-derived growth factor-1 (SDF-1), although it is not specific to MSCs as it can also recruit lymphocytes<sup>62</sup>. Another MSC chemoattractant is platelet-derived growth factor (PDGF)<sup>63</sup> which is also non-specific for MSCs, but PDGF receptors are highly expressed on MSCs. It is worth noting that besides chemokine gradients, the surrounding extracellular matrix (ECM) and the environmental mechanical forces can recruit MSCs as well<sup>64</sup>.

The chemoattractant molecule is generally released from a point source via a carrier that can be in the form of micro/nanospheres<sup>46</sup>, of scaffolds<sup>63 65</sup>, especially when aimed at tissue

engineering applications<sup>66</sup>, or, in fact, of any other implantable structure (stents, subcutaneous patches, sutures, etc.)<sup>65, 67, 68</sup>. Other strategies that are utilized in tissue engineering could also be helpful, including the patterning of scaffolds to induce and guide cell invasion<sup>69</sup>.

Current strategies to recruit endogenous MSCs typically rely on several different techniques to delivery the chemoattractant or MSC boosting factor (reviewed<sup>70, 71</sup>). For example, release of SDF-1 from a poly(lactide ethylene oxide fumarate) (PLEOF) hydrogels or from chitosan/poly( $\gamma$ -glutamic acid) polyelectrolyte complexes have been utilized to recruit MSCs<sup>72 73</sup>. SDF-1 has also been released from poly(lactide-co-glycolide) (PLGA) microspheres to promote MSCs recruitment<sup>74</sup> or alternatively PDGF to enhance both cell migration and vasculogenesis<sup>75</sup>. Modern degradable carriers can now offer a high degree of tunability of the release behavior for any given chemoattractant<sup>76, 77</sup>. Since a controlled release carrier may also be loaded with practically any “instructional” molecules, (e.g. growth factor inducing stem cells differentiation<sup>78</sup>), combining multiple carriers (for instance, different microspheres formulation containing different molecules or a scaffold/microspheres combinatorial structure<sup>79</sup>) allows a more sophisticated cellular control. For instance, this technique could be used for the sequential recruitment of different cells as well as the recruitment of a given cell precursor followed by the release of instructional molecules to direct cell differentiation or tissue production. For instance the sequential delivery of PDGF and vascular endothelial growth factor (VEGF) for sustained neovascularization<sup>80</sup> or the release of PDGF and simvastatin for dentoalveolar regeneration<sup>81</sup>.

In contrast, responsive delivery systems (where the structure of the delivery vehicle is actively altered by endogenous cells) are one of the exciting new frontiers of nanomedicine as they hold promise for instructional-based biomimetic drug delivery. Generally the polymeric components of the carrier incorporate specific sequences that can be cleaved only under the desired

environmental conditions (e.g., low pH) or by specific molecules (e.g. inflammatory cytokines, MMPs, etc.)<sup>82, 83</sup>. Such carriers would allow dynamic release of intended molecules in response to cellular activity, Figure 3.

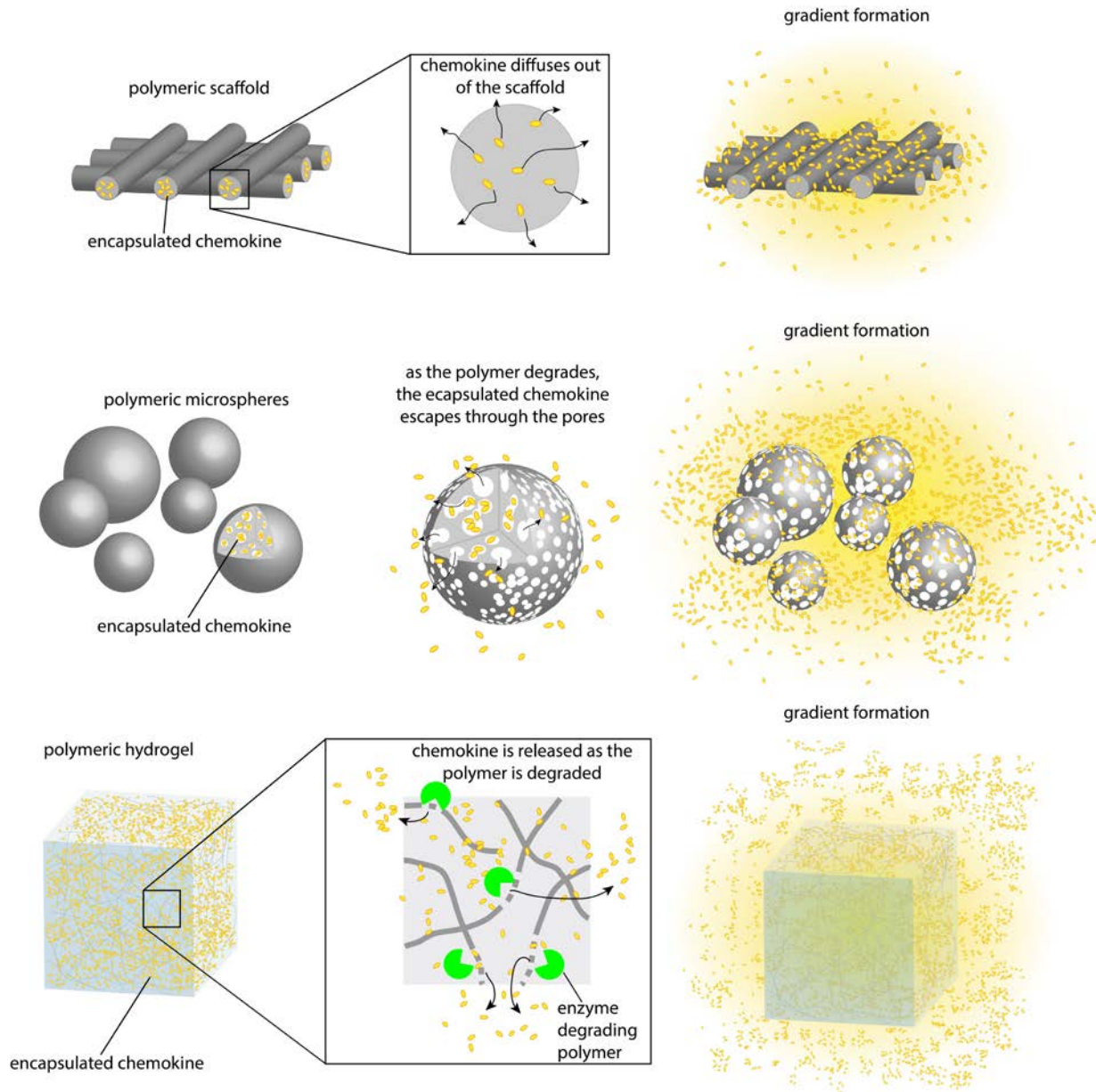


**Figure 3: Synthetic engineering strategies to expand and chemoattract endogenous MSCs and Tregs<sup>59</sup>.**

### **1.1.9 Future vision for engineering treatments for harnessing endogenous regulators for disease**

The role of endogenous regulators, such as Tregs or MSCs, in promoting tissue regeneration via restoration of homeostasis is a promising strategy to treat a number of diseases where current treatments are lacking. Cell therapies utilizing MSCs and Tregs have shown great promise even in the clinic, and have revealed the power of cells to promote immunological and regenerative homeostasis for the treatment of disease. Yet newer, fully synthetic approaches to localized recruitment, expansion and activation of a patient's own endogenous cells bypasses many of the hurdles of cell therapies. Indeed, these synthetic approaches seem to (at least in some capacity) mimic the body's natural mechanisms to cause cell homing or expansion when necessary. Each of these approaches represent potential future medical treatments that harness the body's innate regulatory capacity in a way that is dramatically more sophisticated and complex than what is possible in the clinic today.

## **1.2 STRATEGIES TO RECRUIT AND EXPAND ENDOGENOUS REGULATORY CELLS FOR THE TREATMENT OF PERIODONTAL DISEASE**

Periodontal disease affects over 64 million Americans and is considered one of the most pressing oral health concerns today<sup>84</sup>. Also known as periodontitis, this condition is characterized by destructive inflammation of the periodontium, including the gum tissue, supporting bone, and ligament (Figure 4, periodontal disease progression). Importantly, this disease affects not only tooth loss but also the incidence of cardiovascular disease, kidney disease, respiratory diseases,

diabetes, and even premature childbirth<sup>85-89</sup>. The current standard of care involves debridement of calculus (a procedure called scaling and root planing) and can be accompanied by local delivery of an antibiotic such as minocycline (Arestin®<sup>90</sup>). These treatments temporarily kill pathogens but do not protect against inevitable future infections or address the susceptibility observed in patients disposed to immune dysfunction. In fact, nearly 20% of patients suffering periodontal disease show no response (disease recurrence) to current antibacterial-focused treatment regimes and are labeled as refractory patients<sup>91</sup>.

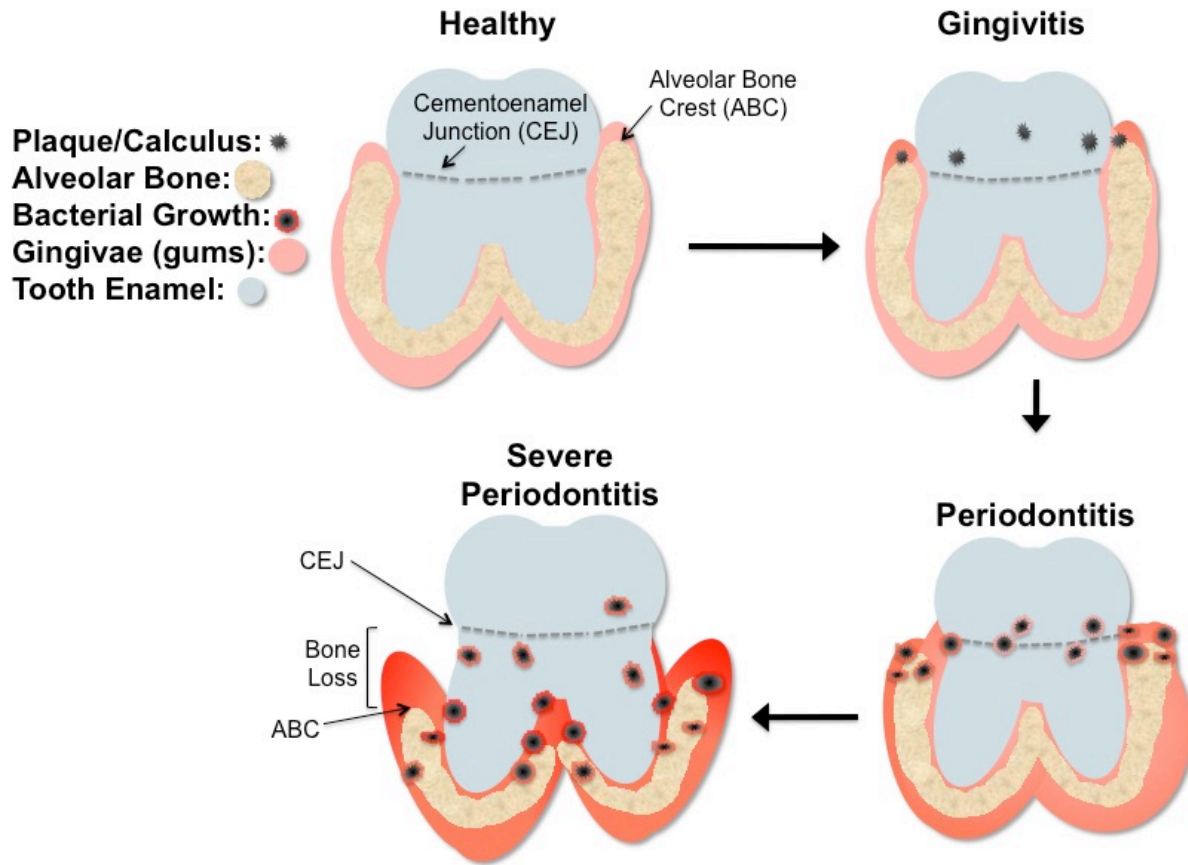


**Figure 4: Periodontal disease structure and progression.** Healthy periodontal tissue is characterized by pink gingivae, absence of plaque and high alveolar bone levels. Gingivitis is characterized by inflammation of the gums (gingiva) and the presence of bacterial biofilms or plaques, however tissue destruction has not occurred or is mild. Disease is categorized as periodontitis once significant tissue damage has occurred, typically displaying periodontal pocket depths of 3 mm or more. Deep pockets, typically greater than 6 mm are categorized as severe or advanced periodontitis. Cementoenamel junction (CEJ) is static architecture of the tooth root often used as a referenced for tissue destruction when performing clinical attachment loss measurements. The alveolar bone crest (ABC) signifies the peak height of the tooth supporting bone, typically clinically measured using dental X-rays.

Although invasive bacterial species are protagonists of the disease, tissue destruction is mediated by an adverse host inflammatory immune response<sup>92, 93</sup>. As the disease progresses,

several populations of lymphocytes are recruited to the periodontium<sup>94-97</sup>, guided by local gradients of specific lymphocyte-attracting chemokines<sup>98, 99</sup>. It is the overall cytokine milieu produced by these specific populations of lymphocytes that ultimately directs hard and soft tissue destruction<sup>100</sup>. Therefore, it is becoming increasingly clear that future treatments of periodontal disease focus not only on invasive bacteria, but also address the underlying immune dysfunction.

### 1.3 PERIODONTAL DISEASE

#### 1.3.1 Prevalence and implications of periodontal disease

Periodontal disease is strikingly prevalent in the United States, affecting 34% of individuals over the age of 30, or an estimated 64 million Americans<sup>84, 101</sup>. It is the number-one cause of tooth loss according to the American Dental Association. Worldwide, periodontal disease is estimated to affect up to 20% of the adult population<sup>102</sup>. Furthermore, the periodontal biofilm hosts a wide variety of bacterial species that are notorious for their role in systemic infection and inflammatory immune diseases. The most predominant periodontal pathogens, *Actinobacillus actinomycetemcomitans*, *Porphyromonas gingivalis*, *Tannerella forsythia*, and *Fusobacterium nucleatum*<sup>93</sup> present virulence factors that have been associated with: 1) systemic infections and consequent complications<sup>103, 104</sup>, 2) a 4-fold increase in premature births<sup>105</sup>, 3) anorexia-cachexia syndrome<sup>106</sup>, 4) atherosclerosis<sup>107</sup>, 5) myocardial infarction and ischemic stroke<sup>108, 109</sup>. As the body of research linking periodontitis to the incidence of these other conditions continues to grow, reducing the prevalence of the disease is of utmost importance. This prevalence is likely

perpetuated by a misunderstanding of how disease symptoms develop, as represented by current treatments that aim only at removing bacterial species.

### **1.3.2 Current clinical treatments for periodontal disease**

The current standard of care for periodontal disease (i.e. scaling and root planing) involves the mechanical removal of calculus and bacteria from beneath the gingiva (debridement), and is typically performed by a periodontal specialist, Figure 5A. In severe cases, antibiotic treatments (Arestin®, PLGA microspheres controllably releasing the antibiotic minocycline for 21 days<sup>90</sup>) may be injected into the periodontal pocket, Figure 5B. Antibiotic treatments, however, only temporarily remove bacterial species. Recurrent infections are common, requiring patients to repetitively undergo these expensive procedures. As a last resort after scaling and root planning, patients with severe or advanced periodontitis may undergo an extremely painful and expensive procedure called open flap surgery, Figure 6. The goal of periodontal flap or open flap surgery is to reshape damaged alveolar bone and tightly reattached the gingiva to the tooth root, to eliminate periodontal pockets that harbor bacteria, Figure 6. Furthermore, these treatment are completely ineffective in 20% of the population (the condition is labeled refractory periodontitis<sup>91</sup>) and may contribute to an ever-increasing resistance to anti-bacterial agents<sup>110</sup>. Indeed, most recent research in the development of new periodontal disease treatments aims to influence the inflammatory immune reaction itself, which is ultimately responsible for tissue destruction.

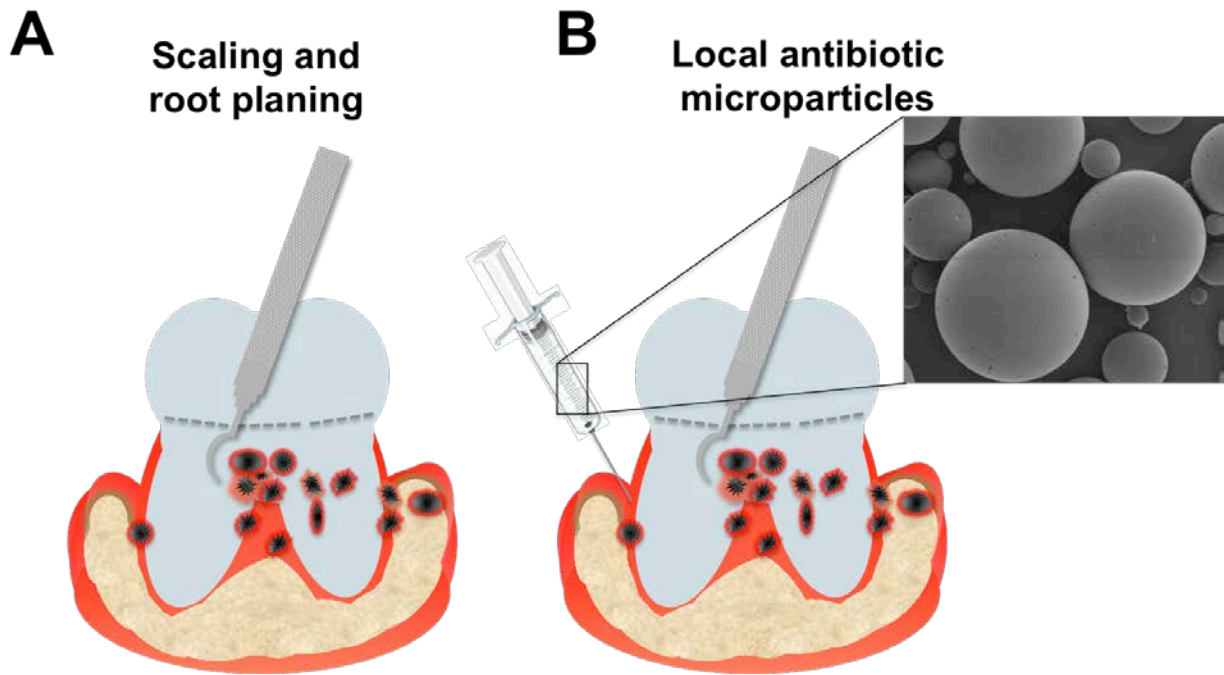


Figure 5: Clinical therapies for periodontitis, scaling and root planing and local antibiotics.

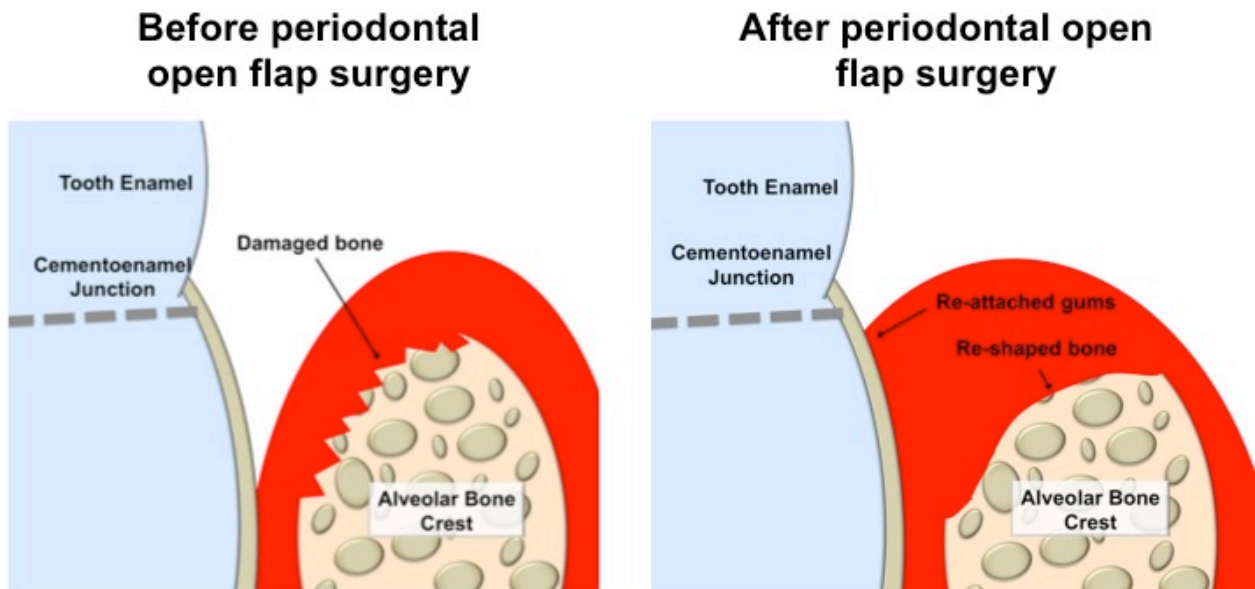


Figure 6: Clinical treatment, periodontal open flap surgery.

### **1.3.3 Current clinically available host modulators**

Tetracyclines like the minocycline and doxycycline are typically used as antibiotic agents, however, a secondary effect of tetracyclines is their ability to inhibit soft tissue destroying enzymes, matrix metalloproteinases (MMPs)<sup>111</sup>. Typically used in low dose formulation (sub antibiotic levels) tetracyclines like doxycycline (Periostat®) have been used to treat periodontal disease by preventing some of the damaging inflammation with greatly altering bacteria levels in patients<sup>112</sup>. Furthermore, minocycline (used clinically in controlled release antibiotic Arestin®<sup>90</sup>) is known to specifically inhibit MMP-8 and MMP-9 presented in periodontal disease patients<sup>111</sup>, and may be present in sub-antibacterial doses as a result of the controlled release nature of Arestin® formulations<sup>90</sup>. However, the use of antibiotics, even at sub-lethal levels, appears to aide in the selection and development of bacterial resistant strains<sup>113</sup>. Bacterial resistance may be perpetuated by prior antibacterial use, for periodontal disease or other conditions<sup>113</sup>, and studies are beginning to assess the effect the use of common antibiotics have on conferring resistance to other pathogenic microbes, ultimately altering the levels of commensal bacteria<sup>114</sup>. Based on recent findings about the characteristics of periodontal disease and the role of the host immune response in the development of tissue destruction, researchers have begun developing new therapies to address damaging inflammation, rather than attempt to halt bacterial growth.

### **1.3.4 Immune reaction, chemokines, and the attraction of lymphocytes to the periodontium**

Recent literature has elucidated that periodontal disease may largely be perpetuated by the inflammatory immune response resulting from initial bacterial insult. Excessive inflammation in

periodontitis is driven by large numbers of leukocytes that infiltrate the periodontium. Early in disease progression, large numbers of protective polymorphonuclear leukocytes (PMNs) are recruited by the presence of bacteria<sup>97, 115</sup>, whereas T lymphocytes predominate in established chronic periodontal lesions<sup>116</sup>. Recruitment of these various leukocyte sub-populations to the periodontium is guided by patterns of proteins that direct cellular translocation (i.e. chemokines). Chemokines interact with specific lymphocyte populations and in turn, bias immune responses<sup>117, 118</sup>. Recently, Th1-type chemokines (CXCL10 formerly IP-10, and CCL3 formerly MIP-1 $\alpha$ ) have been detected in patients with aggressive periodontitis, along with high levels of the pro-inflammatory cytokine IFN- $\gamma$ <sup>119</sup>.

The skewed overabundance of Th1-type or Th17 inflammatory reactions disrupts the delicate homeostatic equilibrium between pro-regenerative and tissue-destroying responses. Inflammatory chemokines and cytokines lead to upregulation of soft tissue destroying matrix metalloproteinases (MMPs)<sup>119</sup> that degrade periodontal ligament and gingivae. Further, this excessive inflammatory environment leads to the local upregulation of receptor activator of nuclear factor- $\kappa$ B ligand (RANKL), a potent activator of bone resorbing osteoclast cells, leading to alveolar bone loss<sup>119</sup> (and eventually tooth loss)<sup>120, 121</sup>.

### **1.3.5 Complications associated with the inhibition or blocking of inflammation**

The most common approach for addressing aberrant inflammation is through the administration of small molecule or protein inflammatory inhibitors<sup>7, 122</sup>. One recent experimental treatment aimed at reducing the host inflammatory response involves the administration of the drug Resolvin. Resolvin blocks neutrophil-mediated inflammation and the associated pro-inflammatory cytokine milieu<sup>123</sup>. However, it has been shown that direct, long-term inhibition of inflammatory cytokines

by traditional blocking (i.e. anti-inflammatory) strategies can compromise periodontal tissue regeneration<sup>124-128</sup>. Furthermore, researchers have shown that traditional blocking of the protective immune responses can result in increased bacterial burden and acute systemic reaction<sup>94, 95</sup>, and increased alveolar bone loss<sup>97</sup>. While the use of anti-inflammatory mediators may provide some disease relief, a technique to harness the body's own regulatory immune response could provide a more robust solution for periodontitis.

### **1.3.6 How the body naturally regulates inflammation**

One possible explanation for the shortcomings of the aforementioned treatment is that our bodies do not regulate harmful inflammatory responses by blocking leukocyte infiltration, but rather by balancing inflammatory leukocyte recruitment with regulatory lymphocyte recruitment<sup>12, 13</sup>. Regulatory T cells (Tregs) exert their control over other lymphocytes both through secreted factors and through direct cell-cell interactions, ultimately leading to targeted inflammatory-immune cell arrest<sup>12, 13</sup>. Although the complete regulatory repertoire possessed by Tregs remains enigmatic, progress has been made toward therapeutic use of Tregs for a wide variety of autoimmune and inflammatory diseases. Adoptive Treg cell transfer (i.e. cell infusion) therapies have seen the most pre-clinical and clinical success, yet clinical translation of the complicated *ex vivo* cellular expansion protocols has proven difficult<sup>15</sup>. We argue that the greatest impact for periodontal disease treatment would come from an off-the-shelf therapeutic — one that harnesses the body's natural mechanisms for immune regulation (recruitment of endogenous Tregs), leading to restoration of local immune homeostasis and not immune inhibition. For this reason, we assert that the recruitment of endogenous Tregs to the periodontium could provide the immune regulation

necessary for abrogation of disease symptoms, while simultaneously maintaining immunity against invasive bacterial species.

### **1.3.7 A biomimetic, engineered approach to promote immune regulation in periodontal disease**

Immune cells are naturally recruited to peripheral sites via chemokines secreted by tissue-resident cells. Specifically, biological gradients of chemokines direct immune cells toward the origin of secretion (presumably the site of infection or injury). Interestingly, one way in which tumors appear to avoid immune surveillance and clearance is through a similar chemokine-based strategy leading to the recruitment of regulatory T cells<sup>44</sup>. Specifically, tumors produce and sustain a biological gradient of CCL22, a Treg-associated chemokine<sup>129-131</sup> that directs Treg migration. Once co-localized with the tumor, Tregs suppress effector immune cells by secreting factors such as IL-10 and TGF- $\beta$ , thereby establishing immunological homeostasis in a milieu that would otherwise present itself as highly inflammatory<sup>132</sup>.

Interestingly, endogenous Regulatory T cells have been shown to be exclusively recruited by to the production of the chemokine CCL22 by some tumors<sup>44</sup>, resulting in tumor immune evasion and exacerbation. Specifically, it appears that Tregs more highly express the receptor for CCL22, CCR4 than other populations of splenocytes<sup>43</sup>, allowing for specific Treg recruitment via CCL22. Furthermore, virally induced CCL22 production in pancreatic islet cells was used therapeutically to prevent the rejection of implanted islet cells to reverse murine diabetes<sup>47</sup>, suggesting that endogenous Treg recruitment via CCL22 may provide a strategy for treating damaging inflammatory immune responses. Therefore, it is foreseeable that using engineering principles, researchers could fabricate controlled release systems that can produce and sustain a

concentration gradient of certain molecules (including CCL22) that may potentially recruit Tregs to the site of microsphere implantation. Utilizing common fabrication techniques, microspheres can be fabricated using a polyester found in a number of FDA-approved systems and will degrade in a well-characterized manner *in vivo*<sup>133, 134</sup>. We theorized that by mimicking the natural immune-evasion mechanisms of tumors using rationally-designed, CCL22-releasing, polymeric microspheres, Tregs could be recruited to a site of destructive inflammation (e.g. diseased periodontium) to slow or stop disease progression.

Further, as an alternative to direct CCL22 controlled release for Treg recruitment, a molecule originally discovered as a vasodilator (vasoactive intestinal peptide, or VIP), has been recently found to induce endogenous CCL22 production by dendritic cells<sup>135</sup>. Originally, VIP was identified as a neuropeptide associated with endothelial cells in the intestinal environment, but later was shown to be a potent immunomodulator<sup>136, 137</sup>. Additionally, VIP was shown to attenuate inflammatory and autoimmune reactions possibly through aiding in the direct induction of regulatory T cells<sup>138-140</sup>. Importantly, VIP was also found to strongly influence bone metabolism by way of inhibiting osteoclastogenesis (bone resorbing cells) and promoting osteoblastogenesis (bone forming cells)<sup>137, 141</sup>. Therefore, VIP may be a viable alternative controlled release therapeutic peptide for periodontal disease, possibly functioning by inducing the local recruitment of Tregs (via inducing CCL22 expression), aiding in the direct induction of Tregs, or even altering the damaging inflammatory response leading to alveolar bone resorption<sup>135-137, 139, 141-143</sup>.

Another way to enhance the numbers of regulatory T cells *in situ* may be through the induction of local T cells towards Treg phenotypes (as opposed to T effector cell phenotypes) via biological enhancers of Treg populations. Several different strategies have been utilized to directly induce Tregs *in vivo*, for example: anti-IL-2 monoclonal antibodies<sup>144</sup>, superagonistic anti-CD28

monoclonal antibodies<sup>145</sup>, and agonistic anti-CD4 monoclonal antibodies<sup>146</sup>. However, the therapeutic mechanisms of these antibodies are not well understood, especially in the context of human trials, where their safety remains a concern. In fact, phase 1 trials of the superagonistic anti-CD28 monoclonal antibodies led to a severe and damaging cytokine storm in all humans who received the treatment<sup>147</sup>. Aside from these antibodies, other molecules have been identified to induce regulatory T cell development, including: IL-2, TGF- $\beta$  and Rapamycin<sup>51</sup>. Specifically, the use of these factors has been shown to aide in the development of Tregs *in vivo* and *in vitro*, even under inflammatory conditions<sup>51, 148-150</sup>.

Recently, the controlled release of IL-2, TGF- $\beta$  and Rapamycin from PLGA microspheres (conducted in our laboratory) has been shown to specifically induce regulatory T cells from naïve CD4+ T cells in both human and mouse cells *in vitro*<sup>51</sup>. Specifically, the combination of IL-2, TGF- $\beta$  and Rapamycin released from PLGA microspheres led to the robust expansion of a 80% pure population of Tregs, as opposed to soluble IL-2 expanded naïve T cells which robustly expanded T cells, but only led to 3% of cells expressing Treg marker FoxP3<sup>51</sup>. Furthermore, Tregs induced from IL-2, TGF- $\beta$  and Rapamycin releasing PLGA microspheres displayed phenotypic markers of Tregs and functionally suppressed T effector cells *in vitro*<sup>51</sup>. Ultimately, multiple strategies utilizing acellular-engineered approaches may help to increase the local populations of regulatory T cells, and have the potential to be used therapeutically in periodontal disease.

### **1.3.8 Hypothesis: increasing the presence of regulatory T cells in the periodontal tissues using Treg-recruiting or Treg-expanding microspheres may attenuate periodontal disease symptoms and promote tissue regeneration**

The proposed delivery system of PLGA microspheres is inherently biocompatible<sup>151</sup>, non-inflammatory<sup>151, 152</sup>, and highly tunable<sup>133, 153</sup>. Furthermore, it represents a biomimetic strategy in that takes advantage of the body's natural mechanisms of regulation and healing during inflammation, as shown in Figure 1. The approach to enhance endogenous Tregs via microsphere formulations provides a potential solution for the immune imbalance and dysfunction associated with periodontal disease, but does not require potentially harmful immune-blocking strategies.

Tregs have been shown to reestablish immune homeostasis through a wide variety of mechanisms, both at the site of inflammation (which for our purposes is the periodontium) and at the draining lymph nodes (in this case, the cervical lymph nodes)<sup>154</sup>. Specifically, Tregs act to balance these pro-inflammatory mediators by secreting anti-inflammatory factors such as IL-10 and TGF- $\beta$ <sup>12, 13</sup>. IL-10 has been shown to play a major role in attenuation of periodontal disease by upregulating an extracellular RANKL inhibitor, osteoprotegerin (OPG), and promoting increased levels of intra-inflammatory-cell 'suppressors of cytokine signaling' (SOCS)<sup>155, 156</sup>. Furthermore, IL-10 not only regulates the inflammatory immune response, but also plays a key role in bone anabolism, leading to maturation of bone-forming osteoblasts<sup>157-159</sup>. Indeed, recent reports have shown IL-10 levels are substantially diminished in patients with severe periodontitis<sup>160</sup>. Finally, TGF- $\beta$  has been shown to play an important role in immune regulation and tissue regeneration specifically with respect to bone growth<sup>161</sup>. The data presented below provides evidence that validates our aforementioned approach to use biomimetic microspheres to harness endogenous Tregs and iTregs for abrogation of periodontal disease symptoms.

## **2.0 CONTROLLED RELEASE OF CCL22 FOR THE RECRUITMENT OF TREGS AND TREATMENT OF PERIODONTAL DISEASE IN A MICE MODEL**

### **2.1 INTRODUCTION**

A large body of literature now suggests that bacterial species (albeit protagonists) are secondary to the host immune response in regard to the etiology of periodontal disease progression<sup>100, 120, 162</sup>. Specifically, various lymphocyte subsets can accumulate in the periodontium, leading to the local expression of soft tissue destroying matrix metalloproteinases<sup>163</sup> (MMPs) and receptor activator of nuclear factor kappa-B<sup>51</sup> ligand (RANKL)<sup>164</sup> (the primary activation factor for osteoclasts), initiating alveolar bone resorption. Several recent reports have also shown that another lymphocyte subset called regulatory T cells (Tregs) can accumulate in the gingival tissues during periodontal disease both in humans and in experimental models<sup>129, 165-167</sup>, and helps protect the host from harmful inflammation. However, it appears that when Tregs are present in insufficient numbers, progression of the disease is accelerated<sup>167</sup>.

Accordingly, this study sought to develop a strategy for increasing local numbers of regulatory lymphocytes through the recruitment of endogenous Tregs<sup>46</sup> (mimicking a mechanism that tumors employ to evade immune responses<sup>44</sup>). Specifically, a natural gradient of a known chemoattractant for regulatory lymphocytes, C-C motif chemokine ligand 22 (CCL22)<sup>46, 47</sup> could be artificially reproduced using controlled release from a local site. Recently, we developed polymer microspheres capable of steadily releasing CCL22 using a model-aided design process that specifies the requisite formulation properties (such as porosity) and polymer composition<sup>46</sup>. Importantly, this process permits the tuning of release behavior using degradable polymers such

as poly(lactic-co-glycolic) acid (PLGA) that are already known to be safe and biocompatible and also exhibit a proven track record of clinical translation<sup>134, 168</sup>. This CCL22-releasing formulation has been shown to be effective at recruiting Treg both *in vitro* and *in vivo*<sup>46</sup>. These recruited Tregs have the potential to influence the local immunological milieu, shifting it toward homeostasis<sup>46</sup>. Based on these observations, the hypothesis of this study is that this biodegradable, controlled release formulation of CCL22 administered locally in the periodontium, may recruit Tregs, and effectively abrogate periodontal disease symptoms without necessarily reducing local bacterial numbers. Furthermore, the presence of Tregs may actually help to balance the pro-inflammatory response and generate an environment that is conducive to both periodontal tissue regeneration as well as bone regeneration possibly through expression of interleukin 10 (IL-10) and osteocalcin (OCN)<sup>167</sup>.

Using both *Actinobacillus actinomycetemcomitans* (Aa)-induced<sup>94, 98-100, 115, 156, 167</sup> and *Porphyromonas gingivalis* (Pg)-induced<sup>97, 169</sup> mouse models for periodontal disease, this study demonstrates that the Treg recruiting formulation significantly halts the progression of periodontitis as determined by significant decreases in alveolar bone resorption (primary disease outcome). Furthermore, the Treg recruiting formulation leads to a significant decrease in the production of proinflammatory cytokines in the periodontal tissues (along with an increase in anti-inflammatory cytokines) as well as a decrease in markers of soft and hard tissue destruction (along with an increase in markers of soft and hard tissue regeneration). Overall, the Treg-recruiting formulations described herein may serve as a tool for the study of the role of Treg in periodontal disease, and even suggest a new treatment modality that intends to harness the body's own sophisticated immune regulatory mechanisms through the recruitment of endogenous cells.

## 2.2 METHODS

### 2.2.1 Microsphere preparation

Poly (lactic-co-glycolic) acid (PLGA) microspheres containing recombinant mouse CCL22 (R&D systems, Minneapolis, MN) were prepared using a standard water-oil-water double emulsion procedure as described<sup>46</sup>. Blank (unloaded) PLGA microsphere controls were fabricated in the same manner with the exception of CCL22 protein encapsulate. Briefly, the PLGA (RG502H, Boehringer Ingelheim, Petersburg, VA) microspheres were prepared by mixing 200  $\mu$ L of an aqueous solution containing 5  $\mu$ g of rmCCL22 and 2 mg of BSA and 15 mmol NaCl with 200 mg of polymer dissolved in 4 mL of dichloromethane. The first water-in-oil emulsion was prepared by sonicating this solution for 10 seconds. The second oil-in-water emulsion was prepared by homogenizing (Silverson L4RT-A) this solution with 60 mL an aqueous solution of 2% polyvinyl alcohol (M.W. ~25,000, 98 mol. % Hydrolyzed, PolySciences, Warrington, PA) for 60 seconds at 3000 RPM. This solution was then mixed with 1% polyvinyl alcohol and placed on a stir plate agitator for 3 hours to allow the dichloromethane to evaporate. The microspheres were then collected and washed 4 times in deionized (DI) water, to remove residual polyvinyl alcohol, before being re-suspended in 5 mL of DI water, frozen, and lyophilized for 72 hours (Virtis Benchtop K freeze dryer, Gardiner, NY; operating at 100mTorr). The overall microsphere fabrication process is shown below in Figure 7.

Additional recombinant mouse CCL22 PLGA microspheres were fabricated in order to find the optimal *in vitro* release characteristics for use in the mouse model of periodontal disease. Microspheres composed of varying PLGAs were used and mixed in combination: 4.2 kDA 50:50 PLGA carboxylic acid capped polymer from Lakeshore Biomaterials (Birmingham, AL), RG502

(acetyl end cap) 50:50 PLGA (Boehringer Ingelheim, Petersburg, VA), RG504 (acetyl end cap) 50:50 PLGA (Boehringer Ingelheim, Petersburg, VA). Briefly, 5  $\mu$ g of rmCCL22 (R&D Systems) was dissolved in 200  $\mu$ L of deionized water and was added to with 200 mg of polymer dissolved in 4 mL of dichloromethane. The first water-in-oil emulsion was prepared by sonicating this solution for 10 seconds. The second oil-in-water emulsion was prepared by homogenizing (Silverson L4RT-A) this solution with 60 mL an aqueous solution of 2% polyvinyl alcohol (M.W. ~25,000, 98 mol. % Hydrolyzed, PolySciences, Warrington, PA) for 60 seconds at 3000 RPM. This solution was then mixed with 1% polyvinyl alcohol and placed on a stir plate agitator for 3 hours to allow the dichloromethane to evaporate. The microspheres were then collected and washed 4 times in deionized (DI) water, to remove residual polyvinyl alcohol, before being re-suspended in 5 mL of DI water, frozen, and lyophilized for 72 hours (Virtis Benchtop K freeze dryer, Gardiner, NY; operating at 100mTorr). The overall microsphere fabrication process is shown below in Figure 7.

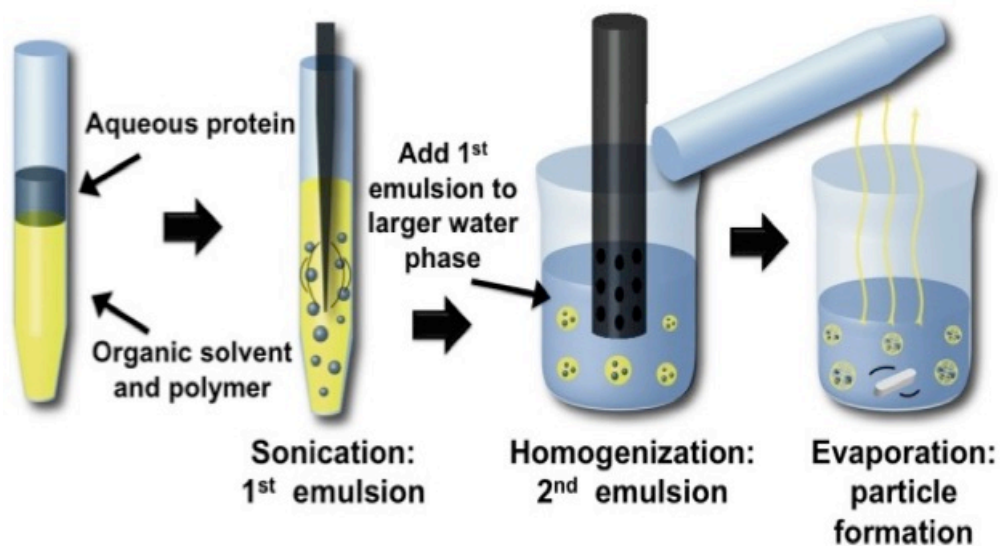


**Figure 7: Fabrication of PLGA microspheres encapsulating aqueous protein.**

### 2.2.2 Microsphere characterization

Surface characterization of microspheres was conducted using scanning electron microscopy (JEOL JSM-6330F, Peabody, MA) and microsphere size distribution was determined by volume impedance measurements on a Beckman Coulter Counter (Multisizer-3, Beckman Coulter, Fullerton, CA). CCL22 release from microspheres was determined by suspending 7-10 mg of microspheres in 1 mL of phosphate buffered saline (PBS) placed on an end-to-end rotator at 37°C. CCL22 release sampling was conducted at various time intervals by centrifuging microspheres and removing the supernatant for CCL22 quantification using ELISA (R&D Systems, Minneapolis, MN), sampling of releasates is shown in Figure 8 Below. Microspheres were re-suspended with 1 mL of fresh PBS and returned to the rotator at 37°C.

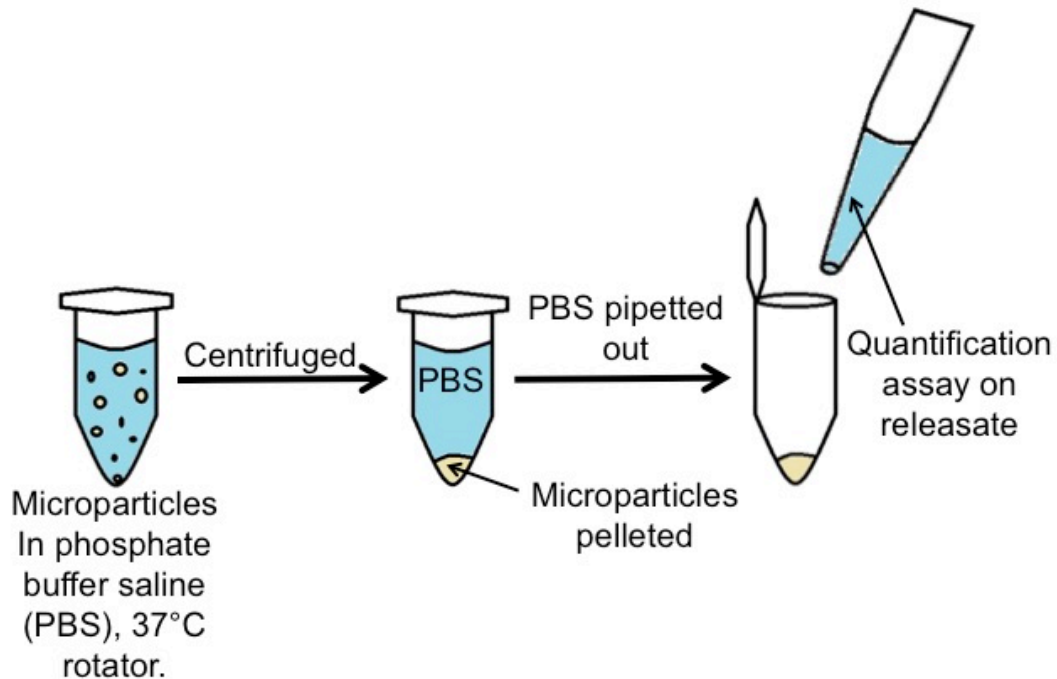


Figure 8: *In vitro* releasate sampling from PLGA microspheres.

### 2.2.3 CCL22 microsphere administration in mice

For mouse investigations microspheres were administered to 4 sites via 2% carboxy methyl cellulose (CMC) in PBS suspension. Specifically, 2-5  $\mu\text{L}$  of solution containing 25 mg/mL of particles were administered to the proximal side of the first molar, each inter-dental site, and distal to the third molar of the right maxilla of the mice, shown in Figure 9 below. Microspheres were injected into maxillary gingiva of mice using 27-28.5 gauged insulin syringes. For C57BL/6JJ mice inoculated with *Actinobacillus actinomycetemcomitans*, microspheres were injected on days -1, 10 and 20 relative to the first bacterial inoculation, shown in Figure 10 below. For BALB/cJ mice inoculated with *Porphyromonas gingivalis*, microspheres were injected on days -1, 20, and 40 relative to the first bacterial inoculation, shown in Figure 11 below. Microspheres were injected in mice at a depth of approximately 100-300 microns within the maxillary gingival tissues. All microsphere injections in mice were performed under a stereomicroscope. Small amounts of the microsphere solution were observed to overflow into the oral cavity of the mice during injections.

# Mouse Maxilla

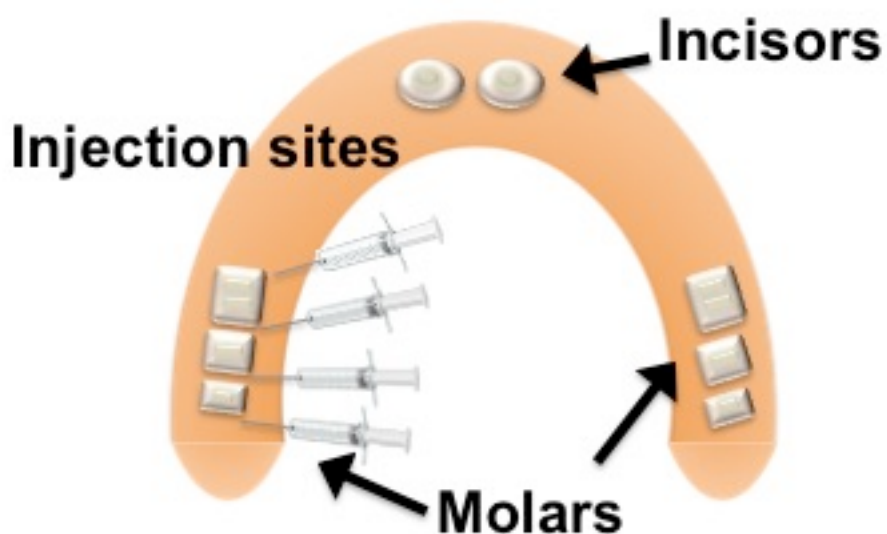


Figure 9: CCL22 microsphere administration route in mice.

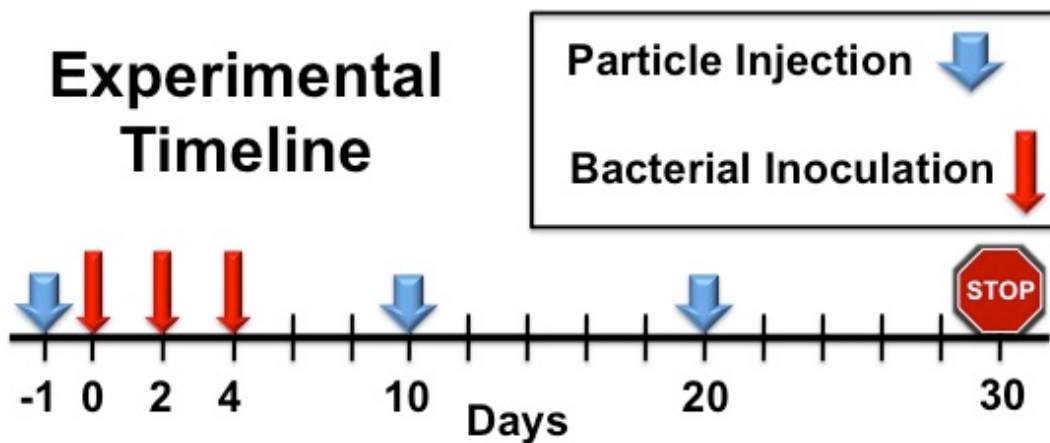


Figure 10: CCL22 microsphere treatment experimental schedule in *Actinobacillus actinomycetemcomitans* infected Black/6 mice.

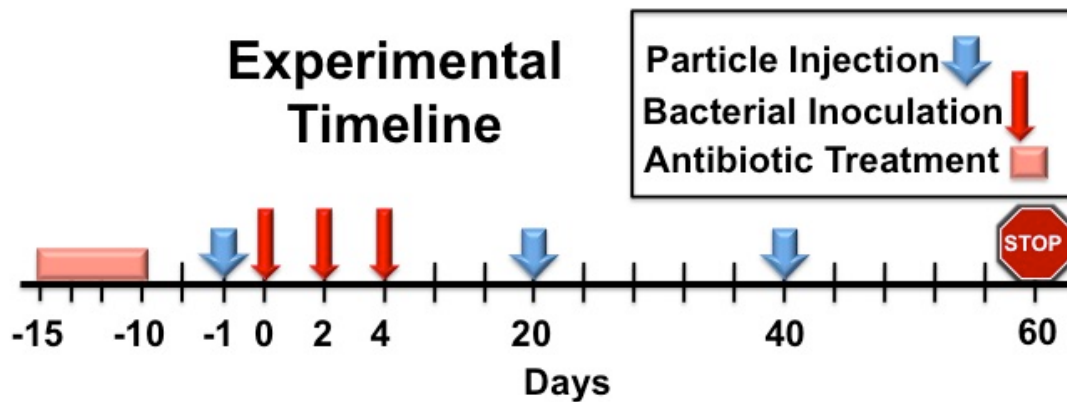


Figure 11: CCL22 microsphere treatment timeline in *Porphyromonas gingivalis* infected BALB/cJ mice.

#### 2.2.4 Periodontal disease induction in mice

The mouse model for periodontitis was conducted as described previously<sup>97, 167</sup>. Briefly, wild type male C57BL/6J mice aged 8-weeks were purchased from Charles River Laboratories International, Inc., (Wilmington, MA) or bred and maintained in the animal facilities of the Department of Biochemistry and Immunology – FMRP/USP. Mice were inoculated with *Actinobacillus actinomycetemcomitans* (ATCC 29522) cultured under anaerobic conditions and suspended in ~100  $\mu$ L of PBS supplemented with 2% carboxymethylcellulose (CMC) at  $1 \times 10^9$  CFU placed in the oral cavity. At 48 hours and 96 hours the inoculation was repeated, as shown in Figure 10. Negative controls received heat-killed-sham bacteria or only PBS supplemented with 2% CMC. All protocols were approved by the local Institutional Animal Care and Use Committees at the University of Pittsburgh and the FMRP/USP.

For experiments using *Porphyromonas gingivalis* as a colonizing periodontopathogen in BALB/cJ mice periodontitis was induced as described<sup>97</sup>. Briefly, male BALB/cJ mice age 6-8

weeks were purchased from Jackson Laboratories. To reduce the commensal oral bacteria, the drinking water of mice was modified with 15 mL/L of Sulfatrim Pediatric Suspension (sulfamethoxazole and trimethoprim, 2 mg/mL wt/vol and 0.4 mg/mL wt/vol, Henry Schein) for 10 days. After 10 days of antibiotic water, the mice were given clean drinking water for 5 days to prevent any direct microbicidal effects of the antibiotic solution on the colonization of the oral pathogen. Mice were then colonized 3 times during the first week at 2 day intervals with *Porphyromonas gingivalis* (*Pg*, ATCC 33277) grown under anaerobic conditions, as shown in Figure 11. Bacteria were plated on brucella blood agar supplemented with hemin and vitamin k1, on days of inoculation, *Pg* was suspended in brain heart infusion (BBL BHI, BD Biosciences, San Jose, CA) supplemented with 2% carboxymethylcellulose at  $1 \times 10^{11}$  CFU. Mice received 0.5 mL of the *Pg* BHI suspension orally administered with gavage feeding needle.

### **2.2.5 Bacteria cultures**

Bacterium, *Actinobacillus actinomycetemcomitans* (ATCC 29522) were cultured under anaerobic conditions. Briefly, *Actinobacillus actinomycetemcomitans* cultures were initiated according to ATCC instructions and plated on brucella blood agar supplemented with hemin and vitamin k1, plates were placed in an anaerobic chamber (Oxoid anaerojar 2.5 L) with an Oxoid anaerogen 2.5 L anaerobic sachet at 37°C. After 1 week of growth, bacteria were isolated with loops from the brucella agar and seeded in 100mL Brain Heart Infusion (BHI) (Becton, Dickson and company, BD) and cultured over night anaerobically (anaerobic jar, Oxoid anaerojar 2.5 L with an Oxoid anaerogen 2.5 L anaerobic sachet) at 37°C. *Actinobacillus actinomycetemcomitans* cultures were isolated from the BHI broth using centrifugation at  $>6000g$ , 10 minutes and washed 2 times with sterile PBS. Finally, *Actinobacillus actinomycetemcomitans* cultures were re-suspended in

Phosphate buffered saline (PBS) supplemented with 2% carboxymethylcellulose (CMC) at  $1 \times 10^9$  CFU.

Bacterium *Porphyromonas gingivalis* (*Pg*, ATCC 33277) were cultured from isolates according to ATCC instructions. Briefly, *Porphyromonas gingivalis* isolates were suspended in tryptic soy broth (TSB) supplemented with hemin, vitamin k1 and L-cystine and cultured anaerobically (anaerobic jar, Oxoid anaerobar 2.5 L with an Oxoid anaerogen 2.5 L anaerobic sachet) at 37°C. After 48 hours *Porphyromonas gingivalis* cultures were isolated from the broth with centrifugation at  $>6000g$ , 10 minutes. Cultures were concentrated with TSB and plated on brucella blood agar supplemented with hemin and vitamin k1 and cultured anaerobically (anaerobic jar, Oxoid anaerobar 2.5 L with an Oxoid anaerogen 2.5 L anaerobic sachet) at 37°C, or glycerol was added to TSB based cultures O.D. 660 ~ 0.6 ABS, and cryopreserved for future use. After 5-7 days *Pg* plated on brucella blood agar supplemented with hemin and vitamin k1 turned black (pigment) and cultures were collected with loop for mouse infection. *Pg* was suspended in brain heart infusion (BBL BHI, BD Biosciences, San Jose, CA) supplemented with 2% carboxymethylcellulose at  $1 \times 10^{11}$  CFU (approximately 1 plate of *Pg* for every 3 mice to be infected).

### **2.2.6 Mouse anti-GITR treatment for Treg inhibition**

Anti-GITR (DTA-1) hybridomas were grown i.p. in mineral oil-injected nude mice as described<sup>167</sup>. Briefly, the antibodies were purified from ascites by precipitation using ammonium sulphate (45%, w/v), and subsequently purified by a G protein column (Amersham Biosciences, Piscataway, NJ, USA), as described previously<sup>167</sup>. A bicinchoninic method was used to quantify protein levels. The in vivo blockage of GITR molecules was performed by i.p. injection of 500 µg/mouse of

purified anti-GITR mAb diluted in phosphate buffered saline (PBS), performed 15 days after bacterial inoculation, Figure 10.

### **2.2.7 Assessment of periodontal disease induced bone loss in mice**

To evaluate the extent of alveolar bone destruction, murine maxillary alveolar bone was quantified as described previously<sup>97, 167</sup>. Briefly, resected maxillae were mechanically defleshed and exposed to dispase or 3% hydrogen peroxide overnight to remove all soft tissue. Palatal and buccal faces of the molars were imaged using dissecting microscopes (Leica, Wetzlar, Germany or Olympus SZX10 with DP72 camera). Digitized images were analyzed using ImageJ (NIH) or ImageTool 2.0 (University of Texas Health Science Center, San Antonio, Texas, USA). The area between the cemento-enamel junction (CEJ) and the alveolar bone crest (ABC) was quantified using arbitrary units of area (AUA) or square micrometers.

### **2.2.8 Assessment of inflammatory cell infiltrate in mice**

Inflammatory cell infiltrate was analyzed from palatal periodontal lesions as described<sup>167</sup>. Whole buccal and palatal tissues of maxillary molars were collected, weighed and incubated in media (RPMI 1640, supplemented with NaHCO<sub>3</sub>, penicillin/streptomycin/gentamycin and 0.28 Wunsch units/mL of liberase blendzyme CI) for 1 hour at 37°C, with the dermal side down. Cell viability was assessed by trypan blue exclusion, and cell count was performed in a Neubauer chamber.

### **2.2.9 mRNA extraction from mouse maxilla**

Total RNA extraction from periodontal tissues was performed using Trizol reagent following the manufacturers instructions (Life Technologies, Rockville, MD, USA) as described previously<sup>167</sup>. Briefly, complementary DNA was synthesized using 3 µg of RNA through a reverse transcription reaction (Superscript III, Invitrogen Corporation, Carlsbad, CA, USA). Real-time polymerase chain reaction quantification of mRNA was performed in a MiniOpticon system (BioRad, Hercules, CA, USA) using SYBR-Green PCR mastermix (Applied Biosystems, Warrington, UK). For mRNA quantification, relative level of gene expression was calculated using β-actin reference expression. The fold change was calculated as  $2^{(-\Delta\Delta CT)} - 1$ . Quantification of *Actinobacillus actinomycetemcomitans* in the palatal tissues was performed as previously described<sup>94</sup>.

### **2.2.10 DNA extraction from mouse maxilla**

Briefly, DNA was extracted from tissues using a DNA purification system (Promega Biosciences Inc., San Luis Obispo, CA, USA) and quantified using a MiniOpticon system, then normalized to tissue weight.

### **2.2.11 Extraction of gingiva proteins from mice**

Measurement of proteins and cytokines from the periodontal tissues were performed as described previously<sup>167</sup>. Briefly, protein was extracted from the palatal gingival after tissue homogenization in PBS. Samples were then centrifuged (100 G) and the supernatants were stored for testing (-70°C). The concentrations of cytokines IL-10, TGF-β, TNF, CTLA-4, RANKL were determined

by ELISA kits (R&D Systems, Minneapolis, MN, USA) and carried out according to manufacturers instructions.

### **2.2.12 Histological sectioning and immunohistochemical staining of mouse maxilla**

Histological analysis of mouse periodontal tissues after *Porphyromonas gingivalis* infection were performed as follows. All samples from *Pg* infected mouse model were fixed in 10% formalin, and embedded in paraffin. Sections were made at 6  $\mu\text{m}$  thickness, and stained with hematoxylin and eosin. FOXP3 positive cells were identified by immunohistochemistry using primary antibody against mouse FOXP3 (14-5773, eBiosciences, San Diego, CA), and SuperPicture™ 3rd Gen IHC Detection Kit (Life Technologies, Grand Island, NY). Brightfield images were taken under microscope (Nikon eclipse TE2000-E: Nikon Instruments, Melville, NY).

### **2.2.13 Statistical analyses**

All data was confirmed to portray a normal distribution (determined by Shapiro-Wilk test) and further analyzed using one-way ANOVA followed by Bonferroni's or Tukey-HSD *post-hoc* test to compare differences between multiple groups. Student's unpaired *t* test was used for all other statistical analyses. Differences were considered significant when  $P < 0.05$ . Statistics were performed using GraphPad Prism or JMP Pro 10 software.

## 2.3 RESULTS

The hypothesis of this study is that biodegradable, controlled release formulation of CCL22 administered locally in the periodontium of mice, may recruit Tregs, and effectively abrogate periodontal disease symptoms. The first step to test this hypothesis was the fabrication and characterization of poly(lactic-co-glycolic) acid (PLGA) microspheres capable of releasing recombinant mouse CCL22.

### 2.3.1 Characterization of rmCCL22 PLGA microspheres

The initial goal of the project was to develop recombinant mouse CCL22 releasing microspheres that portrayed ideal release kinetics for use in the mouse model of periodontal disease. First, the fabrication of recombinant mouse CCL22 releasing poly(lactic-co-glycolic) acid (PLGA) was done using acetyl end capped polymers with 50:50 ratios of lactic acid to glycolic acid residues in three different lengths of PLGAs. Figure 12, below, shows the surface morphology of the three different non-porous, acetyl end capped CCL22 PLGA microspheres using scanning electron microscopy. All three CCL22 microsphere formulations exhibited similar surface morphology, however, the 4.2 kDa PLGA CCL22 microspheres appeared to show a slight increase in surface porosity, Figure 12. The slight increase in porosity of the 4.2 kDa may be attributed to a combination of the smaller polymer chain and the possibility of undesired contaminants as the 4.2 kDa was purchased from a different manufacturer than the other two polymers. Overall, all CCL22 microspheres exhibited similar surface characteristics as seen under scanning electron microscopy, Figure 12.

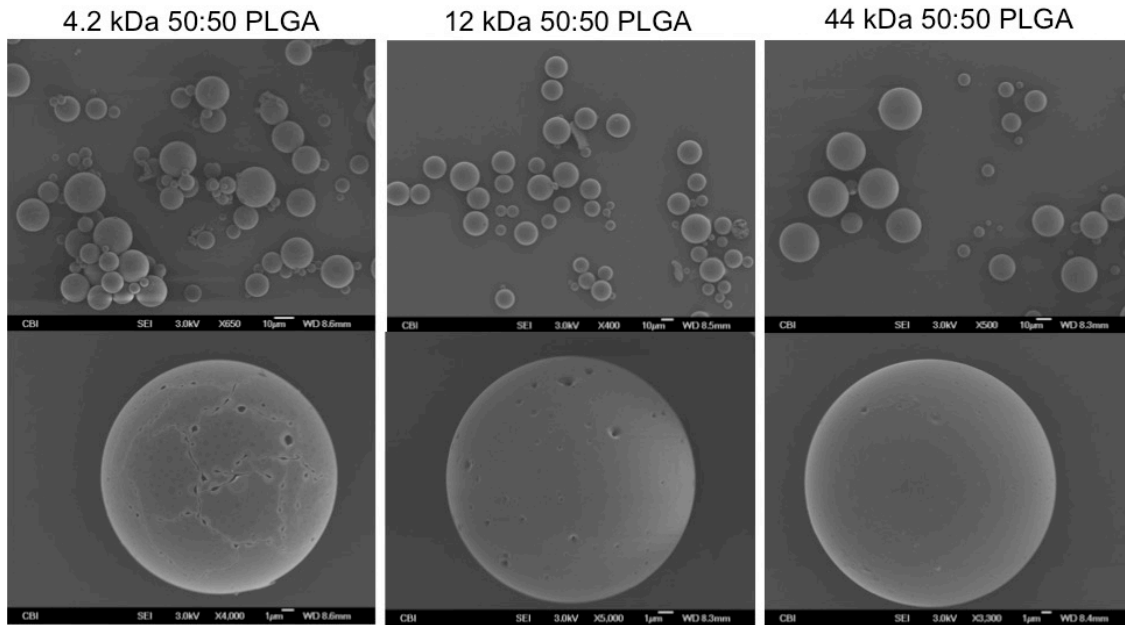


**Figure 12: Surface morphology of non-porous rmCCL22 microspheres (scanning electron micrographs).**

To ensure that three recombinant mouse CCL22 microspheres exhibited similar average particle diameters, volume average size distributions of each PLGA microsphere formulation were investigated. All three microspheres were fabricated using the same exact fabrication parameters, (described in methods section 2.2.1) namely: 200 mg of PLGA (4.2, 12 or 44 kDa 50:50 PLGA), dissolved in 4 mL of dichloromethane, loaded with 5 µg of rmCCL22 dissolved in 200 µL of DI water, inner emulsion sonication at 25% power-10 seconds, second emulsion homogenization at 3000 rpm in 60 mL of 2% poly(vinyl) alcohol (PVA) DI water – 60 seconds, and dichloromethane evaporation in 80 mL of 1% PVA for 3 hours stirred at 600 rpm. Particle diameter is most influenced by the ratio of dichloromethane to water in the second emulsion and the overall homogenization speed. Ultimately, it was important for the recombinant mouse CCL22 microspheres to exhibit average diameters greater than 10 microns to prevent phagocytic removal upon injection into tissue<sup>170</sup>. All three rmCCL22 microspheres exhibited average particle

diameters greater than 10 microns, Figure 13 below. Accordingly, all rmCCL22 microspheres exhibited similar volume average size distributions (determined by size impedance Coulter-counter), Figure 13. Indeed, the average diameter of microspheres composed of 4.2 kDa PLGA, 13.5 microns, was slightly smaller than the average diameter of microspheres composed of 12 kDa PLGA, 19.5 microns, which was slightly smaller than the average diameter of microspheres composed of 44 kDa, 21.4 microns. The slight observed difference in microsphere diameter may be attributed to the inherent viscosity of each polymer, where polymers composed of shorter chains exhibit a lower inherent viscosity, ultimately allowing them to form slightly smaller, stable, droplets during the double emulsion fabrication process under the same power input (i.e. homogenization) for the emulsion process, Figure 7.

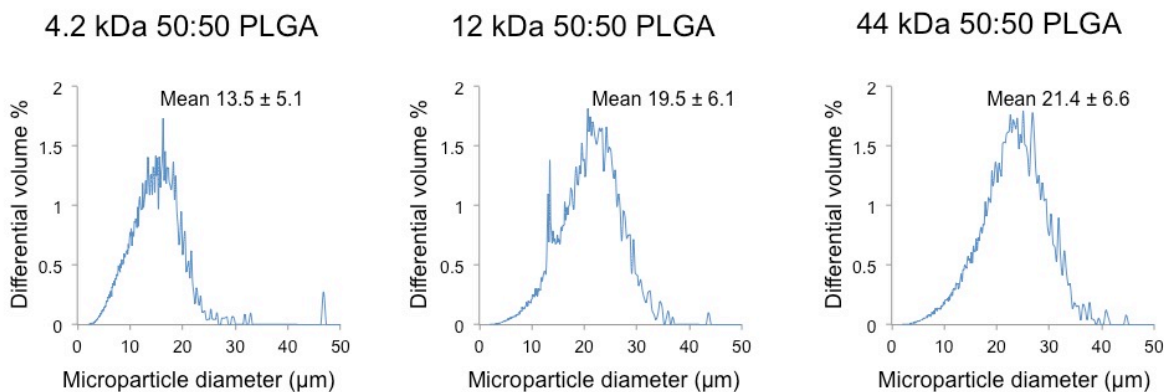


**Figure 13: Volume average size distributions for rmCCL22 microspheres.**

To further characterize recombinant mouse CCL22 microspheres composed of PLGAs of varying size (4.2 kDa, 12 kDa and 44 kDa), *in vitro* release of CCL22 from the microspheres was assessed. *In vitro* release kinetics were observed by sampling rmCCL22 from releasates collected over a period of near 80 days, Figure 14. All three rmCCL22 PLGA microsphere formulations displayed similar initial burst magnitudes and duration, roughly 0.5 ng of CCL22 per mg of PLGA

microspheres over the course of days 0-7, Figure 14. As expected, the rmCCL22 microspheres composed of 44 kDa PLGA exhibited the lowest amount of initial burst, which is typical behavior for microspheres composed of PLGA with longer average polymer chain length<sup>171</sup>. The secondary burst phase of all three microspheres appeared to occur around day 40 of *in vitro* release, Figure 14. Unexpectedly, the rmCCL22 PLGA microspheres composed of 4.2 kDa polymer displayed extended release similar to the 12 kDa and 44 kDa polymers, even though they were expected to release a much more accelerated rate if no microsphere-protein interactions are taken into account. It was believed that the delayed release (delayed secondary burst) from all three microspheres was a result of positively charged CCL22 (isoelectric point of 9.46) interacting with the negatively charged polymer through ionic interactions. Indeed, protein or peptide charge significantly retarded the release of such positively charged proteins and peptides from PLGA microspheres, (published and discussed<sup>172</sup>). Ultimately, all three rmCCL22 PLGA microspheres cumulatively released approximately 3-5 ng of rmCCL22 per mg of PLGA microspheres over the 80 day period of investigation, Figure 14.

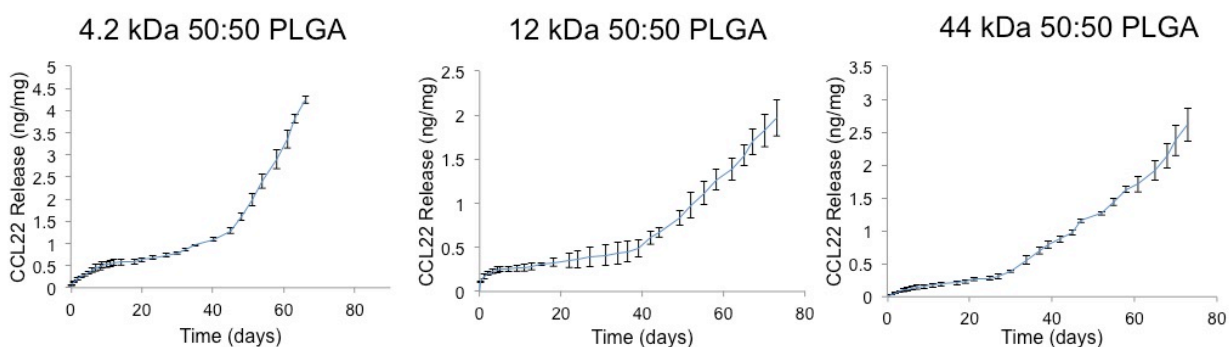


**Figure 14: *In vitro* cumulative release of recombinant mouse CCL22 from non-porous PLGA microspheres.**

In attempt to fabricate a recombinant mouse CCL22 PLGA microsphere formulation capable of sustaining near linear release over (maintaining a constant concentration of CCL22 at the site of microsphere injection) this study hypothesized that mixing rmCCL22 microspheres composed of 4.2 kDa, 12 kDa and 44 kDa polymer may lead to extended linear release by incorporating characteristics of each polymer microsphere. Utilizing a recently developed mathematical model<sup>77, 133, 134, 168</sup>, a recipe was formulated for mixing the three non-porous recombinant mouse CCL22 PLGA microspheres to create one extended release formulation. Model aided predictions suggest that we mix 33.6% of the 4.2 kDa microspheres, 27.9% of the 12 kDa microspheres and 38.5% of the 44 kDa microspheres to create a mixture capable of sustaining linear release over a period of roughly 80 days, Figure 15 A. As expected, mixing the three microsphere formulations achieved a volume average size distribution in the middle of the range of the three individual formulations, with an average diameter of 15.4 microns, Figure 15 B, compared to Figure 12 above. Furthermore, recombinant mouse CCL22 cumulative *in vitro* release from the mixed microsphere formulation exhibited characteristics of all three release profiles of the single microsphere formulations alone, Figure 15 C compared to Figure 14 above. Interestingly, while each microsphere formulation alone portrayed a significant lag phase of between days 7 and 40, Figure 14 above, when combined at model determined ratios the microsphere formulation exhibited very little lag and near constant release of CCL22 over nearly 80 days, Figure 15 C. Ultimately, it was demonstrated that it was possible to formulate a PLGA microsphere system capable of delivering constant release of recombinant mouse CCL22 over a period of 80 days Figure 15.

## Combination of CCL22 releasing microparticles for sustained linear release

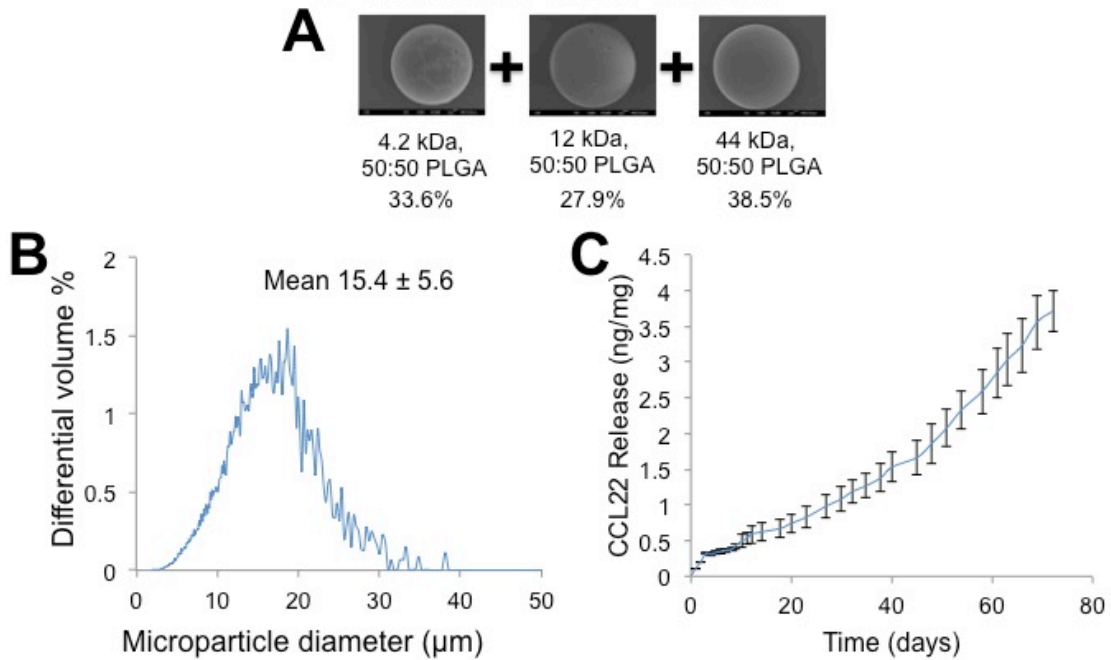


**Figure 15: Combination of non-porous rmCCL22 PLGA microsphere formulations for long-lasting constant release.**

The ultimate goal was to fabricate recombinant mouse CCL22 PLGA microspheres capable of releasing over a physiological relevant timeframe for our mouse model of periodontitis. Therefore, prior to conducting *in vivo* murine periodontal disease studies, the CCL22 controlled release formulation was further optimized. Specifically, to achieve faster complete release of CCL22 that would correspond to the more accelerated (less than 80 days) treatment schedule typically used in the mouse model for periodontal disease<sup>167</sup> CCL22 microspheres were reformulated. To achieve the desired accelerated release of rmCCL22, PLGA microspheres were fabricated with polymer composed of carboxylic acid end-capped, porous, 12 kDa PLGA, Figure 16. To achieve surface porosity, 15 mmol NaCl was incorporated into the first emulsion during microsphere fabrication (15 mmol NaCl + rmCCL22 in DI water for the inner aqueous phase).

Indeed, the surface morphology of the microspheres with the incorporated porogen exhibited significantly more pores than the 12 kDa PLGA microspheres composed without the porogen, Figure 16. Next, it was observed that the carboxylic acid end-capped PLGA microspheres degraded faster than acetyl end-capped, overall accelerating the release of encapsulated agents<sup>172</sup>, therefore the *in vitro* release kinetics of porous, 12 kDa acid end capped rmCCL22 microspheres were investigated.

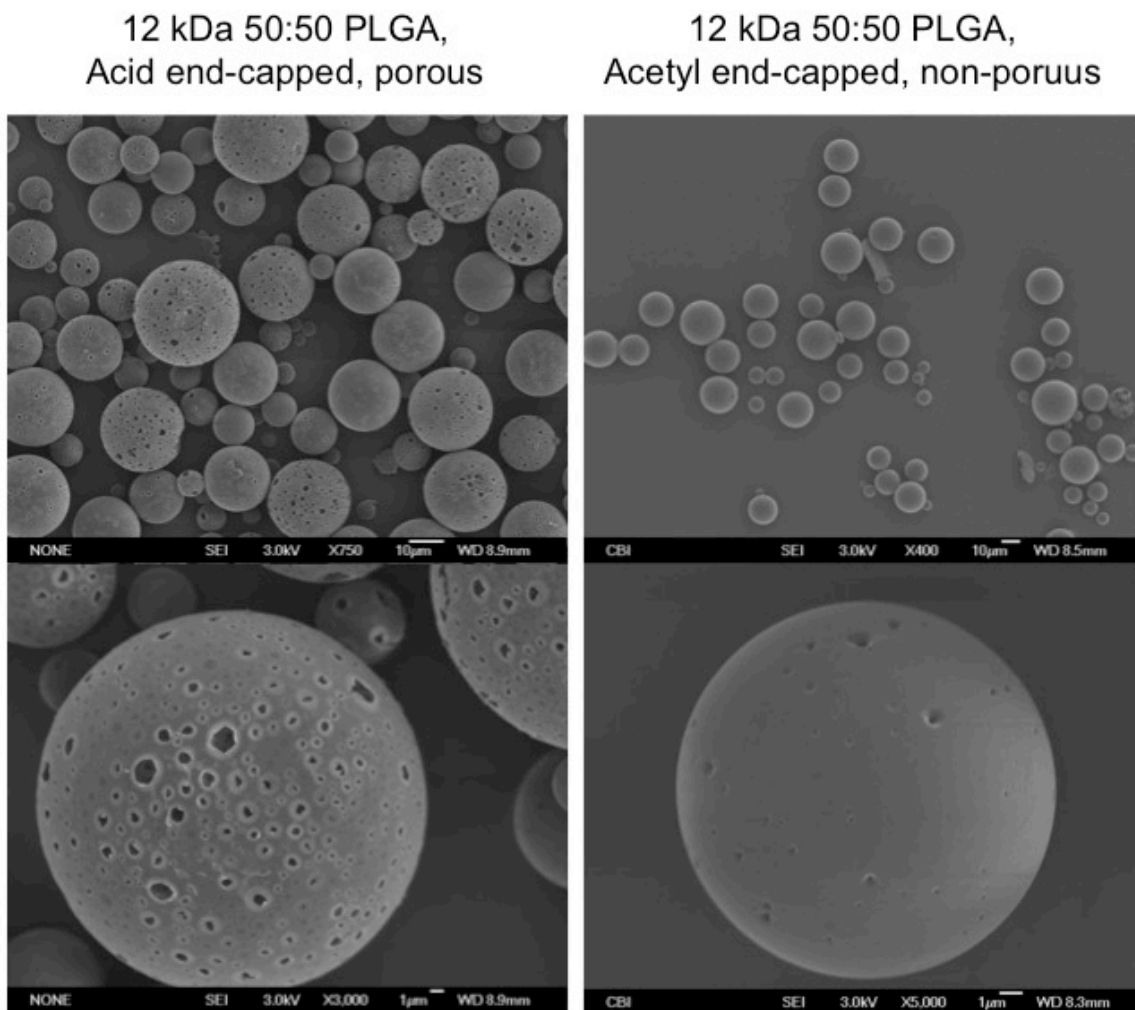


**Figure 16: Comparison of porous, rmCCL22 PLGA microspheres and non-porous rm CCL22 PLGA microspheres.**

Adding porosity by incorporating 15 mmol NaCl into the first emulsion (inner aqueous phase) along with the encapsulated rmCCL22 further helped to accelerate the *in vitro* release of CCL22 from the microspheres to conform to a time-scale more appropriate for *in vivo* therapeutic exploration in the mouse model for periodontal disease, Figure 17 B. A side effect adding a porogen to the rmCCL22 PLGA microspheres is a slight increase in the volume average size distribution, determined by volume impedance, Figure 17 A. Indeed, microspheres fabricated with the NaCl porogen exhibited an average diameter of 20.82 microns, Figure 17 A, compared to the non-porous microspheres that exhibited an average diameter of 19.5 microns, Figure 13 above. Ultimately, rmCCL22 microspheres composed of porous, 12 kDa acid end-capped PLGA, released the entire CCL22 payload in approximately 30 days, significantly faster than the *in vitro* release of CCL22 from non-porous microspheres composed of PLGA with the same molecular weight, Figure 17 B. The porous, acid end-capped rmCCL22 microspheres were chosen for therapeutic investigations in the mouse model for periodontal disease described below.

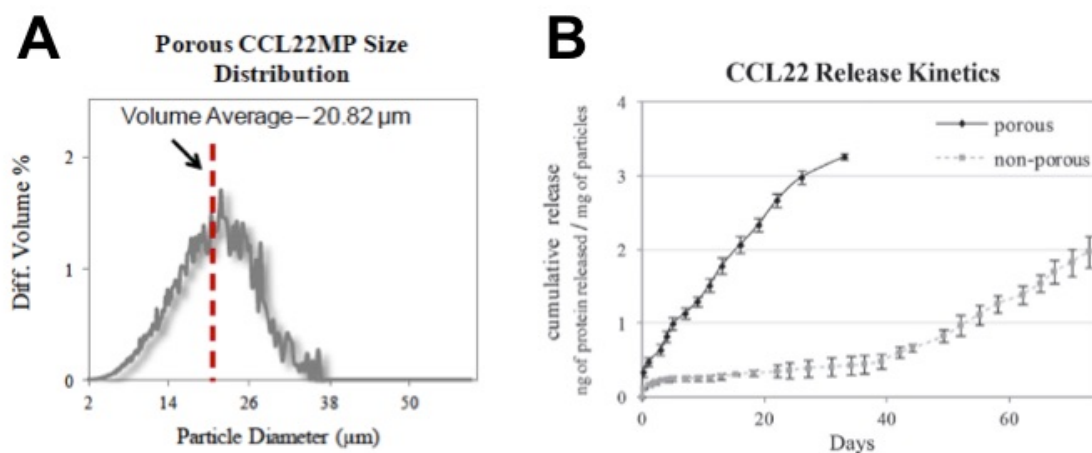


Figure 17: Characterization of porous rmCCL22 microspheres, microsphere size distribution and cumulative *in vitro* release<sup>46</sup>.

### **2.3.2 CCL22 microspheres significantly reduce alveolar bone resorption in mice models for periodontitis**

First, the ability of the Treg-recruiting formulation, porous recombinant mouse CCL22 microspheres<sup>46</sup> to reduce alveolar bone resorption in the periodontium of an experimental mouse model of periodontal disease were tested. It was observed that mice receiving CCL22 releasing microspheres injected into the gingiva (day -1, prior to infection, and days 10 and 20 post infection, based on previous observations that a single treatment was effective in mice for at least 10 days<sup>46</sup>) exhibited less alveolar bone resorption Figure 18 A, as indicated by area quantification measurements between the cemento-enamel junction (CEJ) and the alveolar bone crest (ABC) Figure 18 B. Ultimately, CCL22 microspheres prevented significant alveolar bone resorption in the *Actinobacillus actinomycetemcomitans* induced C57 black/6 mouse model for periodontal disease. However, different bacterial strains are considered to be more prevalent than others based on population demographics<sup>173-175</sup>, and interestingly, different mouse strains appear to have different susceptibilities for alveolar bone loss and infection of periodontal pathogens<sup>169</sup>. Therefore, the ability of CCL22 microspheres to prevent alveolar bone resorption the BALB/cJ mouse model using periodontal disease pathogen *Porphyromonas gingivalis* was also tested.

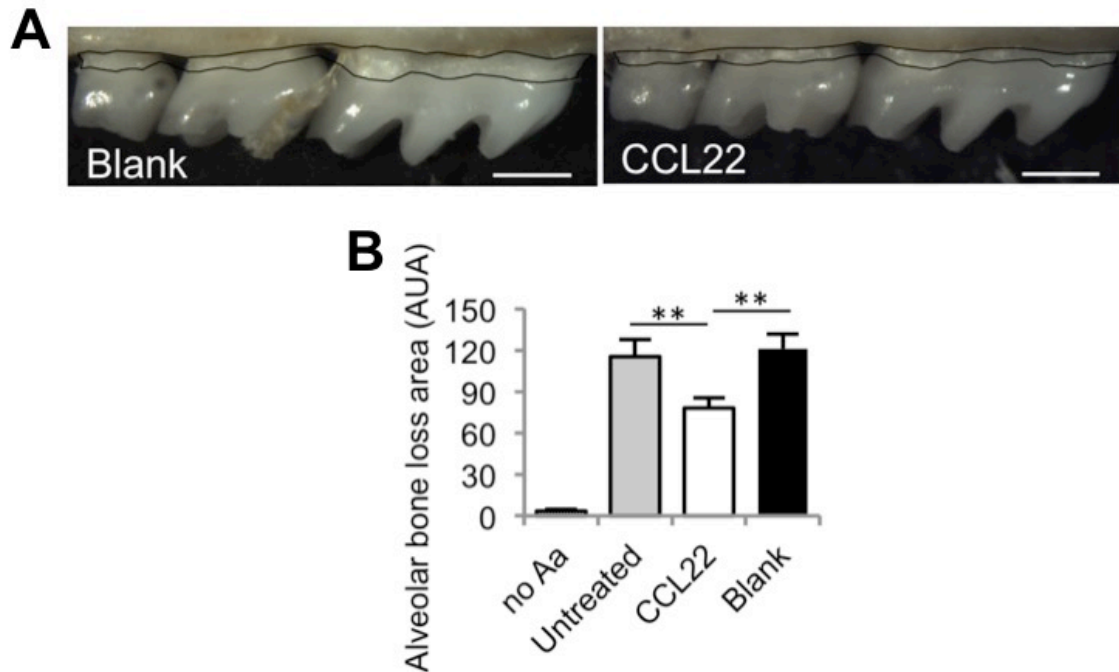


Figure 18: CCL22 microspheres prevent alveolar bone loss in *Actinobacillus actinomycetemcomitans* infected C57 black/6 mice<sup>45</sup>. (A) Representative stereoscope images of defleshed maxilla from C57BL/6J mice infected with *Actinobacillus actinomycetemcomitans* (Aa) 30 days after inoculation. Results of treatment with blank (unloaded) PLGA microspheres (top), and CCL22 microspheres (bottom), injected into maxillary gingiva on days -1, 10 and 20 relative to the first Aa inoculation, scale bar 0.5 mm. (B) Area measurement between the cemento enamel junction (CEJ) and alveolar bone crest (ABC) on the buccal root surface, untreated mice were infected but did not receive microspheres, no Aa served as uninfected controls. N = 5-8 mice. \*\*P < 0.05 determined by One-Way ANOVA followed by Bonferroni's multiple comparisons test, untreated, CCL22 and Blank groups were statistically different from no Aa infection.

To confirm the results that suggest rmCCL22 PLGA microspheres prevent alveolar bone loss (the primary outcome of murine periodontitis) in mice, the ability of CCL22 microspheres to prevent alveolar bone loss in *Porphyromonas gingivalis* infected BALB/cJ mice, Figure 19, was also tested. Indeed, it was observed that mice receiving CCL22 releasing microspheres injected into the gingiva (day -1, prior to infection, and days 20 and 40 post infection) exhibited less

alveolar bone resorption Figure 19 A, as indicated by area quantification measurements between the cementoenamel junction (CEJ) and the alveolar bone crest (ABC) Figure 19 B. Taken together, the results suggest that CCL22 microspheres significantly inhibit alveolar bone loss in both mouse models for periodontal disease.

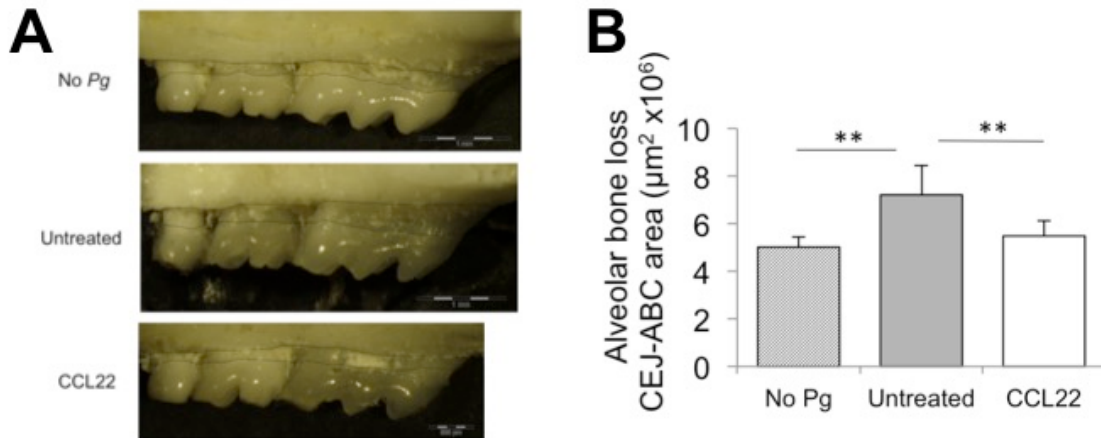


Figure 19: CCL22 microspheres prevent alveolar bone resorption in *Porphyromonas gingivalis* experimental BALB/cJ mouse model. BALB/cJ mice colonized with *Porphyromonas gingivalis* treated with CCL22 microspheres injected in the maxillary gingiva at days -1, 20, 40 showed significant reduction in alveolar bone loss and increased presence of regulatory T cells in the periodontium 60 days after initial colonization. Uninfected mice (no *Pg*) and infected Untreated mice served as controls for CCL22 microsphere treated mice, (CCL22). (A) Representative microscope images of defleshed maxilla, scale bar for CCL22 0.5mm, scale bar for Untreated and no *Pg* 1mm. (B) Quantification of alveolar bone resorption represented by the area between the cementoenamel junction (CEJ) and alveolar bone crest (ABC) in square microns. \*\* P<0.05 determined by ANOVA followed by Tukey HSD post hoc multiple comparison test<sup>45</sup>.

### **2.3.3 CCL22 microspheres reduce the inflammatory infiltrate in mice, without altering bacterial levels**

Using the *Actinobacillus actinomycetemcomitans* induced C57 black/6 mouse model, mice receiving CCL22 microspheres displayed a significant decrease in the total number of inflammatory cells within in the periodontium, Figure 20 A, suggesting these mice had a significant reduction in damaging inflammation. Furthermore, CCL22 microsphere administration did not appear to affect the levels of periodontopathogen *Actinobacillus actinomycetemcomitans* within in the resected gingival tissue of the mice, Figure 20 B. Additionally, overall oral bacterial levels were not significantly altered by CCL22 microsphere treatment, measured by detecting 16s bacterial ribosomal DNA in the resected gingiva of mice, Figure 20 C. In attempt to observe if CCL22 microspheres had any systemic affect on circulating inflammatory mediators, mouse serum was collect and analyzed immediately post-mortem for levels of C-reactive protein (CRP), Figure 20 D. CCL22 microspheres did not appear to have any effect on the serum levels of CRP in mice, Figure 20 D. Taken together, this data suggests that although the invasive bacteria reside within the gingiva of the mice, tissue destruction is mitigated by the treatment of CCL22 microspheres, possibly by regulation of the host immune response.

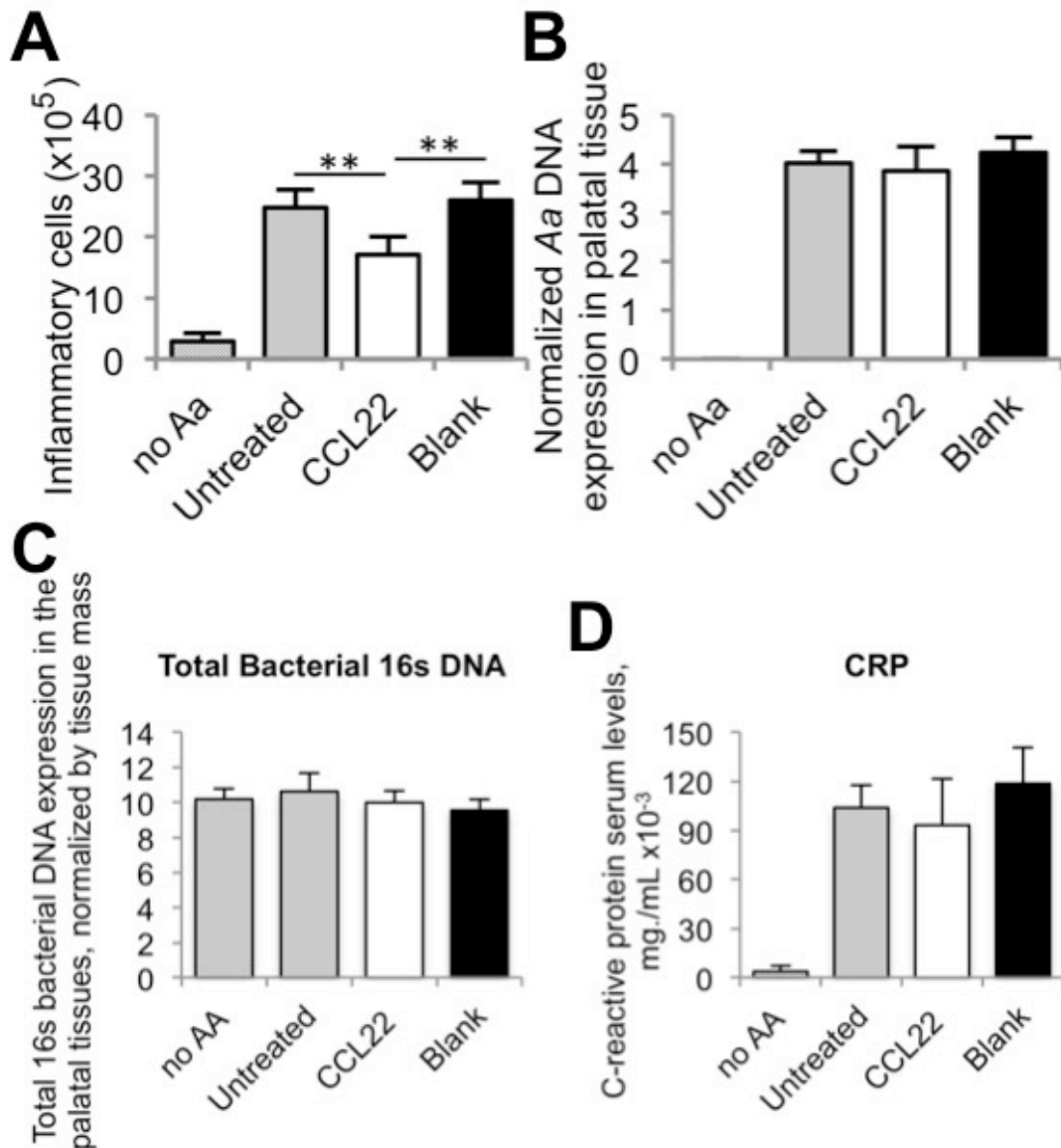


Figure 20: CCL22 microsphere treatment led to a reduction in total inflammatory cells in the mouse gingiva, without affecting the levels of *Actinobacillus actinomycetemcomitans* bacteria found within the periodontium. (A) Inflammatory cell counts in the periodontal tissue following treatments (B) the PCR expression of Aa-specific bacterial 16s ribosomal DNA in the periodontal tissue normalized by palatal tissue weight following treatment, taken from C57BL/6J mice infected with *Actinobacillus actinomycetemcomitans* (Aa) 30 days after inoculation. N = 5-8 mice. (C) Overall bacterial counts were quantified by measuring the 16s ribosomal DNA in the periodontal tissue of mice 30 days after initial inoculation, normalized by palatal tissue weight. No statistical differences were detected among the groups. (D) Serum collected post-mortem 30 days

after *Aa* colonization was analyzed for inflammatory marker C-reactive protein. Untreated, CCL22 and Blank treated mice had statistically higher levels of serum CRP than no *Aa* uninfected controls. No differences were detectable among the infected animals.  $^{***}P < 0.05$  determined by One-Way ANOVA followed by Bonferroni's multiple comparisons test, untreated, CCL22 and Blank groups were statistically different from no *Aa* infection<sup>45</sup>.

### **2.3.4 CCL22 microspheres recruit regulatory T cells to the periodontium of mice, gingival mRNA expression and protein quantification**

This study hypothesized that the observed reduction in alveolar bone loss was a result of an increased presence of Treg in the periodontium. To test this hypothesis, expression of canonical Treg markers and associated molecules (mRNA expression) were measured within the palatal gingival tissues 30 days after disease induction. Mice receiving the CCL22-releasing formulation expressed significantly higher mRNA levels of the hallmark Treg markers, *Foxp3*, *Il10* and transforming growth factor  $\beta$  (*Tgfb*) and cytotoxic T Lymphocyte Antigen 4 (*Ctla4*), Figure 21 A, when compared to untreated or blank (vehicle only) controls. Quantification of IL-10, CTLA-4 and TGF- $\beta$  protein levels, extracted from gingival tissue, confirmed the mRNA trends, showing that mice receiving the CCL22-releasing formulation produced higher levels of the anti-inflammatory proteins when compared to the untreated and blank controls Figure 21 B. Notably, the experimental administration of microspheres had no significant effect on T helper type 2 (Th2) associated marker interleukin 4 (*Il4*) expression or endogenous *Ccl22* production within the periodontium Figure 21 A, suggesting that the local release of CCL22 primarily affected the presence of Tregs as opposed to Th2 cells. Although many activated T-cells will express some level of CCR4 (the receptor for CCL22), it has been previously shown that CCR4 expression in

Tregs is significantly higher level than other T cell subsets<sup>43</sup>, possibly accounting for the preferential recruitment of Tregs seen here and in our prior studies<sup>46</sup>.

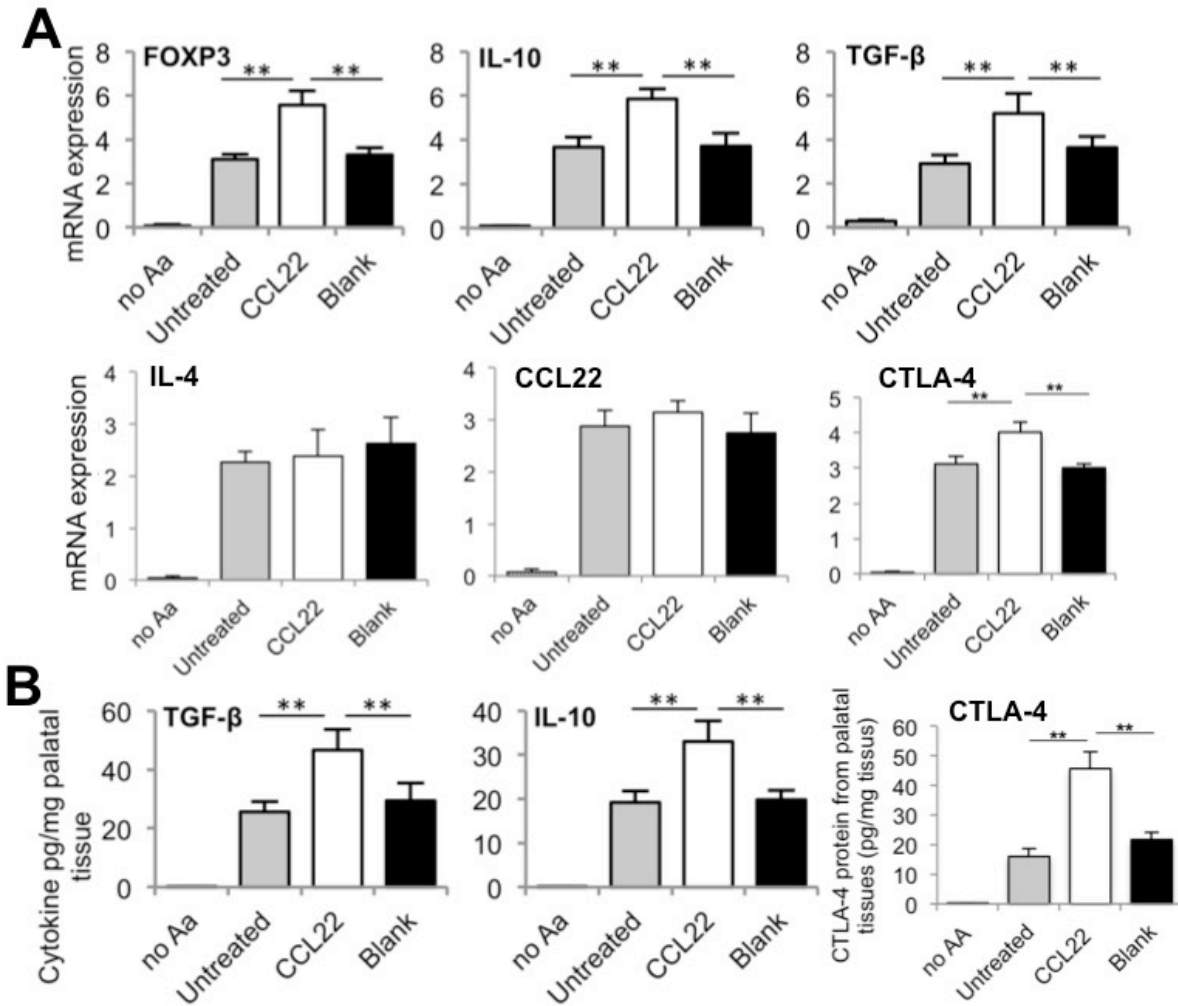


**Figure 21: CCL22 microspheres recruited regulatory T cells (Tregs) to the periodontium of mice. Periodontal tissues were resected from C57BL/6J mice infected with *Actinobacillus actinomycetemcomitans* (*Aa*) 30 days after inoculation, microspheres were injected into maxillary gingiva on days -1, 10 and 20 relative to the first *Aa* inoculation. CCL22 microsphere treated mice, blank (unloaded) microsphere and untreated mice served as infected experimental and control groups, uninfected no *Aa* mice served as positive controls. (A) mRNA expression of *Foxp3*, *Il10*, *Tgfb*, *Il4*, *Ccl22* and *Ctla4* in periodontal tissue as measured by quantitative PCR. The mRNA expression levels were compared by the value of  $2^{-(\Delta Ct)} - 1$ , as compared to  $\beta$ -actin reference.**

**(B) IL-10, TGF- $\beta$ , and CTLA-4 protein levels in periodontal tissues as determined by ELISA from digested periodontal tissues of mice. N = 5 mice. \*\*P < 0.05 determined by One-Way ANOVA followed by Bonferroni's multiple comparisons test, untreated, CCL22 and Blank groups were statistically different from no Aa<sup>45</sup>.**

### **2.3.5 Histological assessment of Tregs presence and reduced osteoclast in the periodontium of mice treated with CCL22 microspheres**

CCL22 microsphere treatments led to observable FOXP3<sup>+</sup> cell (regulatory T cells, Tregs) presence in the periodontium of mice as revealed by immunohistochemistry analysis whereas controls produced no such observable staining Figure 22. Figure 22 A and B show hematoxylin and eosin (H&E) staining of mouse maxilla, Figure 22 C highlights FOXP3<sup>+</sup> Tregs in the periodontium of mice. Importantly, there was no observation of residual PLGA microspheres (or remnants of particles) in the histological sections 20 days after the last microsphere injection (Figure 22), which is to be expected given the relatively low molecular weight distribution of polymer used (12 kDa) and microspheres likely completely degraded, as it has been shown that PLGA microspheres degrade faster *in vivo* than *in vitro*<sup>176</sup>.

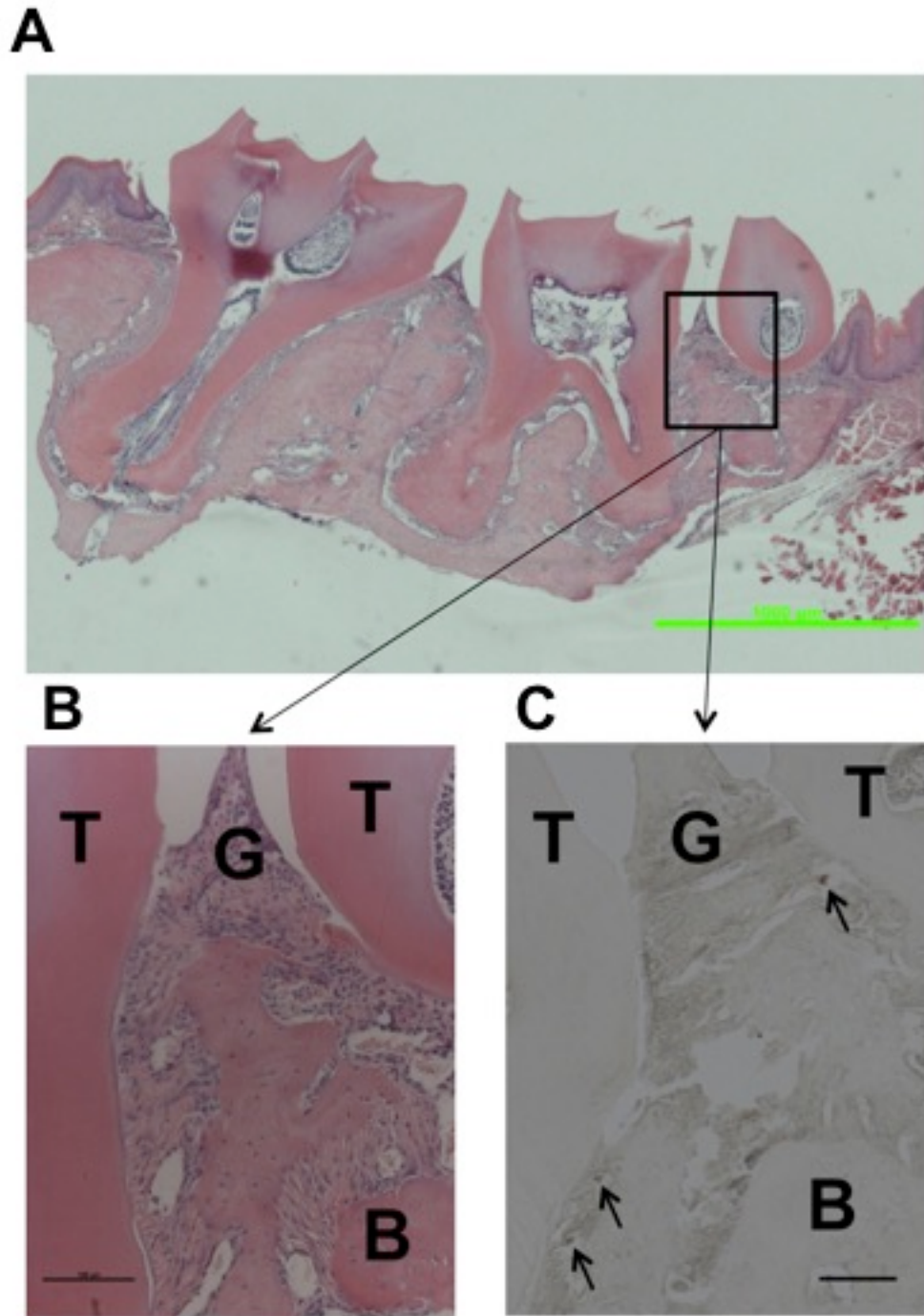
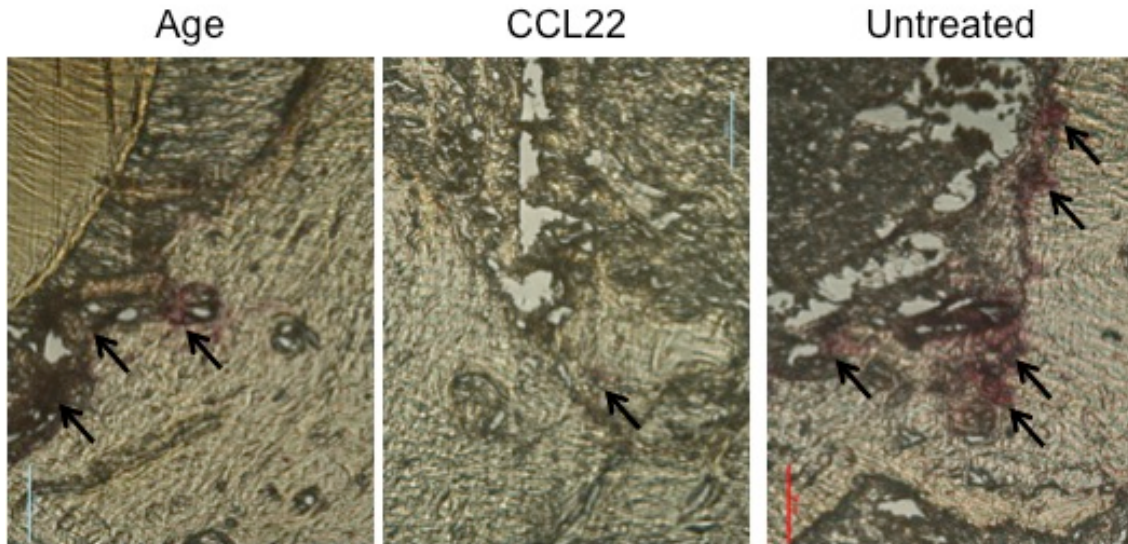


Figure 22: Histological evidence of Treg recruitment to CCL22 microspheres in mice. BALB/cJ mice colonized with *Porphyromonas gingivalis* treated with CCL22 microspheres injected in the maxillary gingiva at days -1, 20, 40 showed significant reduction in alveolar bone loss and increased presence of regulatory T cells in the periodontium 60 days after initial colonization. Uninfected mice (no *Pg*) and infected Untreated mice

served as controls for CCL22 microsphere treated mice, (CCL22). (A-B) Representative immunohistochemistry images of CCL22 microsphere treated mouse maxilla. Sections were stained with H&E (A-B), and immunohistochemistry was performed with anti-mouse FOXP3 antibody (C). FOXP3 positive cells were observed in periodontal tissue (arrows), FOXP3+ cells were only detectable in sections from CCL22 treated mice. Scale bar = A: 1,000 $\mu$ m, B, C: 100 $\mu$ m. *T*: tooth, *G*: gingiva, and *B*: alveolar bone<sup>45</sup>.

Aside from histological evidence of Treg migration to mice treated with CCL22 microspheres, the periodontium histological slices were analyzed for osteoclast (bone resorbing cells) activity. Utilizing a tartrate-resistant acid phosphatase (TRAP) stain, Figure 23 (Red-pink stain), to identify *in situ* osteoclast activity, we observed marked decrease in all sections stained from mice that received CCL22 microspheres compared to untreated, but *Porphyromonas gingivalis* infected mice, Figure 23. Osteoclasts are potent bone resorbing cells that can be induced in bone tissues under inflammatory conditions and show high activity during periodontitis<sup>99, 120, 121</sup>. Decreased osteoclast activity (supported by the decreased TRAP staining) supports the evidence showing CCL22 microsphere treated mice displayed reduced alveolar bone resorption.



**Figure 23: Histological TRAP staining, CCL22 microsphere treated mice show reduced expression of osteoclast (TRAP) activity. BALB/cJ mice colonized with *Porphyromonas gingivalis* treated with CCL22 microspheres injected in the maxillary gingiva at days -1, 20, 40 showed significant reduction TRAP staining. Representative images from age match controlled mice, CCL22 microsphere treated mice and untreated , infected mice, Scale bar (red), 50  $\mu$ m.**

### **2.3.6 Anti-GITR inhibition of Tregs reverses the therapeutic effect of CCL22 microsphere treatments**

To confirm that Tregs are indeed responsible for the decreased disease symptoms and anti-inflammatory cytokine expression, endogenous Tregs were systemically inhibited using anti-glucocorticoid-induced tumor necrosis factor receptor (anti-GITR) antibodies during the onset of periodontitis in *Actinobacillus actinomycetemcomitans* infected mice. Anti-GITR monoclonal antibodies bind to the GITR receptor (which is highly expressed on the surface of Tregs) resulting in reduced Treg functionality in mice<sup>167, 177</sup>. Indeed, administration of anti-GITR antibodies along

with the application of CCL22 releasing microspheres resulted in dramatically increased levels of alveolar bone destruction and a corresponding statistical increase of inflammatory cells into the periodontal tissues 30 days after disease initiation, Figure 24 A, B. Furthermore, Treg impaired mice exhibited a marked decrease in the protein levels of anti-inflammatory cytokines IL-10 and TGF- $\beta$  found in the periodontal tissues after CCL22 microsphere administration compared to mice with unaltered Treg populations, Figure 24 C. Strikingly, Treg inhibition using anti-GITR appears to result in complete reversal (and more so, exacerbated disease symptoms) of the beneficial effects seen with CCL22 microspheres.

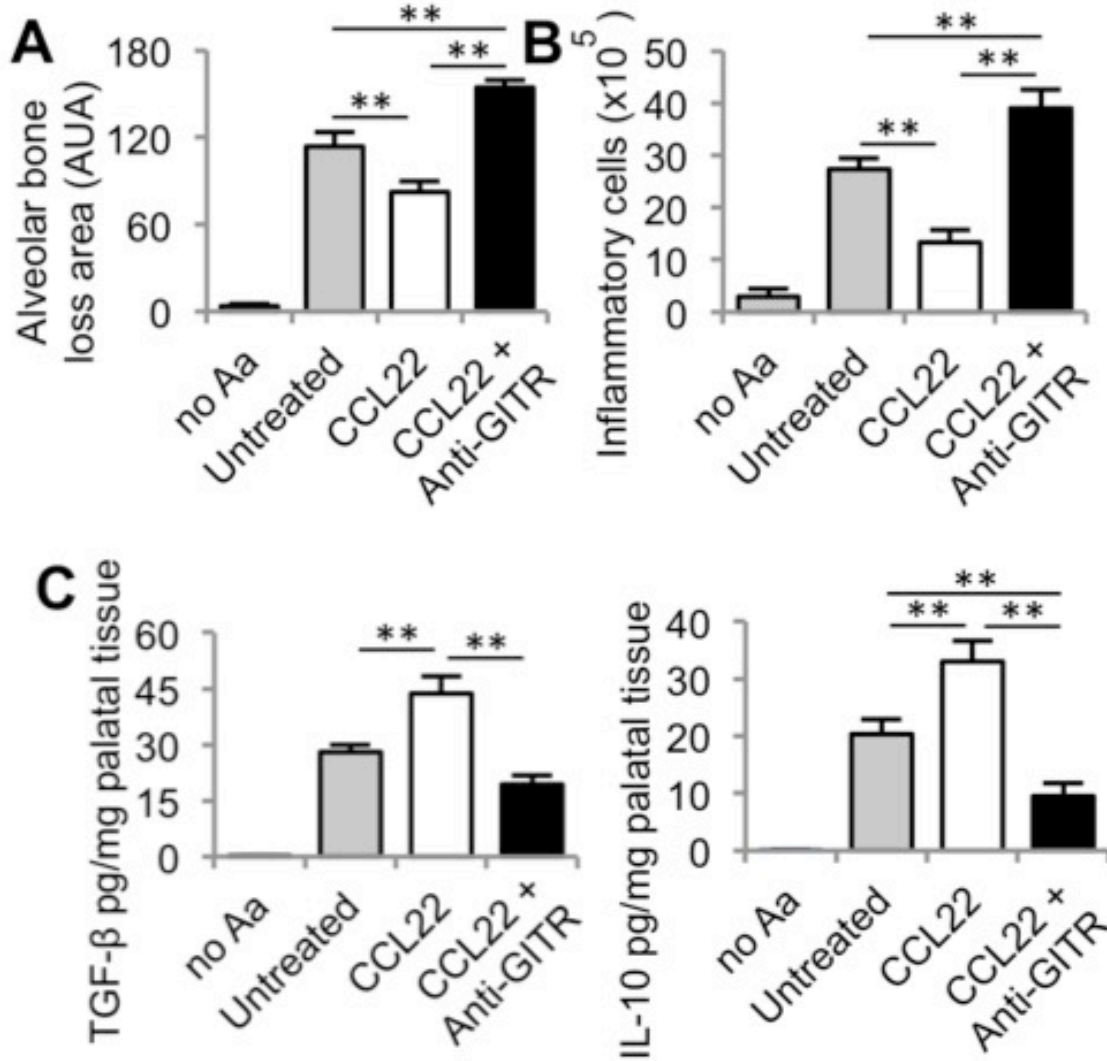


Figure 24: Anti-GITR inhibition of Tregs reverses the therapeutic effect of CCL22 microspheres in mice. Systemic blockage of Tregs was performed by i.p. injection of anti-GITR antibodies in C57BL/6J mice infected with *Actinobacillus actinomycetemcomitans* (Aa), disease indicators were measured after 30 days. CCL22 microsphere injected mice, CCL22 microsphere + anti-GITR, and untreated mice served as infected experimental and control groups, uninfected no Aa mice served as positive controls, microspheres were delivered on days -1, 10 and 20 relative to the first Aa inoculation. (A) Alveolar bone loss as determined by the measuring the area between cemento-enamel junction (CEJ) to the alveolar bone crest (ABC) of resected, defleshed maxilla. (B) The number of inflammatory cells in the periodontal tissues was determined after digesting the periodontal tissues. (C) IL-10 and TGF-β protein levels in digested palatal tissues determined by ELISA.

N = 5 mice. \*\*P < 0.05 determined by One-Way ANOVA followed by Bonferroni's multiple comparisons test, untreated, CCL22 and CCL22 + ant-GITR were statistically different from no Aa<sup>45</sup>.

### **2.3.7 Exploratory PCR array to identify the molecular mechanisms of Treg recruiting CCL22 microsphere treatments**

In order to explore the underlying molecular mechanisms responsible for disease amelioration after CCL22 microsphere administration, changes in the expression of cytokines, chemokines, growth factors and osteogenic markers in the periodontal tissues were screened using an exploratory PCR array. Results suggest that administration of CCL22 microspheres is associated with upregulation of anti-inflammatory cytokine *Il10* and *Tgfb* and a downregulation of the pro-inflammatory cytokines interleukin 1 (*Il1*), interleukin 2 (*Il2*), interleukin 12 (*Il12*), interleukin 17 (*Il17*), interferon-gamma (*Ifny*) and tumor necrosis factor-alpha (*Tnfa*) compared to untreated infected mice Figure 25. In line with evidence of the recruitment of regulatory T cells seen above, it was observed that *Ccr4*, the receptor for CCL22 (expressed highly by Tregs<sup>43</sup>) was significantly upregulated after CCL22 microsphere treatments Figure 25.

Interestingly, the CCL22 microsphere formulation not only led to an upregulation of Treg recruiting chemokine receptor and associated anti-inflammatory molecules, but also a significant and marked upregulation of bone growth factors (bone morphogenic proteins, BMPs) *Bmp4*, *Bmp7* and *Tgfb* Figure 25. Furthermore, significant upregulation of markers of bone formation, including runt-related transcription factor 2 (*Runx2*) (an important transcription factor for bone forming osteoblasts), alkaline phosphatase (*Alp1*) and dentin matrix protein 1 (*Dmp1*) were observed in the CCL22 treated mice Figure 25. Correspondingly, a significant downregulation of *Rank* and *Rankl*,

the receptor and ligand important for osteoclastogenesis leading to bone resorption, was observed after CCL22 microsphere administration. In correlation with the downregulation of *Rankl*, the expression of *Rankl* extracellular inhibitor osteoprotegerin (*Opg*) was moderately upregulated, although not significantly. Moreover, mice receiving the CCL22 formulation exhibited a significant upregulation of extracellular matrix protein collagen type 1 (*Colla1*, *Colla2*) and tissue inhibitors of metalloproteinases *Timp1* and *Timp3*, Figure 25. Again, correspondingly, mice receiving the CCL22 formulation showed a downregulation of extra cellular matrix degrading enzymes *Mmp2*, *Mmp8*, and *Mmp9* compared to untreated control mice 30 days after infection Figure 25.

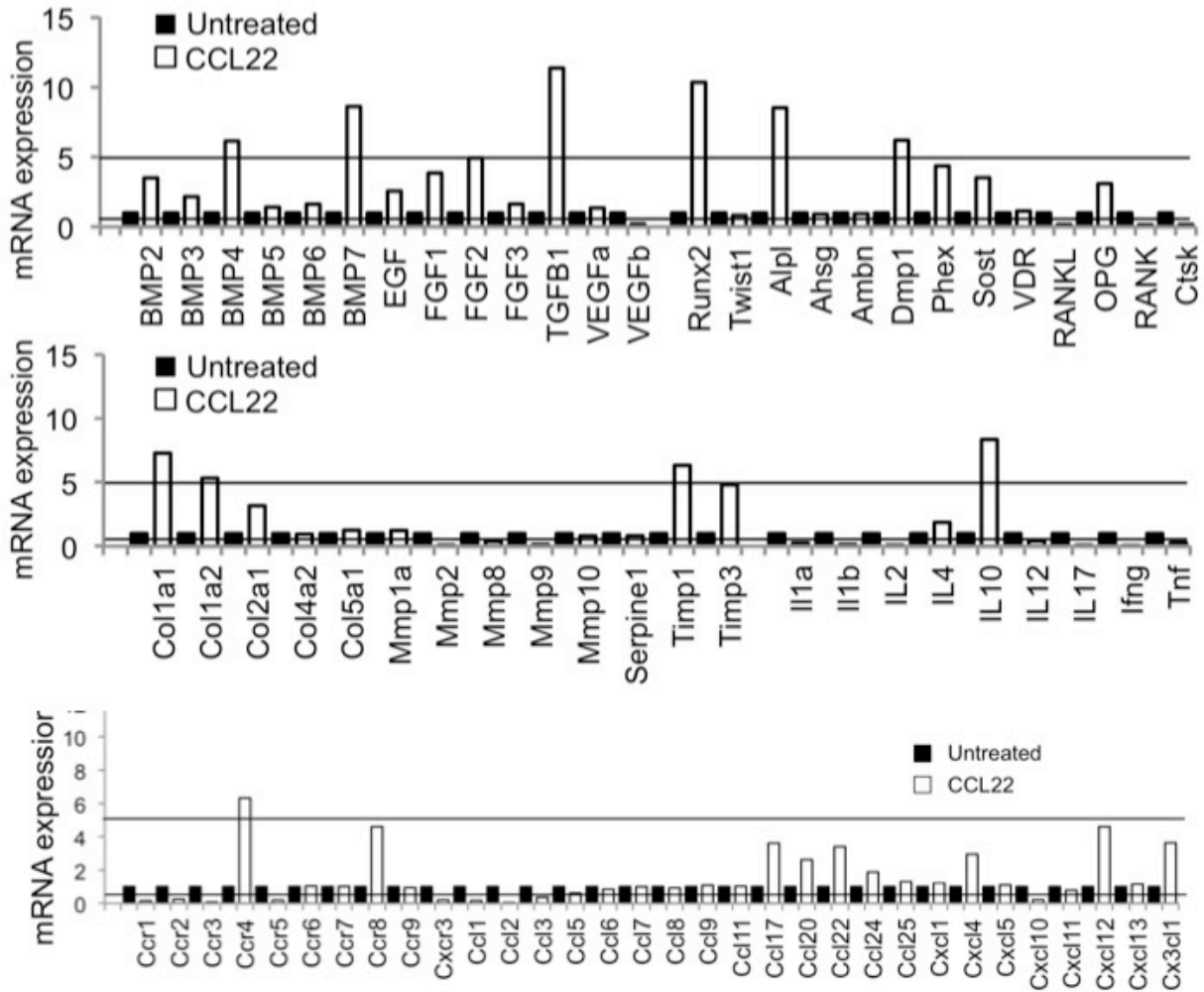
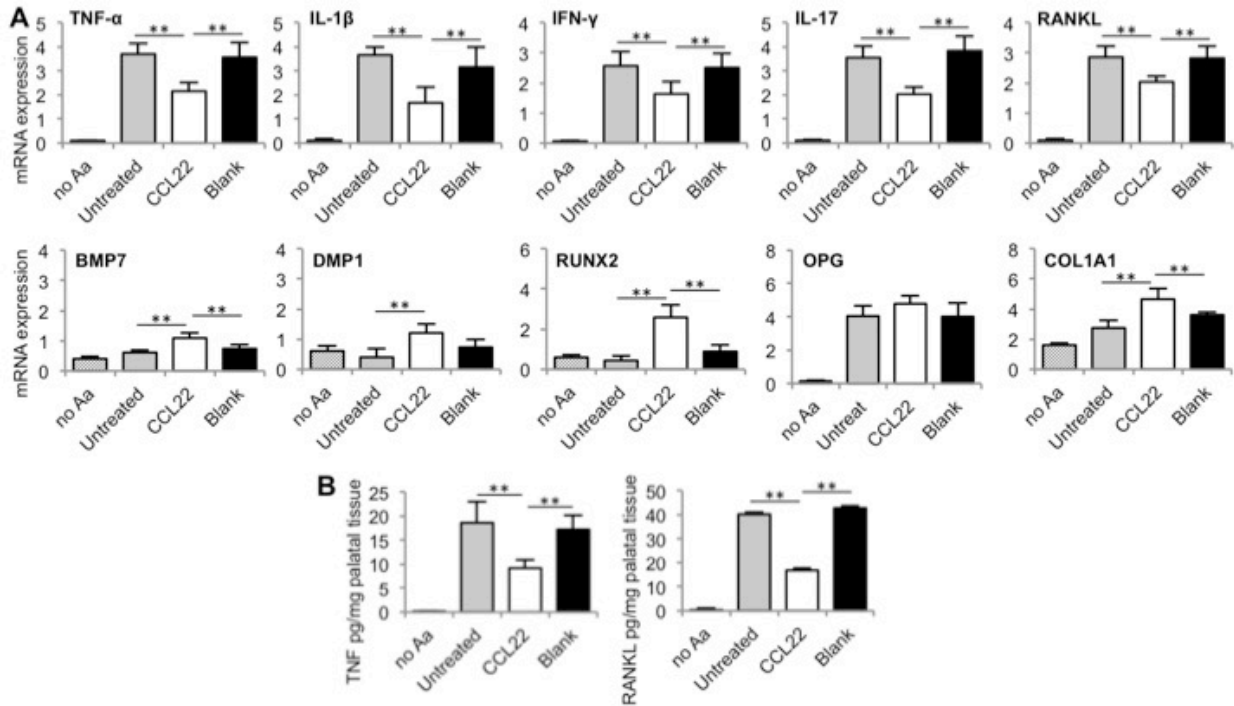


Figure 25: Exploratory PCR array identifying the molecular mechanisms of Treg recruitment by CCL22 microsphere treatment in mice. The Treg-recruiting formulation enhanced the expression of osteogenic, regenerative and anti-inflammatory markers in the periodontium. The expression mRNA in the periodontal tissue of mice 30 days after *Actinobacillus actinomycetemcomitans* (*Aa*) inoculation was analyzed using a custom-designed, exploratory PCR array. Samples were collected from periodontal tissue of C57BL/6J mice that were: infected with *Aa* without treatment (Untreated control, solid bars) and also infected with *Aa* and injected with CCL22 releasing microspheres (CCL22, unfilled bars), microspheres were delivered on days -1, 10 and 20 relative to the first *Aa* inoculation. The threshold for upregulation (more than 5 fold increase) and down regulation (less than 0.5 fold decrease) in CCL22 treated group compared to the control untreated group was indicated with lines<sup>45</sup>.

### **2.3.8 Quantitative mRNA analysis of key markers to elucidate the molecular mechanisms of Treg recruitment by CCL22 microspheres in a mouse model of periodontitis**

To verify the most important results observed with the exploratory PCR array, traditional quantitative PCR assays were utilized and enable the confirmation of statistical significance. Consistent with data obtained from the PCR array, marked decreases in pro-inflammatory cytokines IL-1, TNF (confirmed at the protein level, Fig. 5B), *Ifn $\gamma$* , and *Il17* in the CCL22 microsphere treated animals compared to blank or untreated controls were observed, Figure 26. Furthermore, CCL22 microsphere administration led to statistical increases in pro-regenerative factors in extracellular matrix protein collagen type 1 (*Colla1*), osteoblast transcription factor *Runx2*, *Bmp7*, and *Dmp1*. Accordingly, a decrease in osteoclast maturing *Rankl* both at the transcription and protein level (Figure 26 A, B) was indeed observed in the CCL22 microsphere administered mice.



**Figure 26: Quantitative PCR analysis of periodontal disease mediators in response to Treg recruiting CCL22 microspheres in mice. The Treg recruiting formulation decreased inflammatory cytokine expression and increased the expression of pro-regenerative factors. Periodontal tissues were resected from C57BL/6J mice infected with *Actinobacillus actinomycetemcomitans* (Aa) 30 days after inoculation. CCL22 microsphere injected mice, blank (unloaded) microsphere and untreated mice served as infected experimental and control groups, uninfected no Aa mice served as positive controls, microspheres were delivered on days -1, 10 and 20 relative to the first Aa inoculation. (A) mRNA expression of *Tnfa*, *Il1β*, *Ifnγ*, *Il17*, *Rankl*, *Bmp7*, *Dmp1*, *Runx2*, *Col1a1*, and *Opg* in periodontal tissue was analyzed by quantitative PCR. mRNA expression levels were compared by the value of  $2^{-(\Delta Ct)} - 1$  with reference to  $\beta$ -actin. (B) TNF and RANKL protein levels were measured in digested palatal tissues by ELISA. N = 5 mice. \*\*P < 0.05 determined by One-Way ANOVA followed by Bonferroni's multiple comparisons test, untreated, CCL22 and Blank groups were statistically different from no Aa except for the mRNA expression of BMP7, DMP1 and RUNX2<sup>45</sup>.**

## 2.4 DISCUSSION

As an alternate strategy to current antimicrobial treatments for periodontal disease, we sought to explore the local enrichment of regulatory T lymphocytes (Tregs) in the periodontal space. Tregs have been known to balance inflammation through a number of mechanisms including: anti-inflammatory cytokine secretion including, but not limited to, IL-10, TGF- $\beta$  and CTLA-4<sup>12, 13, 178</sup>, the metabolic disruption of inflammatory cells, perforin mediated direct killing of inflammatory cells, and inhibiting dendritic cell function (reviewed<sup>13</sup>). Correlating with the anti-inflammatory cytokine IL-10 appears to be associated with less aggressive form of periodontitis both in humans<sup>99</sup> and in mice<sup>100</sup>. Furthermore, the anti-inflammatory cytokine TGF- $\beta$  has been studied as a therapeutic in context of periodontal healing and bone regeneration<sup>179</sup>. Previous attempts to harness Tregs in situ involved the use of adenoviral vectors to induce the expression of CCL22 in murine autoimmune diabetes<sup>47</sup>. Here we describe a strategy to recruit Tregs via engineered release of CCL22 protein using biodegradable and biocompatible polymers with an excellent track record of approval by the FDA. More specifically, we utilized rationally-designed controlled release systems to sustain presentation of CCL22 chemokine from an injectable point source, which as previously been shown to successfully localize Tregs *in vivo*<sup>46</sup>.

Indeed, we observe that administration of the CCL22 releasing formulation effectively recruits functional Tregs to the periodontium (Figures 21 and 22), leading to a net decrease of the local inflammatory response and a reduction in alveolar bone loss in a mouse periodontitis model (Figures 18-20). Interestingly, the Treg recruiting formulation is able to achieve this tissue-protective effect without a corresponding increase in bacterial load (*Aa* or total bacterial levels) in the gingival tissues (Figure 20) or increase in systemic inflammation to the infection (C-reactive

protein, CRP, levels in serum, Figure 20), whereas traditional blocking of immune responses can impair the hosts protective defenses<sup>94</sup>.

It was also apparent that impairing Treg function (via anti-GITR administration) reverses the beneficial effects of the Treg-recruiting formulation (Figure 24). These results further underscore the importance of Treg in periodontal health. It is also clear from our data (Figure 21 and 25) that Treg recruitment to the periodontium is accompanied by an increase in IL-10, and TGF- $\beta$  expression. It is well known that these regulatory cytokines are secreted by Tregs, and are a mode by which Tregs exert a protective effect<sup>13</sup>. For instance, these Treg associated mediators are known to diminish the presence of inflammatory cytokines such as IFN- $\gamma$  and IL-17<sup>180, 181</sup>. Notably, T helper type 1 (Th1) and T helper 17 (Th17) cells, which are associated with a high levels of IFN- $\gamma$  and IL-17 expression, have been previously implicated to exacerbate periodontal disease symptoms<sup>97, 182, 183</sup>. Consistent with the idea that recruited Treg may regulate this process, our data (Figures 25 and 26) reveals decreased levels of IFN- $\gamma$  and IL-17 in treated mice. In addition, Treg secretion of IL-10 and TFG $\beta$  are also known to modulate the inflammatory markers TNF<sup>32</sup> and IL1- $\beta$ <sup>184</sup>, which appear to be also down-regulated in CCL22 microsphere treated mice (Figure 25 and 26). Most importantly, it is known that decreased levels of inflammatory cytokines such as IFN- $\gamma$ , IL-17, TNF, and IL-1 $\beta$  are associated with reduced levels of RANK-L (also observed in Figure 25 and 26), with decreasing amounts of this maturation factor previously being correlated with decreased amounts of bone loss<sup>162</sup>. Finally, we also observed an increase in CTLA-4 expression in the periodontal space of CCL22 microsphere treated mice (Figure 21), suggesting that Tregs recruited to the periodontium may suppress inflammation via a cell-cell contact mechanism, as observed previously<sup>185</sup>.

In conjunction with their ability to regulate inflammation, regulatory T cells are also being identified as effective promoters of tissue regeneration<sup>32, 58</sup>. For instance, Tregs negatively modulate pro-inflammatory cytokines responsible for inhibiting various processes during tissue regeneration<sup>32</sup>. Accordingly, CCL22 microsphere treatments led to decreased levels of inflammatory tissue destroying factors, and importantly led to the upregulation of tissue regenerative growth factors (Figure 25 and 26). We also observed that the C-X-C motif chemokine 12 (*Cxcl12*, also known as stromal-cell derived factor 1, *Sdf1*) is upregulated upon CCL22 microsphere treatment (Supplementary Fig. 4), which may mediate the migration of potentially regenerative stem cells into tissues<sup>186</sup>. This result may be particularly important given that the inhibition of *Cxcl12* or corresponding C-X-C chemokine receptor type 4 (*Cxcr4*) was recently reported to delay bone fracture repair<sup>187</sup>. Similarly, the parallel upregulation of the C-X3-C chemokine motif ligand 1 (*Cx3cl1*) observed after CCL22 microsphere treatment (Figure 25) also could account for mesenchymal stem cell recruitment<sup>188</sup>. However, further studies would need to be performed to evaluate whether or not stem cells play a role in the effects observed in this study. Regardless, the results described above suggest that recruitment of Tregs may not only halt destructive inflammation but also promote an environment amenable to tissue regeneration.

### **3.0 CONTROLLED RELEASE OF CCL22 FROM PLGA MICROSPHERES FOR THE TREATMENT OF PERIODONTAL DISEASE IN A DOG MODEL**

#### **3.1 INTRODUCTION**

A multitude of animal models have been used to evaluate the new treatments and to advance the understanding of the pathogenesis of periodontal disease<sup>189,190</sup>. Each animal model for periodontal disease represents different characteristics of the human condition, and the utility of each model can depend on the study's ultimate goal. Rodent models of periodontal disease offer cheap and timely advantages compared to models conducted in larger species<sup>93</sup>. Furthermore, the use of rodents allows investigators to use a wide variety of molecular tools (e.g. antibodies, gene knockout strains etc.) to analyze and differentiate certain characteristics of the disease, and such investigations have been crucial to develop the comprehensive understanding of the disease etiology<sup>93</sup>. However, small animal or rodent models for periodontal disease do not always accurately replicate the complex development of periodontal disease seen in the human condition<sup>189,190</sup>. Therefore, testing therapeutic agents in larger animal models that more accurately represent the human periodontal disease condition is often a key step in the translation therapies from the bench-top to the bedside.

##### **3.1.1 Advantages and disadvantages of rodent models for periodontal disease**

Rodent models for periodontal disease, utilizing various strains of rats or mice, are typically initiated by feeding or inoculating rodents with human pathogenic bacteria<sup>93</sup>. Mouse molars are

used for periodontal disease investigations as opposed to the incisors, which exhibit continuous tooth eruption (and are degraded by wear). The most common mouse models for periodontal disease utilize the periodontal pathogen *Actinobacillus actinomycetemcomitans*<sup>45, 95, 99, 100, 167, 191</sup> or the periodontal pathogen *Porphyromonas gingivalis*<sup>45, 97, 169, 192</sup>. Interestingly, *Actinobacillus actinomycetemcomitans* is typically associated with aggressive or juvenile periodontitis, whereas *Porphyromonas gingivalis* is typically associated with adult or chronic periodontitis<sup>93</sup>. While these are the two most commonly used mouse model bacteria, there is not a lot research on whether or not the resulting infection is polymicrobial, or what role commensal or resident bacteria play in the development of the disease models. Furthermore, mouse strain appears to play a role in experimental periodontal disease development, and BALB/cJ mice appear to be more susceptible to alveolar bone loss initiated by *Pg* than mice of C57 black/6 backgrounds<sup>169</sup>. Regardless, mouse models enable researchers to utilize a large number of immunological and cellular reagents that are available, along with a long history of background information on mouse molecular mechanisms and immune system. While the human periodontal disease condition can assert itself as both a chronic or an acute disease (possibly with periods of both) mouse models are typically considered to better represent acute disease conditions. Some work has utilized aged mice (~2 year old mice) to better simulate chronic periodontal disease conditions seen clinically<sup>183</sup>, but such models require a lot of resources and are better for investigating molecular mechanisms of disease than testing new treatment modalities<sup>193</sup>. Others have used lipopolysaccharides derived from invasive bacterial species (LPS derived from *Actinobacillus actinomycetemcomitans*) to initiate periodontal immune responses (via toll-like receptor 4, TLR4, signaling) in mice, possibly allowing for more controlled inflammatory conditions compared to infection-based mouse models<sup>194-196</sup>.

Rat models for periodontal disease typically use infection with *Actinobacillus actinomycetemcomitans* or *Porphyromonas gingivalis*, with or without molar ligatures<sup>93</sup>. Typically Wistar or Sprague-Dawley rat strains are used for periodontal disease models, and ligatures (silk sutures) are typically placed (tied) around the middle molar (middle of 3 molars) of the mandible of rats. Whereas in mice, ligatures are not typically used (although some have reported successful use<sup>183</sup>) because of the limited space and size of mice mandibles, ligature placement in mice typically is associated with significant trauma making alveolar bone destruction due to periodontal disease conditions difficult to discern from forced trauma. However, the size of rats mandibles and molars easily allows for the use of ligatures to induce periodontal disease. Ligatures, with or without additional external bacteria inoculation, allow for the growth of endogenous or native bacterial biofilms and are thought to be more representative of acute periodontal disease conditions seen clinically<sup>93, 189</sup>. Overall, rodent models for periodontal disease progress extremely fast compared to humans, however, the ease of use with limited resources and a large library of immunological and cellular tools make them ideal model species for basic hypothesis testing<sup>93, 189, 190</sup>.

Furthermore, some investigators have utilized hamsters, ferrets or minks as species for experimental models of periodontal disease<sup>189, 190</sup>. While these species are larger than mice, they have comparable dimensions to rats, but lack many of the immunological and cellular tools widely available for rats and mice.

### **3.1.2 Advantages and disadvantages of non-human primates for experimental periodontal disease models**

Generally, non-human primates are the most similar to humans in experimental models for periodontal disease<sup>189, 190</sup>. While non-human primates share many of the dental features of humans, they typically display less depth in disease related periodontal pockets compared to humans<sup>190</sup>. Periodontal disease conditions have been reproduced in non-human primate models by typically by placement of silk sutures (ligatures) around the base of investigated teeth to simulate acute periodontitis, or by surgically creating defects by removing alveolar bone and gingiva and observing the healing response, or surgically creating defects accompanied with steel bands around the teeth or ligatures to simulate chronic disease<sup>197</sup>. The most common non-human primate model is the ligature induce acute periodontitis, where silk sutures are placed around the base of teeth and disease progression (often with treatment) is monitored using clinical measures of periodontal disease over the course of 1-6 months<sup>189, 190, 197, 198</sup>. Clinical measures of bleeding on probing, probing depth and clinical attachment loss can be assessed in non-human primates just as they are done clinically (these measures cannot be performed on rodents due to the dimensions and the nature of rodent experimental periodontitis). Although non-human primates are ideal candidates for experimental periodontitis as they most accurately represent human conditions, they are extremely difficult to work with (ferocious), extremely resource intensive and lack many of the immunological and cellular tools available for rodents<sup>189, 190</sup>.

### **3.1.3 Advantages and disadvantages of dog models for periodontitis**

Unlike non-human primates, dogs offer a less resource intensive, and less difficult (dogs are docile and obedient compared to non-human primates) experimental model for periodontal disease<sup>189, 190</sup>. Unlike rodents, but similar to non-human primates, dog models for periodontitis allow for the measure of clinically relevant disease outcomes such as periodontal probing depth, bleeding on probing and clinical attachment loss<sup>189, 190, 199</sup>. Similar to non-human primates, periodontal disease is induced via ligature induced periodontitis to simulate acute disease or surgically created defects to model healing and repair responses<sup>189, 190</sup>. Typically, beagle dogs are used for periodontal research to help ensure reproducibility and because they have demonstrated natural susceptibility periodontal disease<sup>199</sup>. However, dogs typically exhibit less of an increase in anaerobic gram negative rod-bacteria compared to human conditions, after ligature placement and endogenous or native bacterial build-up<sup>200</sup>. Overall, dog models for periodontitis are the most widely used large animal model due to their ease of experimentation, reproducibility (with beagle research strains being readily available) and human disease replication, including clinical measurements of disease<sup>189, 190</sup>.

### **3.1.4 CCL22 microspheres for the treatment of periodontitis in the ligature induced dog model of periodontitis**

Utilizing one of the most widely accepted preclinical model of periodontitis, ligature induced canine periodontitis<sup>190, 199</sup>, the efficacy of CCL22 microspheres was explored in a this more clinically relevant translational experimental model. Treg-recruiting CCL22 microspheres were administered into periodontal pockets at multiple time-points (for maximum effect) and measured

symptoms using both a common clinical measure (probe of gingival sulcus) as well as quantitative CT measurement of alveolar bone loss.

## 3.2 METHODS

### 3.2.1 Microsphere preparation

Poly (lactic-co-glycolic) acid (PLGA) microspheres containing recombinant human for canine investigations CCL22 (R&D systems, Minneapolis, MN) were prepared using a standard water-oil-water double emulsion procedure as described<sup>46</sup>. Mouse and human CCL22 share 63% of amino acid identities and score 83% positives using a BLAST analysis. Canine CCL22 and Human CCL22 share 71% of identities and score 84% positives using a BLAST analysis. Blank (unloaded) PLGA microsphere controls were fabricated in the same manner with the exception of CCL22 protein encapsulate. Briefly, the PLGA (RG502H, Boehringer Ingelheim, Petersburg, VA) microspheres were prepared by mixing 200  $\mu$ L of an aqueous solution containing 25  $\mu$ g of rmCCL22 and 5 mmol NaCl with 200 mg of polymer dissolved in 4 mL of dichloromethane. The first water-in-oil emulsion was prepared by sonicating this solution for 10 seconds. The second oil-in-water emulsion was prepared by homogenizing (Silverson L4RT-A) this solution with 60 mL an aqueous solution of 2% polyvinyl alcohol (M.W.  $\sim$ 25,000, 98 mol. % Hydrolyzed, PolySciences, Warrington, PA) for 60 seconds at 3000 RPM. This solution was then mixed with 1% polyvinyl alcohol and placed on a stir plate agitator for 3 hours to allow the dichloromethane to evaporate. The microspheres were then collected and washed 24 times in deionized (DI) water, to remove residual polyvinyl alcohol, before being re-suspended in 5 mL of DI water, frozen, and

lyophilized for 72 hours (Virtis Benchtop K freeze dryer, Gardiner, NY; operating at 100mTorr). The overall microsphere fabrication process is shown in Figure 7, above.

### **3.2.2 Microsphere characterization**

Surface characterization of microspheres was conducted using scanning electron microscopy (JEOL JSM-6330F, Peabody, MA) and microsphere size distribution was determined by volume impedance measurements on a Beckman Coulter Counter (Multisizer-3, Beckman Coulter, Fullerton, CA). CCL22 release from microspheres was determined by suspending 7-10 mg of microspheres in 1 mL of phosphate buffered saline (PBS) placed on an end-to-end rotator at 37°C. CCL22 release sampling was conducted at various time intervals by centrifuging microspheres and removing the supernatant for CCL22 quantification using ELISA (R&D Systems, Minneapolis, MN), sampling of releasates is shown in Figure 8 Above. Microspheres were re-suspended with 1 mL of fresh PBS and returned to the rotator at 37°C.

### **3.2.3 Recombinant human CCL22 microsphere administration in dogs**

Dogs received approximately 2-4 mg of dry particles to the subgingival pockets (periodontal pocket) of the 4<sup>th</sup> premolars and carnassial (first molar) of both mandibles. Dry microspheres were deposited in the subgingival pockets using empty, cleaned, and refilled Arestin® injector tips. The dry microspheres hydrated (in gingival crevicular fluid of the dogs) and swelled immediately, retaining them within the periodontal pocket of dogs, and we observed no microsphere leakage from the pockets. Dogs received microspheres the start of the ligature induced periodontitis (week 0) and at 4 weeks, according to the schedule shown below in Figure 27.

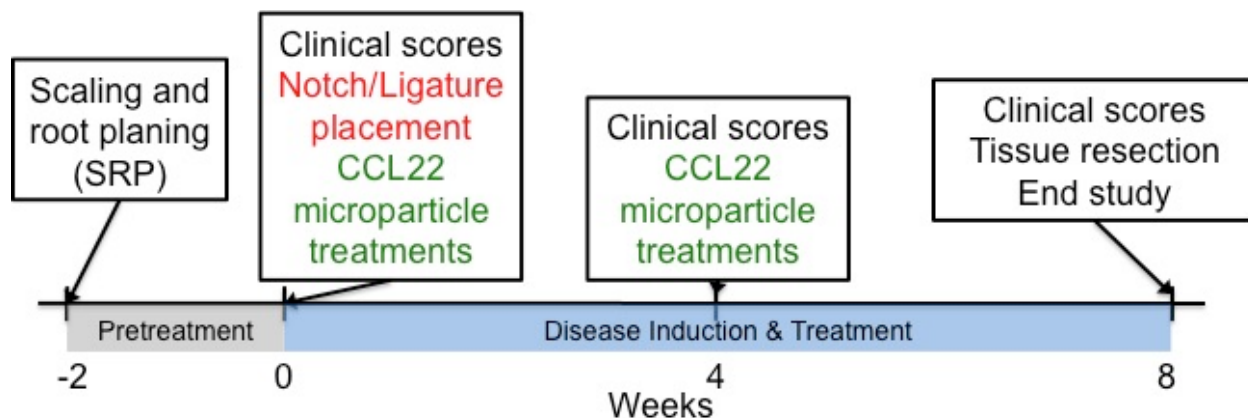


Figure 27: rhCCL22 treatment schedule and ligature induced periodontal disease induction in dogs.

### 3.2.4 Periodontal disease induction in beagle dogs

Nine ~12 month old female beagle dogs were purchased from Marshall BioResources (North America). Periodontal disease was induced as previously described<sup>199</sup>. Briefly, all dogs received dental scaling and root planing on mandibular 4<sup>th</sup> premolar, and carnassial teeth two weeks prior to ligature placement as a pretreatment to create a baseline for oral health. Every dog received 2 times daily tooth brushing during the two week pretreatment to maintain oral hygiene. To induce periodontitis, 2.0 silk sutures were placed at the cervix of the gingiva of the mandibular 4<sup>th</sup> premolar, and carnassial teeth. Ligatures were held in place on the proximal and distal sides of each tooth by shallow notch made using a round bur. Ligatures that had fallen off were replaced immediately and a small amount of dental composite resin was used to ensure ligature maintenance. Microspheres were administered immediately after ligature placement and again 4 weeks after ligature placement. Overall disease induction and treatment schedule can be seen in Figure 27 above.

### **3.2.5 Assessment of periodontal disease in dogs, alveolar bone loss and clinical scores**

Pocket depth was measured at six points of each tooth, mesial and distal corner, and middle of both buccal and lingual sides. Bleeding on probing was recorded at each probing site. All the clinical assessment was performed at 0, 4, and 8 weeks after treatment. Gingival pocket depth is the distance between the cervixes of gingival to the attachment point of gingival epithelia to the tooth. The increase of pocket depth was calculated by subtracting the pocket depth at 0 week from 4 weeks or 8 weeks using the mean of all the sites.

To quantify alveolar bone loss, dog mandibles were scanned in 70% ethanol by SCANCO vivaCT 40 micro-computed tomography (microCT) system (SCANCO, Bruttisellen, Switzerland). 3D images were reconstructed with SCANCO software at the same threshold across all the samples. Each scan was reoriented with DataViewer (GE Healthcare, London, ON). The images were reoriented by the planes adjusted to the cemento-enamel junction (CEJ), bucco-lingual center of the roots, and parallel to the root canal in the center of distal root of 4<sup>th</sup> premolar and mesial root of first molar. To assess the vertical bone reduction, the distance between CEJ and alveolar bone crest (ABC) was measured at the distal face and buccal face of the fourth premolar and the first molar after microCT image reorientation. Along the distal face of the tooth, the ABC-CEJ distance was measured at 5 points 0.3 mm apart, along the buccal face of the tooth the ABC-CEJ distance was measured at 14-16 sites on premolar 4, and 26-28 sites on the molar spaced 0.6 mm apart from mesial to distal. To quantify an overall value of alveolar bone resorption per dog, we used a total summation of the linear CEJ-ABC distances over the (averaged left and right) premolars (19 sites per tooth) and molars (31 sites per tooth) of each dog. Bone loss was also represented as the average linear CEJ-ABC at the buccal and distal sites of premolar 4 and the 1<sup>st</sup> molar, averaged on a per tooth basis.

### 3.2.6 Statistical analyses

All data was confirmed to portray a normal distribution (determined by Shapiro-Wilk test) and further analyzed using one-way ANOVA followed by Bonferroni's or Tukey-HSD *post-hoc* test to compare differences between multiple groups. Student's unpaired *t* test was used for all other statistical analyses. Differences were considered significant when  $P < 0.05$ . Statistics were performed using GraphPad Prism or JMP Pro 10 software.

## 3.3 RESULTS

### 3.3.1 Characterization of rhCCL22 PLGA microspheres

The initial goal of the project was to develop recombinant human CCL22 releasing microspheres that portrayed ideal release kinetics for use in the dog model of periodontal disease. rhCCL22 PLGA microspheres were fabricated and composed of carboxylic acid end-capped 12 kDa 50:50 (lactic:glycolic) poly(lactic-co-glycolic) acid microspheres, Figure 28. Surface mapping of the microspheres, Figure 28 A, shows that rhCCL22 PLGA microspheres exhibited slightly porous morphology as a result of the incorporation of 5 mmol NaCl into the inner aqueous phase (first emulsion) of the fabrication procedure, scanning electron micrograph Figure 28 A. The *in vitro* release of rhCCL22 from PLGA microspheres displayed extended release of the chemokine over a period of 30 days, Figure 28 B. Finally, the rhCCL22 PLGA microspheres volume average size distribution revealed that the microspheres had an average diameter of 16.6 microns (very similar to the rmCCL22 microspheres used in murine studies), ultimately suggesting that the microspheres

would avoid phagocytic clearance (larger than 10 microns<sup>170</sup>) once placed in the periodontium of dogs, Figure 28 C.

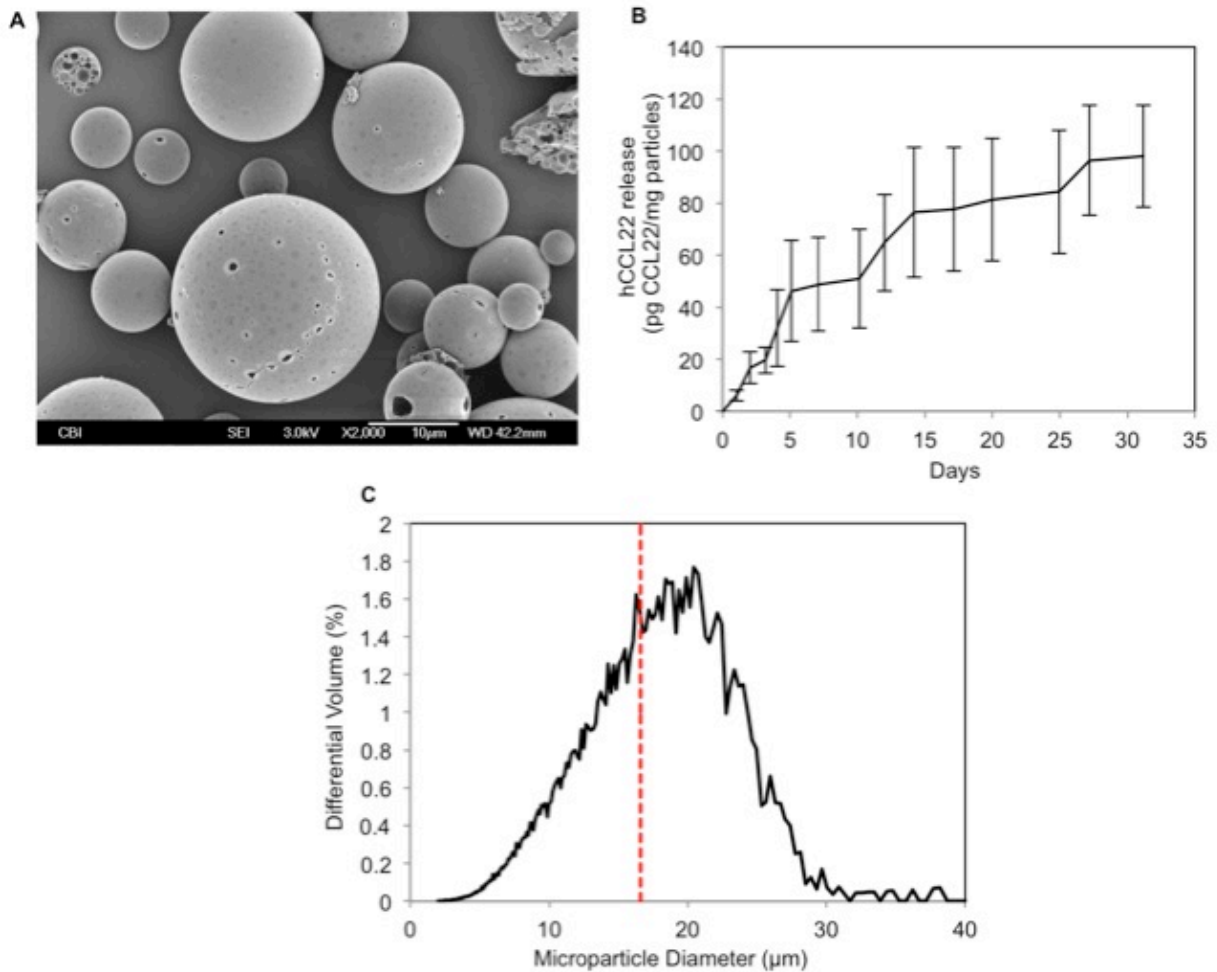


**Figure 28: Characterization of rhCCL22 PLGA microspheres for treatment of periodontal disease in the ligature induced dog model. (A) Scanning electron microscope image of poly(lactic-co-glycolic) acid microspheres encapsulating rhCCL22. (B) Cumulative fraction released from rhCCL22 microspheres determined by *in vitro* in phosphate buffered saline and measured by ELISA. (C) Volume impedance**

microsphere size distribution, average particle diameter 16.6  $\mu\text{m}$  represented by red-dashed line, standard deviation  $\pm 5.8 \mu\text{m}$ <sup>45</sup>.

### **3.3.2 rhCCL22 microspheres reduce the clinical scores of periodontal disease and inflammation in ligature induced dog periodontitis**

In order to explore the potential for clinical translatability of Treg-recruiting treatments, a ligature induced canine model that tested the ability of the CCL22 releasing formulation to perform under severe inflammatory conditions and a diverse periodontopathogen milieu was used<sup>93, 201</sup>. Specifically, disease was induced in nine beagle dogs (3 dogs per group, both left and right mandibles) by placement of ligature at the gingival cervix. The study was terminated eight weeks subsequent to ligature placement, and plaque had manifested on the ligatures, and cervical gingiva appeared inflamed in all animals (Figure 29). Whereas the mouse experiments relied upon CCL22 microspheres encapsulating recombinant mouse CCL22<sup>46</sup>, for canine experiments a formulation that released recombinant human CCL22 (Figure 28 above) deposited in the subgingival pocket at time-points 0 and 4 weeks was used, which mirrors the duration of human CCL22 release from the treatment.

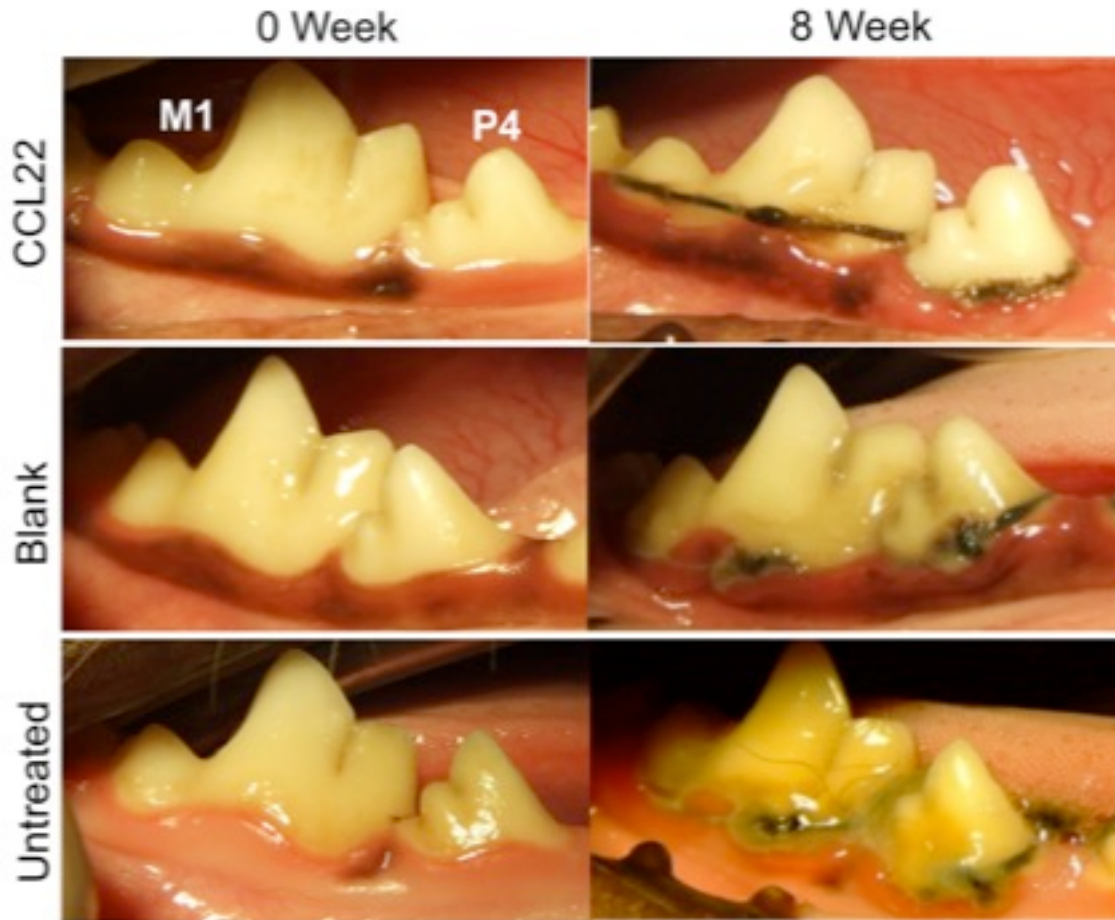


**Figure 29:** rhCCL22 microspheres reduced observational swelling and plaque build up in ligature induced dog periodontitis. Dogs received scaling and root planing followed by ligature placement (untreated), or followed by ligature placement and CCL22 microsphere treatment or blank (unloaded) microsphere controls, microspheres were deposited into the subgingival pocket at 0 and 4 weeks after ligature placement. Representative digital pictures as taken on the date of ligature placement (0 week) and after the 8 weeks of treatment (8 weeks, terminal endpoint) of the premolars and carnassial teeth of beagle dogs<sup>45</sup>.

To assess periodontal health and the degree of inflammation, the gingival pocket probing depth and the bleeding on probing sites were measured and recorded at 0, 4, and 8 weeks after the ligature placement Figure 30. Recombinant human CCL22 microsphere treatments administered during disease induction led to noticeable reduction in probing depths compared to blank and

untreated controls at 4 and 8 weeks after disease initiation, Figure 30 A. Additionally, bleeding on probing score was lower at 4 and 8 weeks in dogs receiving CCL22 microspheres, compared to controls Figure 30 B.

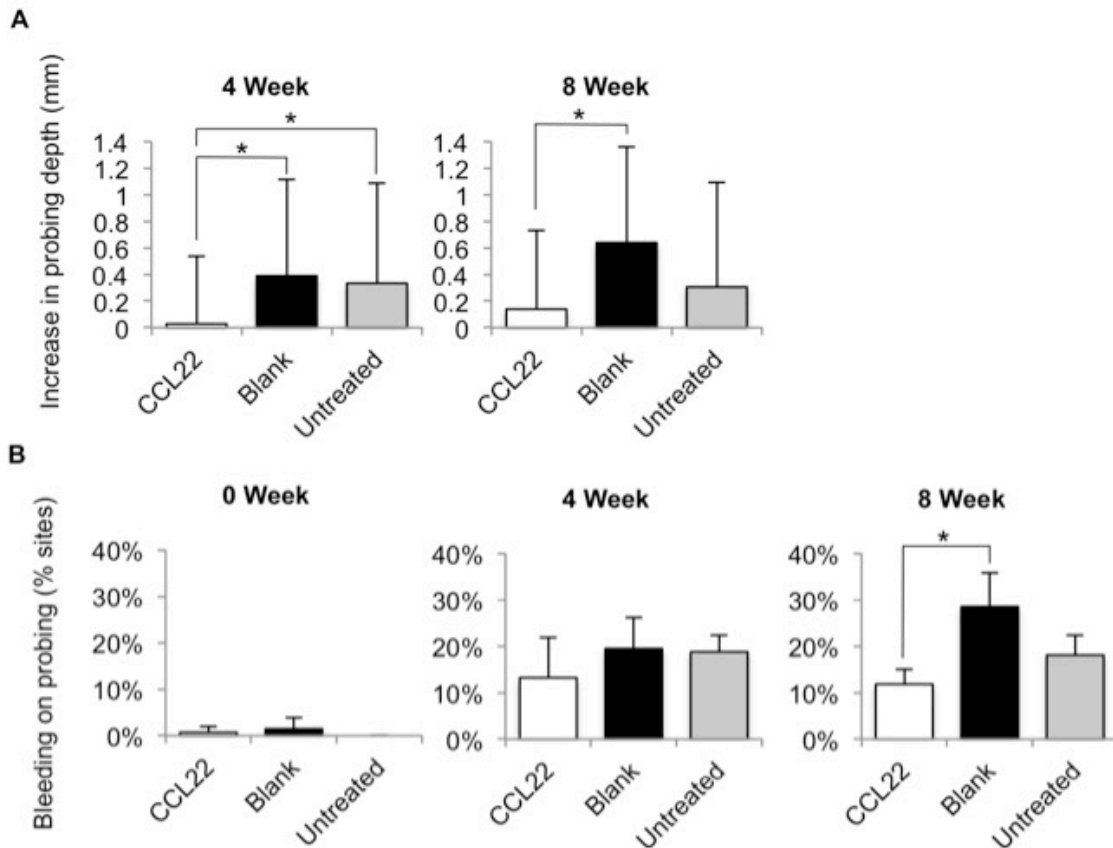


**Figure 30: rhCCL22 microsphere administration prevents exacerbation of clinical probing depths and bleeding upon probing scores in dogs. Beagle dogs receiving periodontal disease inducing ligatures at week 0 were monitored for pocket depth and bleeding on probing at 6 sites per tooth (3 buccal, 3 lingual) of their second, third, fourth premolars as well as their carnassial tooth. (A) Periodontal pocket depth increase as measured at 4 weeks – 0 week and 8 week – 0 week after treatment for molar sites. (B) The percentage of bleeding sites on probing of all the probed sites at 0, 4, and 8 weeks. Dogs treated with CCL22 microspheres deposited into the periodontal pocket at times 0 and 4 weeks (CCL22) were compared to untreated (Untreated) and empty microspheres (Blank) controls. \*P<0.05, student t-test<sup>45</sup>.**

### **3.3.3 rhCCL22 microspheres prevent alveolar bone loss in dogs**

CCL22 microsphere administration also appears to significantly reduce alveolar bone resorption as compared to controls, Figure 31. Using X-ray microtomography (microCT) at the termination of the study 8 weeks after ligature placement, alveolar bone resorption was quantified in the 9 beagle dogs. Figure 31 A-B, shows the buccal face all dog mandibles used in the study, CCL22 microsphere treated dogs display reduced alveolar bone resorption.

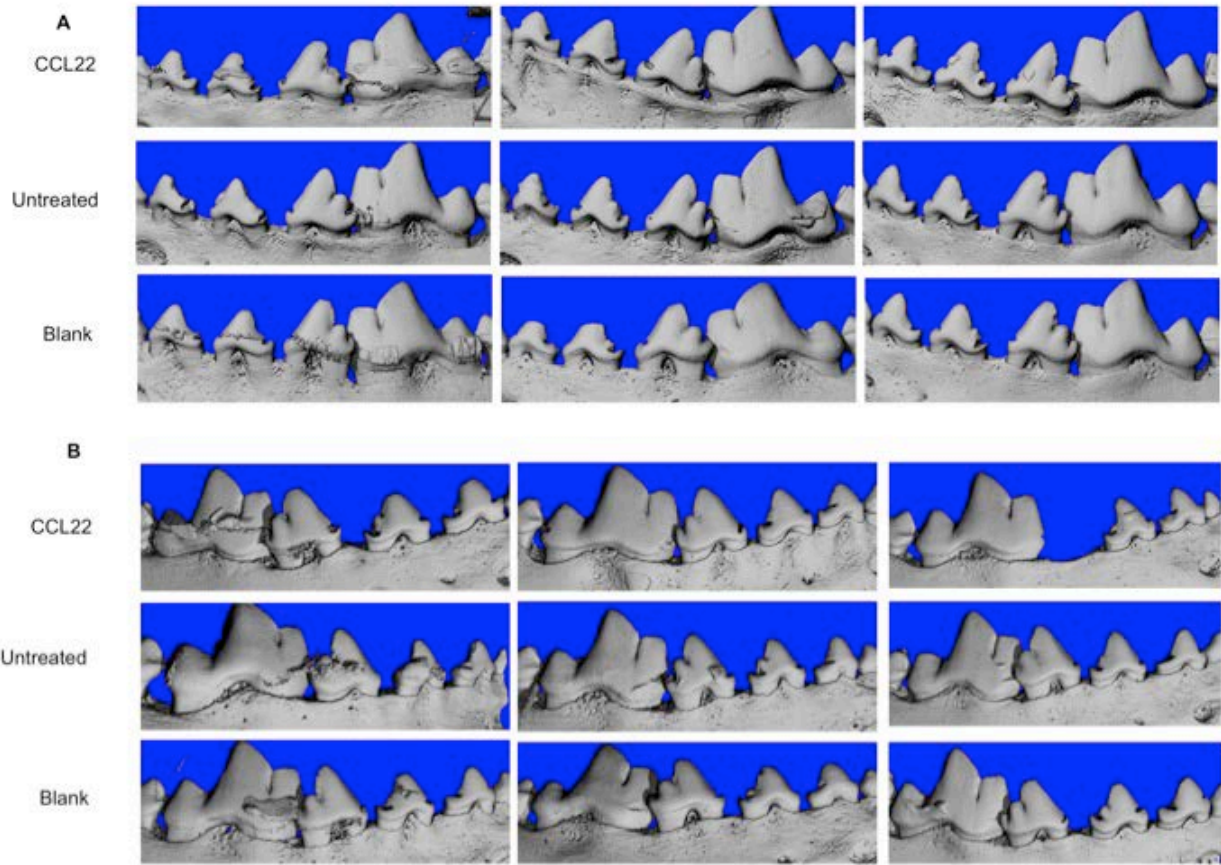


**Figure 31: 3D-reconstructed microCT images of the buccal face of dog mandibles. (A) Representative 3D microCT images from mandibles of each animal on the buccal face of the left mandible post mortem, 8 weeks of ligature placement, and (B) right mandible, n = 3 animals per group. One dog was missing premolar 4 on birth (top row, third panel, (B), therefore no ligatures were placed on this tooth and it was excluded from the study. Dogs treated with CCL22 microspheres deposited into the periodontal pocket at times 0 and 4 weeks (CCL22) were compared to untreated (Untreated) and empty microspheres (Blank) controls<sup>45</sup>.**

Alveolar bone loss in dogs was measured by taking linear measurements along the buccal and distal faces of the fourth premolar and first molar (carnassial) teeth of beagle dogs after 8 weeks of ligature placement and microsphere treatment, Figure 32. Figure 32 A, shows a 3D reconstructed microCT image highlighting the fourth premolar (P4) and first molar (M1) of the

dog mandibles. Fourteen linear measurements were taken on the buccal face of the cementoenamel junction (CEJ) to the alveolar bone crest (ABC) on the P4 tooth, and 26 linear measurements sites (CEJ to ABC) were taken on the buccal face of the M1 tooth, Figure 32 A. Figure 32 B shows an example re-oriented 2D microCT X-ray slice, and an example CEJ to ABC measurement is shown. Figure 32 C graphs the alveolar bone loss trends along the buccal face of the P4 and M1 teeth for dogs treated with rhCCL22 microspheres, blank microsphere controls and untreated controls.

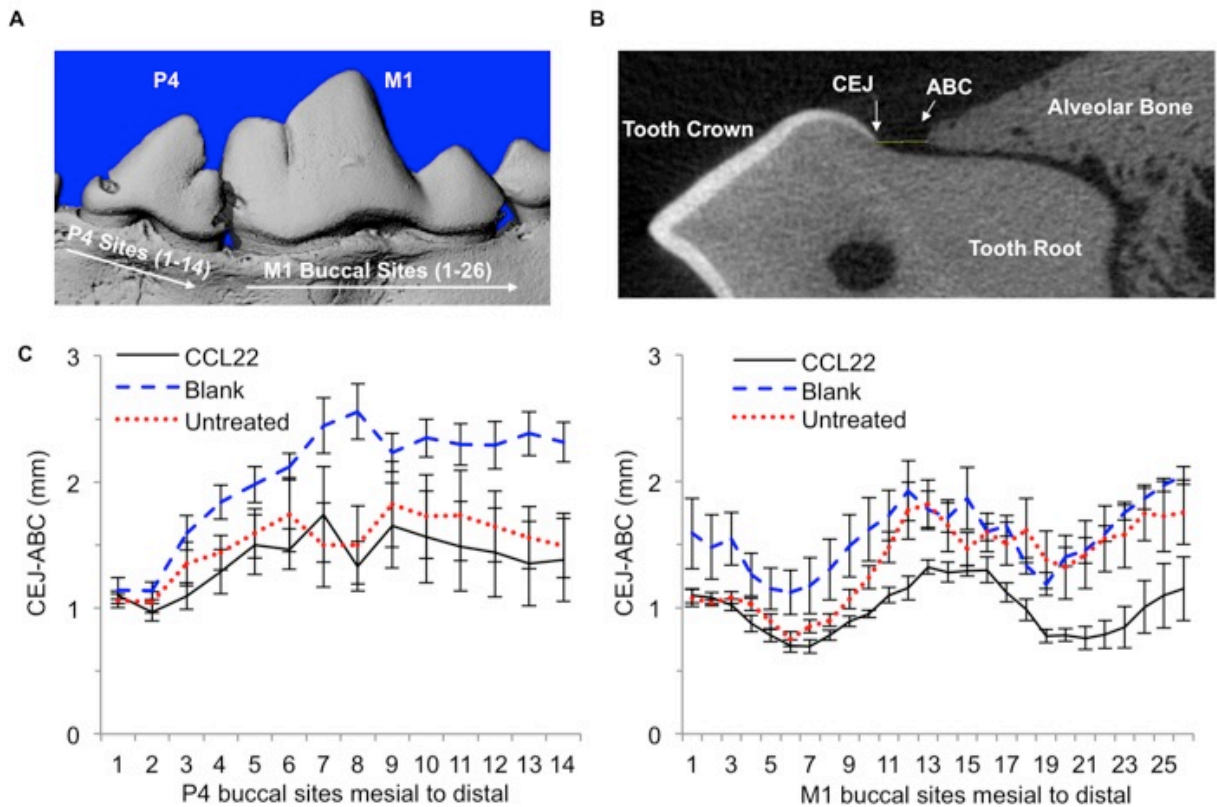


**Figure 32: Quantification of alveolar bone loss in ligature induce dogs. MicroCT quantification of alveolar bone loss prevention in dogs treated with CCL22 microspheres. (A) Representative 3D X-ray microtomography image of beagle dog fourth premolar (P4) and first molar (M1). To quantify alveolar bone loss, 5 linear measurements of the distance between the cementoenamel junction (CEJ) and alveolar bone crest (ABC) were taken at 0.3 mm spacing on the distal face of the P4 and M1 (quantified and shown in Fig. 6).**

Additionally, the CEJ to ABC distance was measured at sites spaced 0.6 mm apart along the buccal face of the P4 (14 sites) and M1 (26 sites). (B) A representative image showing the measurements of the CEJ to the ABC were performed after re-orientation of the microCT slices to align the apical roots and CEJ. (C) Linear bone loss between the CEJ and ABC along the buccal face of the left and right premolars (P4) and molars (M1) displaying the trends in alveolar bone resorption. Dogs treated with CCL22 microspheres deposited into the periodontal pocket at times 0 and 4 weeks (CCL22) were compared to untreated (Untreated) and empty microspheres (Blank) controls<sup>45</sup>.

Quantification of the buccal and distal cemento-enamel junction to alveolar bone crest (CEJ to ABC) showed that rhCCL22 microspheres significantly prevented alveolar bone resorption in ligature induced dog periodontitis, Figure 33. Substantial bone loss was apparent on all dogs, particularly at the buccal side of 4<sup>th</sup> premolar and first molar, Figure 33 A. Quantifying total alveolar bone loss (on a per animal basis) as a summation of the linear distance between CEJ and ABC, CCL22 treated dogs revealed significantly reduced bone resorption after 8 weeks, Figure 33 B. More specifically, CCL22 treated dogs displayed on average 0.5-1.0 mm less CEJ-ABC bone loss than controls at buccal and distal tooth sites, Figure 33 C, akin to the linear reduction in clinical attachment loss reported after clinical periodontal flap surgery<sup>202</sup>.

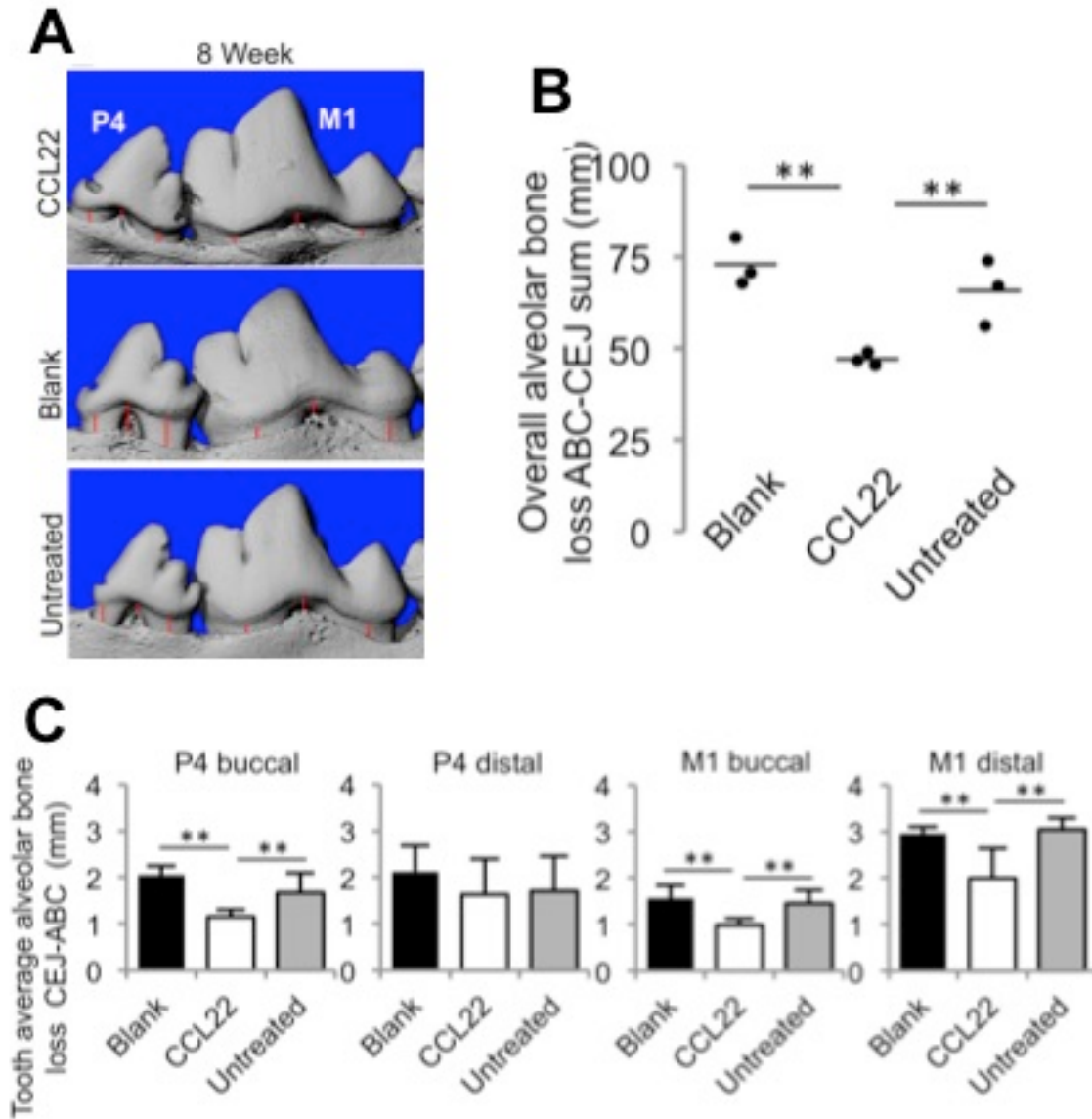


Figure 33: Administration of CCL22 microspheres significantly prevented alveolar bone resorption in dogs with periodontitis. Dogs received scaling and root planing followed by ligature placement (untreated), or followed by ligature placement and CCL22 microsphere treatment or blank (unloaded) microsphere controls, microspheres were deposited into the subgingival pocket at 0 and 4 weeks after ligature placement. (A) Representative 3D images of left mandibular buccal surface of treated and control fourth premolar and carnassial teeth taken post-mortem with microCT scans. Red lines illustrate representative CEJ-ABC distances, which were measured using 2D slices of the tooth as described in Fig. S8. (B) Quantification of overall alveolar bone loss per dog determined as a summation of linear distances between the alveolar bone crest (ABC)

and cementoenamel junction (CEJ) on the buccal and distal sites of the fourth premolar (P4) and carnassial (first molar, M1). (C) Quantification of the average linear bone loss on the P4 and M1 distal and molar sites, calculated on a per tooth basis.. N = 3 dogs per group. **\*\*P < 0.05, determined by ANOVA followed by Tukey-HSD multiple comparisons post test<sup>45</sup>.**

### 3.4 DISCUSSION

To confirm the effects of the Treg recruiting formulation in a model that is more representative of human disease, we utilized a widely accepted canine model, where disease is established by placement of ligatures followed by a soft diet, encouraging retention of a more diverse microbial insult and, correspondingly, more complex disease progression<sup>190</sup>. CCL22 microspheres were administered as a dry powder directly to the periodontal pocket, much in the same way as minocycline-loaded particles are delivered as adjunctive treatment to scaling and root planing in the clinic today<sup>90</sup>. Consistent with the results in our mouse model, we observed slower disease progression with reduced clinical measures of probing depth and bleeding on probing in canine subjects treated with CCL22 releasing particles (Figure 30 above). Clinical probing depths and bleeding on probing scores are typically sufficient to determine the therapeutic efficacy of potential treatments in large animal models<sup>199</sup>. Interestingly, CCL22 microsphere treated dogs displayed reduced amounts of bacterial plaques (seen in Figure 29). The reduction of bacterial plaques was hypothesized to be a result of reduced inflammation leading to a microenvironment less favorable for plaque formation, (as CCL22 is not known to have any antibacterial effects alone).

In addition, we also quantified alveolar bone resorption using microCT image analysis (Figures 32 and 33 above), the first time this has been done to our knowledge. Using these methods, we observed that alveolar bone loss was significantly reduced in groups treated with

CCL22 microspheres (Figure 31-33 above) by up to 1 mm, even at extremely low doses of active protein (less than one microgram of CCL22 per kilogram body weight). This amount of bone loss is significant given that current clinical gold standard periodontal flap surgeries appear to halt approximately 0.5 mm of clinical attachment level after one year<sup>202</sup>. Furthermore, dogs receiving control PLGA microspheres exhibited increased bone loss compared to untreated control animals (Figures 31-33), similar to clinical results seen using other PLGA microsphere control vehicles<sup>90</sup>. It is hypothesized that the PLGA microspheres alone may contribute to inflammation during the acidic breakdown of the polymer chains<sup>203</sup>. As possible limitations of this study, one animal in the CCL22 treatment group exhibited an abnormality (crookedness) of the 4<sup>th</sup> premolar that likely contributed to the observed statistical variance with the P4 distal sites (Figure 31). In addition, another animal in the CCL22 treatment group arrived with a missing premolar as a congenital defect. In this animal, an analysis was performed to ensure that the plaque burden and bone resorption was not reduced at adjacent sites, and in fact, bone resorption was actually the greatest at this site compared to other animals. Overall, future studies using micro-CT analysis should prioritize the selection of animals so as to exclude these sources of variance prior to initiation of the study.

The treatment of inflammatory and autoimmune diseases through the use of Tregs is an emerging trend with significant potential<sup>204</sup>. Indeed, several methods are currently being investigated in preclinical models<sup>47</sup> and clinical trials for autoimmune disease such as type 1 diabetes and transplant rejection<sup>15</sup>. However, these current methods involve complicated *ex vivo* Treg expansion protocols, and have been difficult to replicate in humans<sup>15</sup>. Here we describe a method to harness endogenous Tregs and recruit them to specific sites of aberrant inflammation in a stable, dry powder form that can be stored and easily administered in the clinic. We also foresee

that these Treg recruiting microspheres may be useful for the *in situ* expansion of Tregs<sup>51</sup> for a number of other inflammatory and autoimmune diseases where local re-establishment of immune hypo-responsiveness or inflammatory homeostasis would be beneficial to halting destructive inflammation and even establishing a pro-regenerative milieu.

## **4.0 CONTROLLED RELEASE OF VASOACTIVE INTESTINAL PEPTIDE (VIP) FOR THE RECRUITMENT OF TREGS AND TREATMENT OF EXPERIMENTAL PERIODONTAL DISEASE IN MICE**

### **4.1 INTRODUCTION**

#### **4.1.1 Introduction to vasoactive intestinal peptide and periodontal disease**

Vasoactive intestinal peptide (VIP) is a 28-aminoacid neuropeptide originally isolated from the intestine that has numerous biological and regulatory functions<sup>136</sup>. VIP down-regulates a variety of pro-inflammatory responses and up-regulates anti-inflammatory responses, and has been used with therapeutic success in experimental collagen-induced arthritis, sepsis, Crohn's disease, and experimental autoimmune encephalomyelitis (EAE) in mice<sup>138, 205</sup>. Additionally, VIP appears to shift the Th1-Th2 balance in the favor of Th2 by promoting Th2-type cytokine production and, at the same time, by inhibiting Th1 development and responses<sup>143, 205</sup>.

More recently, new mechanisms have been proposed that identify the role of VIP in inducing and recruiting regulatory T (Treg) cells (Figure 34), important for maintaining immune homeostasis<sup>143</sup>. Both natural and inducible regulatory T cells are involved in immune tolerance and regulation. Natural Treg cells develop in the thymus as CD4<sup>+</sup>CD25<sup>+</sup>FoxP3<sup>+</sup> Tregs, and expand in the periphery<sup>140</sup>. So-called inducible Treg cells can be generated from CD4<sup>+</sup>CD25<sup>-</sup> and CD8<sup>+</sup>CD25<sup>-</sup> naïve T cells under certain stimulation patterns. Treg induction by VIP occurs in two primary pathways. First, VIP may directly activate naïve CD4<sup>+</sup>CD25<sup>-</sup> T cells to have a regulatory phenotype<sup>138, 140</sup>. Secondly, VIP steers immature dendritic cells (DCs) toward a tolerogenic

phenotype. Such tolerogenic DCs can then induce CD4+ and CD8+ naïve T cells toward a regulatory phenotype (inducible Tregs)<sup>140</sup>. Finally, VIP can induce tolerogenic dendritic cells to produce CCL22<sup>135</sup>. CCL22 is a chemokine important for the recruitment of regulatory T cells<sup>138</sup>.

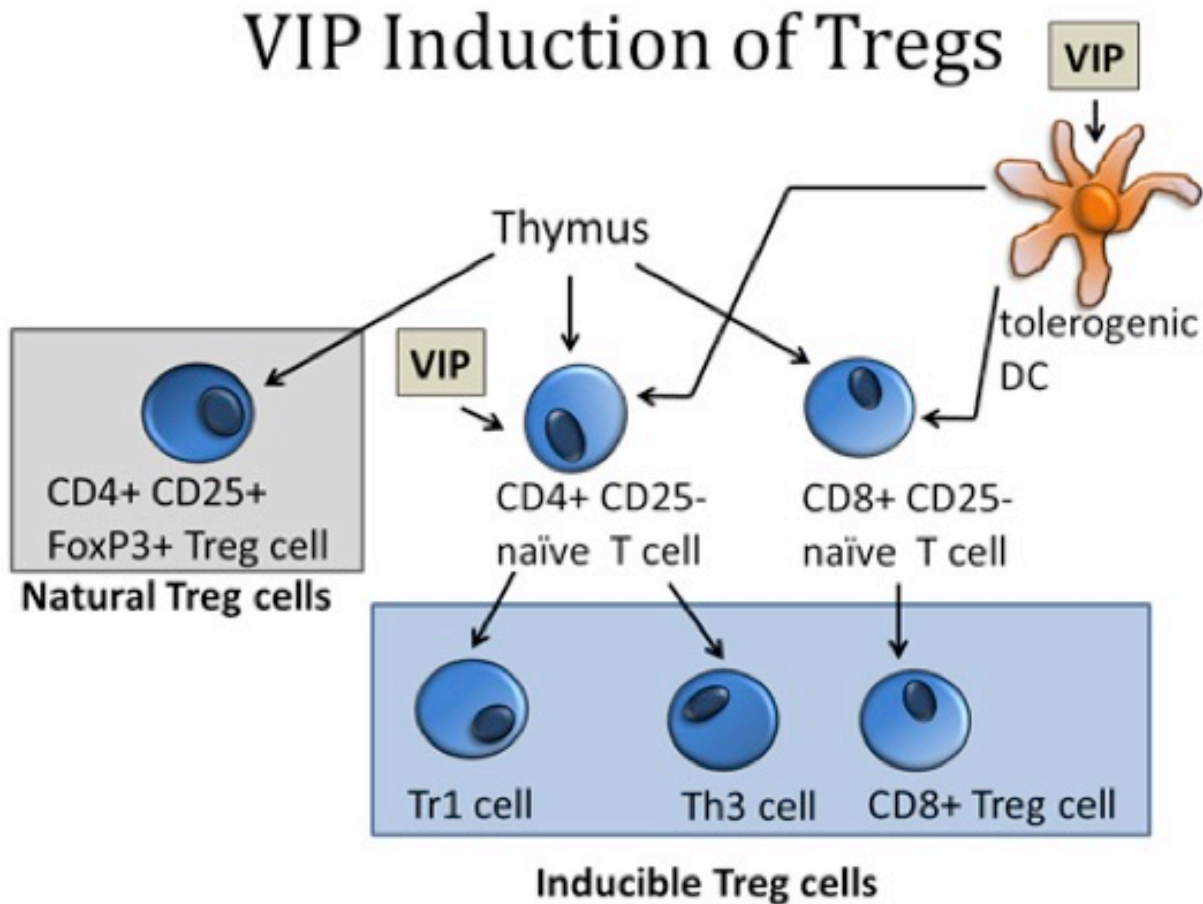


**Figure 34: Vasoactive intestinal peptide (VIP) may induce Tregs through multiple pathways. First, direct activation of CD4+CD25- naïve T cells to inducible Tregs, and second, activation of tolerogenic dendritic cells which then promote inducible Treg generation through activation of CD8+CD25- naïve T cells<sup>143</sup>.**

The major difficulty in VIP based therapies is the short half-life of VIP in the body<sup>206</sup>. One approach to address this challenge is developing VIP analogs which deliver the same therapeutic benefits as VIP but are metabolically stable<sup>207</sup>. Another approach is to protect the VIP by encapsulation into sterically stabilized liposomes<sup>206</sup>. However, VIP analogues only extend the half-life to 4 hours and the liposomes offer only short-term release, releasing 77-87% of encapsulated VIP within the first two hours *in vitro*<sup>206</sup>. Microspheres which deliver a longer lasting release profile are therefore a more promising approach to a VIP-based therapy.

## 4.2 METHODS

### 4.2.1 Vasoactive intestinal peptide (VIP) microsphere preparation

VIP PLGA microspheres were prepared following a model guided fabrication protocol using a double emulsion technique<sup>133</sup>, Figure 7 microsphere fabrication above. Four batches of microspheres were fabricated, and then combined in model specified ratios to obtain complex release behaviors. Three batches were comprised of individual PLGA polymer molecular weights using 4.2 kDa polymer, RG502H PLGA polymer (12.6 kDa), and RG505 polymer (55 kDa). Additionally, a fourth batch was fabricated with the 12.6 kDa polymer which contained Poly(ethylene glycol) (PEG) at approximately  $4 \times 10^{-4}$  mM in the inner aqueous phase. The inner aqueous phases of all VIP microspheres consisted of 1250  $\mu\text{g/ml}$  VIP. Unloaded (or “blank”) sets of particles were also fabricated for each batch.

In a separate study, nonporous and porous (with an inner aqueous phase comprised of 7.5 mM NaCl) VIP microspheres were prepared using RG502H polymer (approximately 12.6 kDa).

The inner aqueous phases of the nonporous and porous microspheres consisted of 1250 µg/ml VIP. Blank sets of nonporous and porous particles were also fabricated.

#### **4.2.2 VIP microsphere characterization**

The size distribution of each set of microspheres was determined using a Beckman Coulter Counter (Multisizer-3, Beckman Coulter, Fullerton, CA). Additionally, scanning electron microscopy was used to analyze the surface morphology microspheres (JEOL JSM-6330F, Peabody, MA).

#### **4.2.3 VIP microsphere *in vitro* release assays**

Release samples were collected for each of the batches of microspheres. Release was also measured for two sets of microspheres with varying polymer ratios determined by the computer model and by estimation to achieve linear and multi-bolus release. For the linear group, the model suggested microsphere ratios of 10.6% of the 4.2 kDa polymer, 31.9% of the 12.6 kDa polymer (without PEG), and 57.5% of the 100 kDa polymer. For multi-bolus release, 33.3% each of the 4.2 kDa, 12.6 kDa (with PEG), and 100 kDa polymers were mixed. Release was also measured for the porous and nonporous microsphere groups. Additionally, eight sets of blank microspheres for each group were also collected at each time-point. Release assays in PBS conducted for each set of microspheres. Ten milligrams of particles and 1 mL of PBS were incubated at 37°C. Vials were centrifuged at 2000 rpm, and 800µL of supernatant was removed and saved at -80°C, and replaced with fresh PBS for each time point. VIP concentration was determined using a VIP EIA kit purchased from Phoenix Pharmaceuticals. Samples were diluted up to 10x.

#### 4.2.4 Primary mouse dendritic cell isolation

Dendritic cells were isolated from murine bone marrow following the DC isolation lab protocol. Briefly, mouse hind limbs were harvested immediately post mortem and processed to extract murine dendritic cells. Mouse hind limbs were placed in 10 mL of MACS buffer in a petri dish, flesh and muscle was removed from the tibia and femur with scissors and tweezers. Cleaned leg bones were placed in another sterile petri dish containing 10 mL of MACS buffer. Both ends of the leg bones (tibia and femur) were cut with scissors. Using a 27.5 gauge needle and syringe, MACS buffer was washed through the center of the bone to elute bone marrow contents, and the process was repeated until all reddish tint (bone marrow) was removed from the bones. The remaining bone marrow MACS solution was filtered through 70  $\mu\text{m}$  filters into a 50 mL conical tube using a 5 mL syringe. The filtered bone marrow cells were centrifuged at 500g for 5 minutes at room temperature. Supernatant was aspirated and 1 mL of red blood cell (RBC) lysis buffer was added to the pelleted cells and cells were re-suspended and left to sit for 2 minutes, swiftly after incubation time 10 mL of dendritic cell complete media was added to the cells in RBC lysis buffer. Complete dendritic cell media (same as primary mouse T cell media) was composed of 500 mL of RPMI 1640 base media, 5 mL of HEPES buffer (100x), 5 mL of NEAA (100x), 5 mL of sodium pyruvate (100x), 0.5 mL of mercaptoethanol (1000x), 50 mL of fetal bovine serum (FBS) 10x, 5 mL of antibiotic/antimycotic concoction (100x) and 5 mL of L-glutamine (100x). The bone marrow cells in 1 mL of RBC lysis buffer and 10 mL of complete DC media were then centrifuged at 500g for 5 minutes at room temperature. Cells were re-suspended in complete DC media and viable cells were counted using trypan blue and a hemocytometer. Finally, 3 million bone marrow precursors were plated per petri dish after counting.

Dendritic cells were cultured from primary mouse bone marrow precursors in complete DC media supplemented with 2 ng/mL GM-CSF and 1 ng/mL IL-4. Media changes were conducted every 3 days, by tilting the petri dish and removing 5 mL of spent media and replacing with 10 mL of fresh complete DC media. On day 6 DC precursors were isolated from other remaining bone marrow cells using a CD11c positive isolation kit (Miltenyi Biotec catalog # 130-052-001) according to manufacturer instructions. After DC specific isolation, dendritic cells were matured with ipopolysaccharide (*E. coli* derived, Sigma) 1 µg/mL for 12 hours. Investigations using VIP, VIP was added as specified below.

#### **4.2.5 Primary mouse dendritic cell cultures with VIP**

Dendritic cell cultures were performed following a modified lab protocol. For CCL22 production studies, GMCSF and IL-4 were added to supernatants of bone marrow cell cultures during media changes on Days 0, 3 and 6. On Day 6, CD11c<sup>+</sup> DC cells were isolated using Macs cell sorting beads and plated into three 24-well plates at 100,000 cells/well. A mature DC control group received only LPS. An immature DC control group did not receive LPS. Soluble VIP was added in concentrations of 10<sup>-6</sup> M, 10<sup>-8</sup> M, and 10<sup>-9</sup> M to both immature DC groups and DCs matured with LPS. Twelve different groups were matured with LPS and received different concentrations of either blank porous, blank nonporous, VIP porous, or VIP nonporous microspheres (of the 12.6 kDa polymer). Microspheres were added in concentrations of either 2.77 mg/mL, 1.39 mg/mL, and 0.277 mg/mL. In a second DC culture, the low concentration of microspheres was reduced to 0.0556 mg/mL. At time-points of 7, 24, and 48 hours, 100 µl was removed from each well and frozen for ELISA analysis. 100 µl of fresh media was then added to each well after sample removal to maintain a total well volume of 600 µl.

For chemotaxis studies, in the first two experiments, both GM-CSF and IL-4 were added to DC media (modified RPMI 1640) of bone marrow cell cultures during media changes on Days 0, 3 and 6. In the third experiment, the IL-4 was purposely omitted and GM-CSF was added in 5x concentration. On Day 6, CD11c<sup>+</sup> DC cells were isolated using MACS cell sorting beads and plated in a 24-well plate at 100,000 cells/well. Five different groups of four wells each were analyzed and received treatment. An immature DC control group did not receive LPS. A mature DC control group received only LPS. Three different groups were matured with LPS and received different concentrations of either soluble VIP or releasates of VIP microspheres or blank microspheres (using the 12.6 kDa polymer). Soluble VIP was added to the third group in concentration of  $2.5 \times 10^{-8}$  M. Ten milligrams of microspheres were first incubated for 4-6 hours in media and 250  $\mu$ L of releasates were added to each well. After treatment, the DCs were incubated for approximately 18 hours. Prior to the CD4<sup>+</sup> T cell chemotaxis study, the 24-well plate was centrifuged and the media was removed. The cells were then starved with 600  $\mu$ L PBS+1%BSA and incubated for one hour prior to chemotaxis studies.

#### **4.2.6 Measuring CCL22 production by VIP treated DCs**

Measuring recombinant mouse CCL22, an ELISA test purchased from R&D Systems was used to measure CCL22 production by dendritic cells following modified lab protocol. An alternate blocking buffer of 1 mL Tween dissolved in 50 mL PBS was used. Cell culture media samples were diluted up to 500x.

#### 4.2.7 Primary mouse CD4<sup>+</sup> T cell isolation and chemotaxis

Murine CD4<sup>+</sup> T-cells were isolated from the spleen and lymph nodes of a mouse using Dynal beads following the lab protocol. Briefly, lymph nodes and spleen resected from mice were mechanically broken down in complete T cell (DC) media. Complete T cell was composed of 500 mL of RPMI 1640 base media, 5 mL of HEPES buffer (100x), 5 mL of NEAA (100x), 5 mL of sodium pyruvate (100x), 0.5 mL of mercaptoethanol (1000x), 50 mL of fetal bovine serum (FBS) 10x, 5 mL of antibiotic/antimycotic concoction (100x) and 5 mL of L-glutamine (100x). Cells were isolated from spleen and lymph nodes by using forceps to tear apart the tissue in a petri dish. Next a 5 mL syringe was used to further break down the tissue with repeated filling and excretion. Finally, cells were passed through a 70 µm filter. Cells were centrifuged at 300g for 5 minutes at 4 °C. Media was aspirated and 1 mL RBC lysis buffer was added to the cells (per spleen). After a 2 minute incubation, 5 mL of complete T cell media was added to the RBC lysis buffer re-suspended cells. Cells were centrifuged at 300g, for 5 minutes at 4 °C. Next, cells were counted by hemocytometer. Primary mouse CD4<sup>+</sup> T cells were negatively isolated using a Dynal® CD4 Negative Isolation kit (Invitrogen) according to manufacturer instructions.

For T cell chemotaxis, 3 µm Transwells were added to the 24-well plate containing the DCs in the bottom chamber and 100 µL of PBS and 1% BSA containing 500,000 CD4<sup>+</sup> cells were added to each transwell top chamber and incubated for two hours. T Cells that flowed through were analyzed for CD4<sup>+</sup>FoxP3<sup>+</sup> expression using flow cytometry.

#### 4.2.8 Murine periodontal disease induction

The mouse model for periodontitis was conducted as described previously<sup>97, 167</sup>. Briefly, wild type male C57BL/6J mice aged 8-weeks were purchased from Charles River Laboratories International, Inc., (Wilmington, MA). Mice were inoculated with *Actinobacillus actinomycetemcomitans* (ATCC 29522) cultured under anaerobic conditions and suspended in ~100  $\mu$ L of PBS supplemented with 2% carboxymethylcellulose (CMC) at  $1 \times 10^9$  CFU placed in the oral cavity. At 48 hours and 96 hours the inoculation was repeated, as shown in Figure 10, above. Negative controls received heat-killed-sham bacteria or only PBS supplemented with 2% CMC. All protocols were approved by the local Institutional Animal Care and Use Committees at the University of Pittsburgh.

#### 4.2.9 Bacteria cell culture

Bacterium, *Actinobacillus actinomycetemcomitans* (ATCC 29522) were cultured under anaerobic conditions. Briefly, *Actinobacillus actinomycetemcomitans* cultures were initiated according to ATCC instructions and plated on brucella blood agar supplemented with hemin and vitamin k1, plates were placed in an anaerobic chamber (Oxoid anaerojar 2.5 L) with an Oxoid anaerogen 2.5 L anaerobic sachet at 37°C. After 1 week of growth, bacteria were isolated with loops from the brucella agar and seeded in 100mL Brain Heart Infusion (BHI) (Becton, Dickson and company, BD) and cultured over night anaerobically (anaerobic jar, Oxoid anaerojar 2.5 L with an Oxoid anaerogen 2.5 L anaerobic sachet) at 37°C. *Actinobacillus actinomycetemcomitans* cultures were isolated from the BHI broth using centrifugation at  $>6000g$ , 10 minutes and washed 2 times with sterile PBS. Finally, *Actinobacillus actinomycetemcomitans* cultures were re-suspended in

Phosphate buffered saline (PBS) supplemented with 2% carboxymethylcellulose (CMC) at  $1 \times 10^9$  CFU.

#### **4.2.10 Assessment of periodontal disease-induced bone loss in mice**

To evaluate the extent of alveolar bone destruction, murine maxillary alveolar bone was quantified as described previously<sup>97, 167</sup>. Briefly, resected maxillae were mechanically defleshed and exposed to dispase or 3% hydrogen peroxide overnight to remove all soft tissue. Palatal and buccal faces of the molars were imaged using dissecting microscopes (Leica, Wetzlar, Germany or Olympus SZX10 with DP72 camera). Digitized images were analyzed using ImageJ (NIH) or ImageTool 2.0 (University of Texas Health Science Center, San Antonio, Texas, USA). The area between the cemento-enamel junction (CEJ) and the alveolar bone crest (ABC) was quantified using arbitrary units of area (AUA) or square micrometers.

### **4.3 RESULTS**

#### **4.3.1 VIP microsphere characterization**

Vasoactive intestinal peptide (VIP) was encapsulated in poly(lactic-co-glycolic) acid (PLGA) microspheres to achieve extended release and maintain bioactivity. VIP microspheres were fabricated using the 12.6 kDa PLGA in both a porous and non-porous formulation in order to find the most effective VIP release kinetics. Figure 35 below, shows the surface morphology of VIP

encapsulating PLGA microspheres. Porous PLGA microspheres, containing 7.5 mmol NaCl (porogen) in their inner aqueous phase (first emulsion) showed a slight increase in surface porosity as seen by the scanning electron micrograph, Figure 35 right. The PLGA microspheres had mean diameters of 16.9  $\mu\text{m}$  and 18.9  $\mu\text{m}$  for nonporous and porous particles, respectively, Figure 35 bottom. Importantly, both the non-porous and porous VIP microsphere formulations had average particle diameter greater than 10 microns, ensuring that they would avoid phagocytic removal upon implantation *in vivo*<sup>170</sup>.

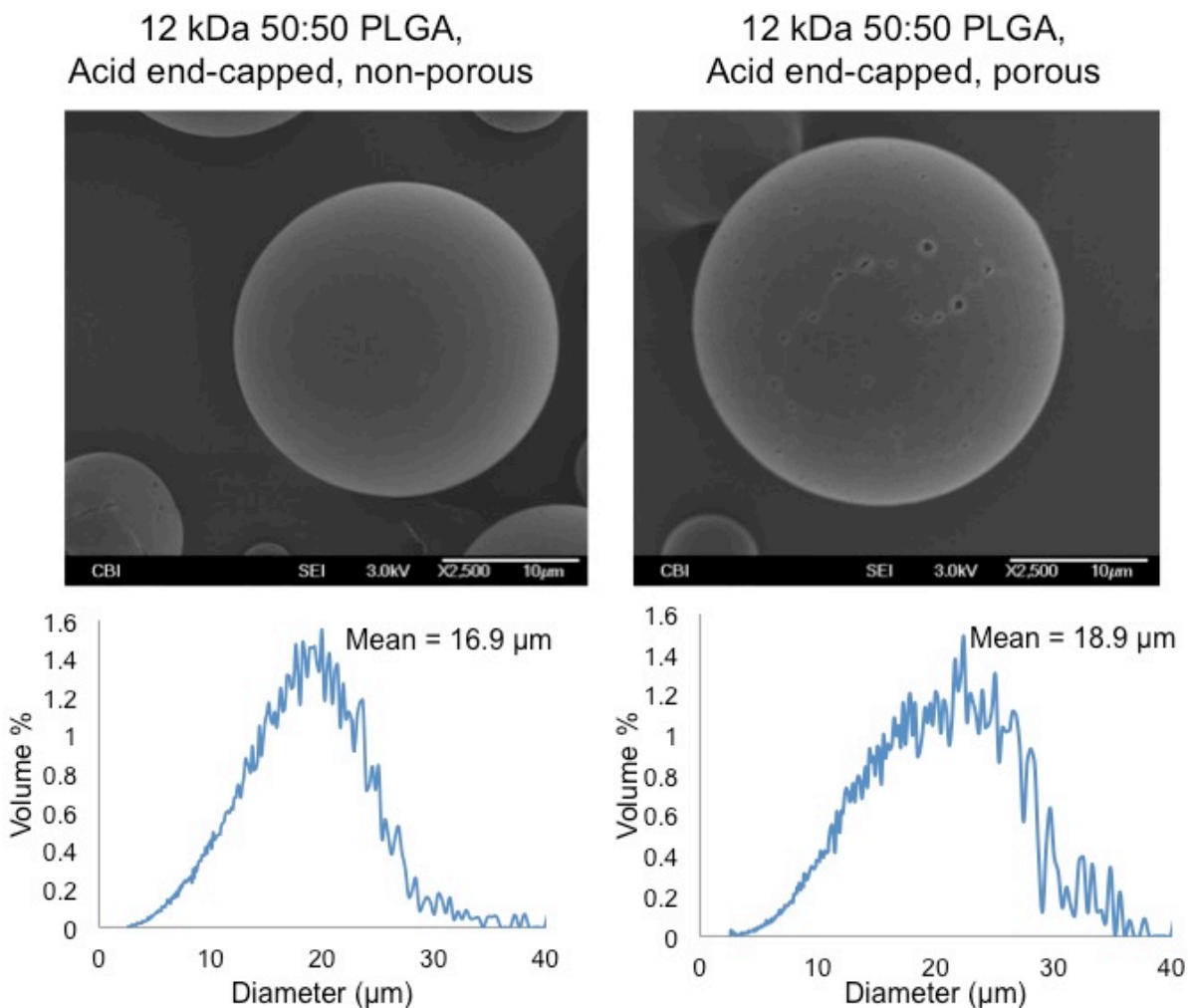


**Figure 35: Vasoactive intestinal peptide loaded PLGA microspheres. VIP microspheres composed of 12.6 kDa PLGA (50:50) showed non-porous and porosity on scanning electron micrographs. Furthermore, size distributions of the microspheres revealed that the non-porous microspheres had a mean diameter of 16.9 microns, and the porous microspheres had a mean diameter of 18.9 microns.**

#### 4.3.2 VIP *in vitro* release from PLGA microspheres

Prior to *in vitro* bioactivity assay and *in vivo* efficacy, VIP microsphere cumulative release was measured from both porous and non-porous 12.6 kDa PLGA. Porous VIP microspheres were

fabricated with 7.5 mmol NaCl in the inner aqueous phase (first emulsion), were non-porous microspheres did not have any porogen added. The nonporous VIP microspheres experienced a slight initial burst and a secondary burst around Day 14, Figure 36. The porous VIP particles experienced less of an initial burst and slower release than the nonporous particles, Figure 36. Overall, both VIP PLGA microspheres exhibited extended release of VIP over a period of 30 days, Figure 36.

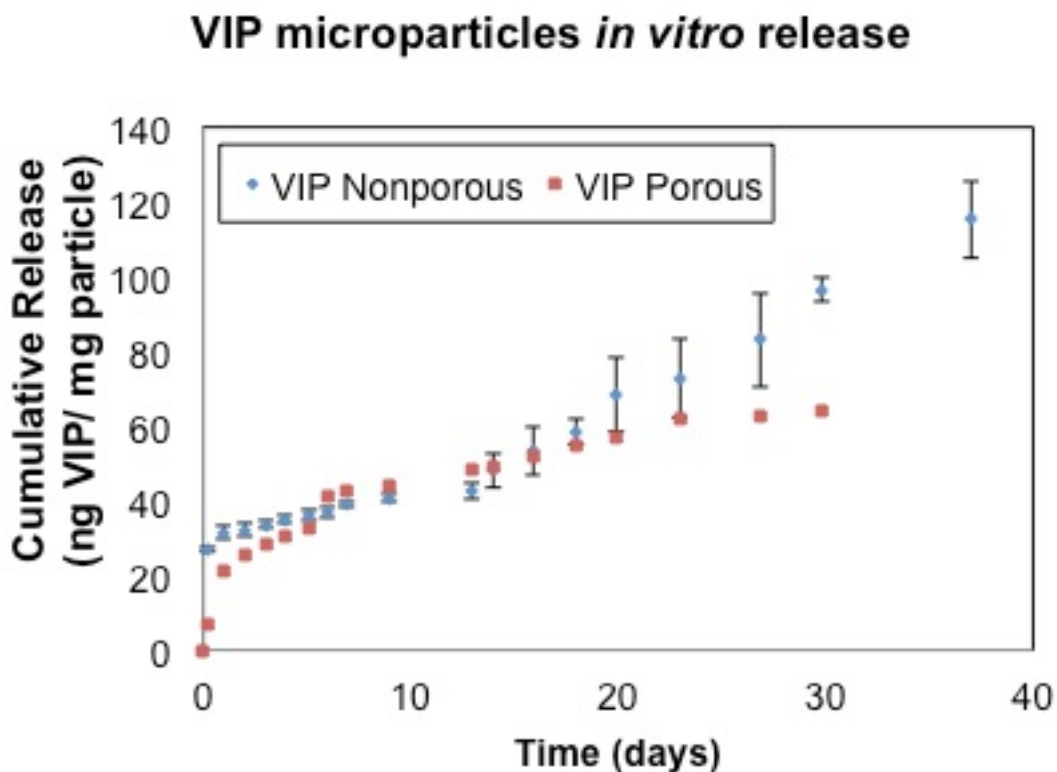
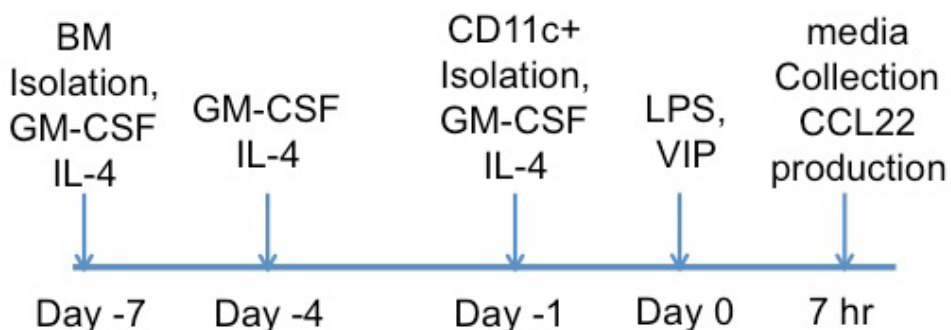


Figure 36: Controlled release of vasoactive intestinal peptide (VIP) from PLGA microspheres. Porous microspheres were fabricated with 7.5 mmol NaCl in the first emulsion, inner aqueous phase, non-porous microspheres received no porogen. Cumulative release of VIP shown in phosphate buffered saline (PBS).

### 4.3.3 VIP microspheres induce CCL22 production by dendritic cells

Primary mouse dendritic cell cultures were completed with and without VIP microspheres to measure the reported production of CCL22, a chemokine known to recruit regulatory T cells<sup>45, 46, 135</sup>. Dendritic cells were cultured and treated according to the schedule below, Figure 37, and CCL22 production was measured from DC cultured media (ELISA).



**Figure 37: CCL22 production by dendritic cells treated with VIP microspheres experimental schedule.**

Primary mouse dendritic cells, cultured with GM-CSF and IL-4 were purified using CD11c+ MACS beads to isolate dendritic cells from other bone marrow cells. Dendritic cells (DCs) were matured with lipopolysaccharide (LPS) derived from *E. coli*, a TLR4 activator of dendritic cells. Dendritic cells matured and treated with soluble vasoactive intestinal peptide (VIP) exhibited a slight increase in CCL22 production (Figure 38), however, CCL22 production was very comparable to DCs matured without VIP treatment, contrary to published reports<sup>135</sup>. Importantly, both VIP porous and non-porous PLGA microsphere treated DCs exhibited increased CCL22 production compared to blank PLGA microsphere controls, Figure 38. While, VIP porous microspheres appeared to induce less CCL22 production from DCs, non-porous VIP microspheres

led to comparable amounts of CCL22 from dendritic cells, Figure 38. Based on these results, VIP non-porous microspheres appeared to be releasing more bioactive VIP given similar treatment schedules than porous VIP microspheres and therefore the non-porous VIP microspheres were used for further *in vitro* and *in vivo* testing.

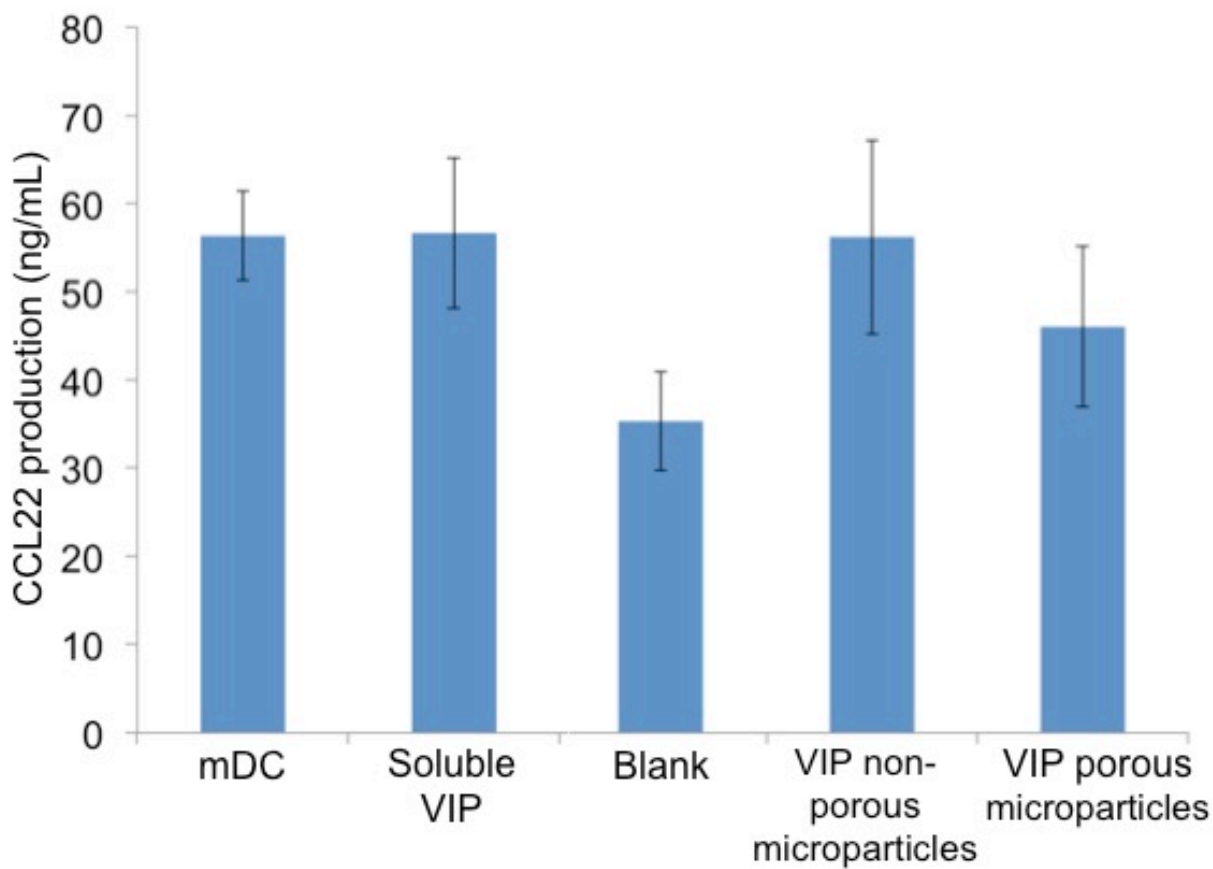


**Figure 38: CCL22 production from VIP microsphere treated murine dendritic cells. Primary mouse dendritic cells were cultured and matured with LPS, then treated with soluble VIP, or VIP microspheres, blank PLGA microspheres served as controls. Media was sampled for CCL22 production (measured by ELISA) 7 hours after LPS and VIP treatment.**

#### **4.3.4 VIP microsphere-treated dendritic cells recruit CD4<sup>+</sup>FoxP3<sup>+</sup> regulatory T cells *in vitro***

Next, to determine how effectively dendritic cells treated with VIP microspheres could recruit regulatory T cells (Tregs) an *in vitro* chemotaxis assay was used. Utilizing transwell migration assay tissue culture filters, VIP microsphere treated dendritic cells were placed as well as (separately) control treated DCs in the bottom wells, and primary mouse CD4 positive T cells in the top wells. Natural Tregs that migrated toward the VIP microsphere treated DCs were analyzed using flow cytometry for FoxP3 positive expression. All wells were normalized against immature (no LPS) treated dendritic cells. Mature (LPS treated) DCs, Soluble VIP treated, VIP non-porous microsphere treated and Blank PLGA microsphere-treated DCs all exhibited more Treg recruitment than immature DC controls, values greater than 1 (normalized against immature DCs, Figure 39), suggesting immature DCs do not produce high amounts of Treg recruiting factors. Soluble VIP treated mature DCs showed the most Treg specific recruitment, followed by VIP non-porous PLGA microspheres, suggesting VIP microspheres do release bioactive vasoactive intestinal peptide, Figure 39. Based on these *in vitro* bioactivity assays, it was decided to test the efficacy of the non-porous VIP microspheres in the mouse model for periodontal disease.

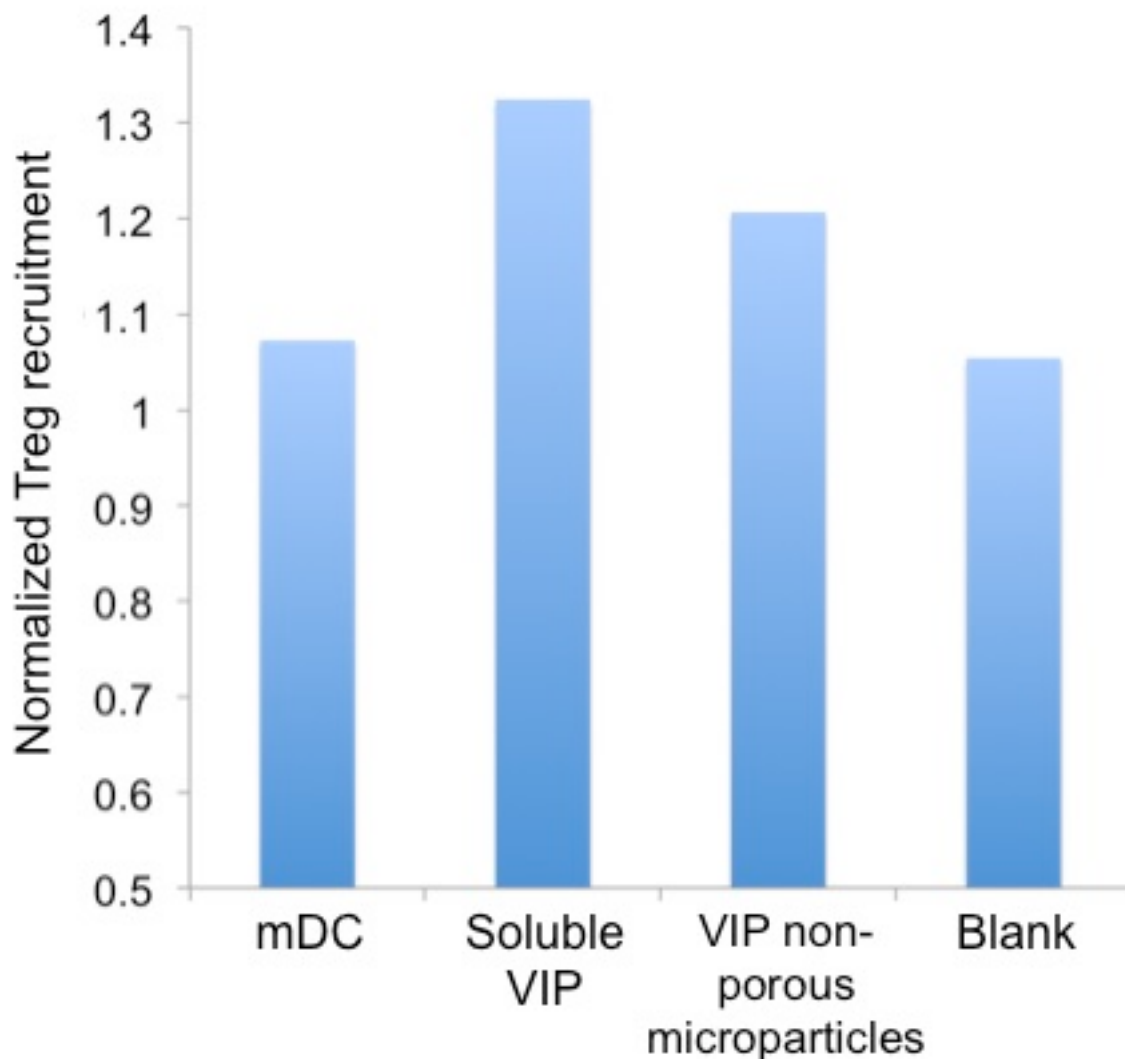


**Figure 39: Mature dendritic cells (DCs) treated with vasoactive intestinal peptide (VIP) released from PLGA microspheres recruit more Tregs than mature DCs or blank PLGA microsphere treated DCs. Transwell migration assay using 3  $\mu\text{m}$  transwell filters, primary dendritic cells matured with LPS (or immature, no LPS normalized control) were treated with soluble VIP  $2.5 \times 10^{-8}$  M concentration, VIP non-porous PLGA microspheres (estimated quantity comparable to  $2.5 \times 10^{-8}$  M VIP) or blank PLGA microspheres were placed in the bottom wells. Primary mouse CD4<sup>+</sup> T cells were placed in the top transwell chambers, and left for 2 hours to migrate to the VIP treated dendritic cells. Cells from the bottom well were collected and analyzed using flow cytometry to quantify the number of CD4<sup>+</sup>FoxP3<sup>+</sup> Regulatory T cells that migrated through the transwell filters.**

#### **4.3.5 Vasoactive intestinal peptide PLGA microspheres reduce alveolar bone loss in murine periodontitis**

Utilizing the *Actinobacillus actinomycetemcomitans* experimental mouse model for periodontal disease in C57 black/6 mice, mice received VIP non-porous PLGA microspheres or CCL22 microspheres on days -1, 10 and 20 relative to disease induction. Figure 40 A shows representative dissecting microscope images of resected and defleshed maxilla from mice treated with Blank PLGA microsphere controls, CCL22 microspheres and non-porous VIP microspheres. CCL22 microsphere treated, and VIP microsphere treated mice exhibited significantly less alveolar bone loss 30 days after disease induction, Figure 40 A and B. Taken together, this data suggest that VIP microspheres release bioactive VIP that can recruit Tregs and ameliorate periodontal disease symptoms in mice.

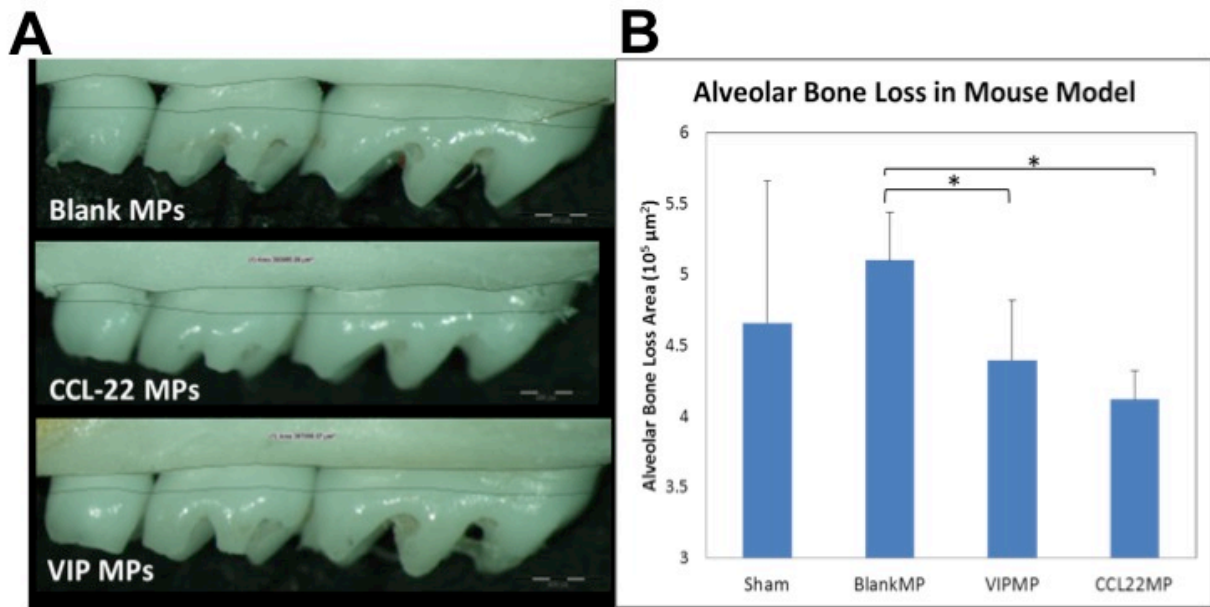


**Figure 40: Vasoactive intestinal peptide microspheres reduce alveolar bone loss in an experimental mouse model of periodontal disease. (A) Representative stereoscope images of defleshed maxilla from C57BL/6J mice infected with *Actinobacillus actinomycetemcomitans* (*Aa*) 30 days after inoculation. Results of treatment with blank unloaded PLGA controls, CCL22 microsphere, and VIP microspheres injected into the maxillary gingiva at days -1, 10 and 20 relative to first *Aa* inoculation. (B) Quantification of the area between the cemento enamel junction (CEJ) and alveolar bone crest (ABC) on the buccal tooth surface. Sham infected mice received heat killed *Actinobacillus actinomycetemcomitans* and served as positive controls. \*P < 0.05 determined by student T test.**

#### 4.4 DISCUSSION

As an alternative to direct CCL22 controlled release for Treg recruitment (presented earlier), a molecule originally discovered as a vasodilator (vasoactive intestinal peptide, or VIP), has been found to possibly enhance Treg recruitment and induction of Tregs locally through a variety of mechanisms<sup>142, 143</sup>. Originally, VIP was identified as a neuropeptide associated with endothelial

cells in the intestinal environment, but later was shown to be a potent immunomodulator<sup>136, 137</sup>. Additionally, VIP was shown to attenuate inflammatory and autoimmune reactions possibly through aiding in the direct induction of regulatory T cells<sup>138-140</sup>. Importantly, VIP was also found to strongly influence bone metabolism by way of inhibiting osteoclastogenesis (bone resorbing cells) and promoting osteoblastogenesis (bone forming cells)<sup>137, 141</sup>. Therefore, VIP may be a viable alternative controlled release therapeutic peptide for periodontal disease, possibly functioning by inducing the local recruitment of Tregs (via inducing CCL22 expression), aiding in the direct induction of Tregs, or even altering the damaging inflammatory response leading to alveolar bone resorption<sup>135-137, 139, 141-143</sup>.

Various tactics can be employed to alter the release of encapsulated VIP from PLGA microspheres. VIP release was slowed as with the use of non-porous PLGA microspheres, whereas the addition of NaCl slightly increased the initial release rate of VIP from PLGA microspheres. However, both the porous and non-porous PLGA microspheres released VIP at a very similar rate, suggesting that other interactions may be effecting the release of VIP from PLGA. Indeed, VIP has an isoelectric point of 11.8 (~ 3 higher than CCL22 microspheres, which also display charge interactions with PLGA microspheres<sup>172</sup>), meaning VIP is very positively charged at neutral pH while PLGA is negatively charged, leading to ionic interactions<sup>172</sup>. Regardless, VIP encapsulation in PLGA microspheres significantly extended the release of VIP compared to previous attempts to controllably release VIP, extending the release from hours to up to 30 days<sup>206</sup>, Figure 36 above, VIP release from PLGA microspheres.

The data above suggests that VIP released from PLGA microspheres appeared bioactive in the *in vitro* dendritic cell (DC) cultures (Figures 38 and 39 above). The observed CCL22 production of DCs treated with microspheres was significantly higher than that of the respective

blank microspheres and showed significant increase at 7 hours in the nonporous VIP group. The effects of the presence of LPS for an extended time period have not been determined but are thought to be detrimental for the cells, therefore time-points after 7 hours were not ideal. Additionally, the microspheres themselves may negatively impact the cells and cause lower CCL22 production by DCs relative to the control and soluble VIP groups. It is well known that PLGA degrades into acidic lactic acid and glycolic acid residues in an aqueous environment<sup>151</sup>, and this could help explain the observed decrease in the bioactivity of blank PLGA unloaded control treated DCs. The particle degradation products, such as PLGA fragments or lactic or glycolic acid, may disrupt the cells and may cause some cells to die<sup>151</sup>.

Additionally, it was expected that the DCs cultured with soluble VIP would show a more significant increase in CCL22 production relative to the mature DC control group, as was shown in previous studies<sup>135</sup>. IL-4 has been proposed to skew DC differentiation to exhibit a regulatory phenotype<sup>208</sup>, so there was a concern that the IL-4 used to culture the DCs diminished the difference in CCL22 production between the groups. In future chemotaxis studies that measure FoxP3<sup>+</sup> T-cell recruitment by DCs treated with VIP microsphere releasate, omission of IL-4 during cell culture may increase the distinction between FoxP3<sup>+</sup> T cell recruitment. Overall, it appears that VIP induction of CCL22 from dendritic cells led to significant FoxP3<sup>+</sup> Treg migration *in vitro*.

After demonstration of the bioactivity of VIP microspheres *in vitro*, it was shown that the VIP microspheres also promote therapeutic effects *in vivo*. VIP microspheres significantly reduced bone loss in mice infected with periodontal disease relative to mice treated with blank microspheres. Next steps would be to repeat the mouse model of VIP microsphere treated periodontitis and obtain additional data supporting the recruitment or the expansion of Tregs

locally in response to VIP microsphere treatments. QPCR analysis and flow cytometry can be conducted in the future to measure the expression of FoxP3<sup>+</sup> T cells (Tregs) in draining lymph nodes and in the periodontal pocket. A higher expression of FoxP3<sup>+</sup> T cells (Tregs) in draining lymph nodes is expected to show that VIP microspheres induce the production of Tregs. Additionally, an increase in tolerogenic DCs in draining lymph nodes is expected and can be evaluated by observing a decrease in CD86 and CD80 and MHCII on the DCs using flow cytometry.

## 5.0 ENGINEERING LOCAL TREG-INDUCING MICROSPHERES FOR THE TREATMENT OF PERIODONTAL DISEASE IN A MOUSE MODEL

### 5.1 INTRODUCTION

Aside from recruitment (using molecules such as CCL22 or VIP described above), regulatory T cells populations are naturally bolstered by the combination of specific anti-inflammatory cytokines in the presence of antigen presenting cells (APCs). Specifically, some tumors have been shown to secrete IL-10 and TGF- $\beta$  ultimately resulting in APC-mediated induction of regulatory T cells (iTregs), ultimately aiding in tumor evasion of anti-cancer immune responses<sup>209</sup>. This strategy can be replicated *ex vivo* in order to boost and expand Tregs for therapeutic re-administration<sup>15</sup>. Although many groups have reported success in animal models in several disease models, translation of the complicated *in vitro* protocols (often using difficult to maintain and culture, genetically modified dendritic cells) to the clinical setting has been difficult, faulting reproducibility and reliability<sup>15</sup>. For this reason, we hypothesized that formulations could be created to accomplish this task *in situ*, locally in the periodontium rather than having to resort to *ex vivo* expansion of cells

Another way to enhance the numbers of regulatory T cells *in situ* may be through the induction of local T cells towards Treg phenotypes (as opposed to T effector cell phenotypes) via biological enhancers of Treg populations. Several different strategies have been utilized to directly induce Tregs *in vivo*, for example: anti-IL-2 monoclonal antibodies<sup>144</sup>, superagonistic anti-CD28 monoclonal antibodies<sup>145</sup>, and agonistic anti-CD4 monoclonal antibodies<sup>146</sup>. However, the therapeutic mechanisms of these antibodies are not well understood, especially in the context of

human trials, where their safety remains a concern. In fact, phase 1 trials of the superagonistic anti-CD28 monoclonal antibodies led to a severe and damaging cytokine storm in all humans who received the treatment<sup>147</sup>. Aside from these antibodies, other molecules have been identified to induce regulatory T cell development, including: IL-2, TGF- $\beta$  and Rapamycin<sup>51</sup>. Specifically, the use of these factors has been shown to aide in the development of Tregs *in vivo* and *in vitro*, even under inflammatory conditions<sup>51, 148-150</sup>.

Recently, the controlled release of IL-2, TGF- $\beta$  and Rapamycin from PLGA microspheres (conducted in our laboratory) has been shown to specifically induce regulatory T cells from naïve CD4<sup>+</sup> T cells in both human and mouse cells *in vitro*<sup>51</sup>. Specifically, the combination of IL-2, TGF- $\beta$  and Rapamycin released from PLGA microspheres led to the robust expansion of a 80% pure population of Tregs, as opposed to soluble IL-2 expanded naïve T cells which robustly expanded T cells, but only led to 3% of cells expressing Treg marker FoxP3<sup>51</sup>. Furthermore, Tregs induced from IL-2, TGF- $\beta$  and Rapamycin releasing PLGA microspheres displayed phenotypic markers of Tregs and functionally suppressed T effector cells *in vitro*<sup>51</sup>. Ultimately, multiple strategies utilizing acellular-engineered approaches may help to increase the local populations of regulatory T cells, and have the potential to be used therapeutically in periodontal disease. Ultimately, multiple factor-releasing strategies utilizing acellular-engineered approaches may help to increase the local populations of regulatory T cells, and have the potential to be used therapeutically in periodontal disease.

Furthermore, *in situ* expansion of Tregs may be an even more promising strategy to increase the local presence of regulatory T cells given the high prevalence of naïve CD4<sup>+</sup> cells that could be differentiated into Treg<sup>167, 210</sup>. Additionally, the IL-10 and TGF- $\beta$  (cytokines secreted from Tregs) have been shown to induce both soft and hard tissue regeneration even in disease<sup>52, 53</sup>,

<sup>55-57, 211</sup>, suggesting Tregs may have a paracrine effect on periodontal regeneration. Additionally, the IL-10 and TGF- $\beta$  secreted by Tregs may have an autocrine effect and further promote the induction and differentiation of Tregs from naïve T cells<sup>12, 13</sup>. We hypothesize that the *in situ* induction and recruitment of Tregs using engineered biomimetic microspheres strategies (IL-2, TGF- $\beta$  and rapamycin microspheres) may provide the optimal adjunct therapy for the treatment of periodontal disease.

To test this hypothesis, that Treg inducing formulations, capable of *in situ* expansion of Treg populations from naïve T cell precursors, may provide a more robust adjunct therapy for the treatment of periodontal disease, the mouse model for periodontal disease was utilized. Although the recruitment of natural endogenous regulatory T cells (nTregs) via CCL22 microspheres is a very promising technology for the treatment of periodontitis, it is foreseeable that some patients may have insufficient numbers of nTregs or dysfunctional nTregs (in fact, researchers have begun exploring disease mechanisms that could be a result of dysfunctional nTregs<sup>212, 213</sup>). Therefore, a combination of microspheres that release factors capable of inducing and expanding Tregs from naïve conventional T cells (generating induced Tregs or iTregs) may provide a potent adjunct therapy for periodontal disease.

## **5.2 METHODS**

### **5.2.1 Treg inducing microsphere fabrication**

Poly (lactic-co-glycolic) acid (PLGA) microspheres containing recombinant mouse interleukin 2 (IL-2, R&D systems, Minneapolis, MN) or recombinant human transforming growth factor beta 1

(TGF- $\beta$ 1 Cat.# 101-B1-001, Peprotech, Rocky Hill, NJ) were prepared using a standard water-oil-water double emulsion procedure as described<sup>46</sup>, Figure 7. Blank (unloaded) PLGA microsphere controls were fabricated in the same manner with the exception of the protein encapsulate. Briefly, the TGF- $\beta$  PLGA (RG502H, Boehringer Ingelheim, Petersburg, VA) microspheres were prepared by mixing 200  $\mu$ L of an aqueous solution containing with 10  $\mu$ g of recombinant human TGF- $\beta$ 1 (Peprotech, Rocky Hill, NJ) in deionized water (DI water). For TGF- $\beta$  microspheres, 170 mg of RG502H (Boehringer Ingelheim, Petersburg, VA) were mixed with 30 mg of 20 kDa PLGA co-blocked with polyethylene glycol (PEG) to make up the 200 mg of polymer for microsphere fabrication, and was dissolved in 4 mL of dichloromethane. The first water-in-oil emulsion was prepared by sonicating this solution for 10 seconds. The second oil-in-water emulsion was prepared by homogenizing (Silverson L4RT-A) this solution with 60 mL an aqueous solution of 2% polyvinyl alcohol (M.W. ~25,000, 98 mol. % Hydrolyzed, PolySciences, Warrington, PA) for 60 seconds at 3000 RPM. This solution was then mixed with 1% polyvinyl alcohol and placed on a stir plate agitator for 3 hours to allow the dichloromethane to evaporate. The microspheres were then collected and washed 4 times in deionized (DI) water, to remove residual polyvinyl alcohol, before being re-suspended in 5 mL of DI water, frozen, and lyophilized for 72 hours (Virtis Benchtop K freeze dryer, Gardiner, NY; operating at 100mTorr).

For IL-2 microspheres, 5  $\mu$ g of recombinant mouse interleukin 2 (IL-2, R&D systems, Minneapolis, MN), aliquoted in phosphate buffer saline (PBS) 50  $\mu$ L, was added to 150  $\mu$ L of DI water, creating an inner aqueous phase with 76.6 mmol osmolality. 200 mg of RG502H PLGA polymer (Boehringer Ingelheim, Petersburg, VA) for microsphere fabrication, and was dissolved in 4 mL of dichloromethane. The first water-in-oil emulsion was prepared by sonicating this solution for 10 seconds. The second oil-in-water emulsion was prepared by homogenizing

(Silverson L4RT-A) this solution with 60 mL an aqueous solution of 2% polyvinyl alcohol (M.W. ~25,000, 98 mol. % Hydrolyzed, PolySciences, Warrington, PA), supplemented with 61.6 mmol of NaCl, for 60 seconds at 3000 RPM. This solution was then mixed with 1% polyvinyl alcohol, supplemented with 61.6 mmol of NaCl, and placed on a stir plate agitator for 3 hours to allow the dichloromethane to evaporate. The microspheres were then collected and washed 4 times in deionized (DI) water, to remove residual polyvinyl alcohol, before being re-suspended in 5 mL of DI water, frozen, and lyophilized for 72 hours (Virtis Benchtop K freeze dryer, Gardiner, NY; operating at 100mTorr). A total 10 mmol osmolality was used inside the first emulsion inner aqueous phase to generate porous IL-2 microspheres.

For rapamycin microspheres, a single emulsion fabrication technique was used to encapsulate rapamycin in PLGA microspheres, Figure 41. Briefly, 100  $\mu$ L aliquots of 10 mg/mL rapamycin in DMSO was added to 4 mL of dichloromethane along with 200 mg of polymer for microsphere fabrication. The single emulsion microspheres (oil-in-water) was prepared by homogenizing (Silverson L4RT-A) this solution with 60 mL an aqueous solution of 2% polyvinyl alcohol (M.W. ~25,000, 98 mol. % Hydrolyzed, PolySciences, Warrington, PA) for 60 seconds at 3000 RPM. This solution was then mixed with 1% polyvinyl alcohol and placed on a stir plate agitator for 3 hours to allow the dichloromethane to evaporate. The microspheres were then collected and washed 4 times in deionized (DI) water, to remove residual polyvinyl alcohol, before being re-suspended in 5 mL of DI water, frozen, and lyophilized for 72 hours (Virtis Benchtop K freeze dryer, Gardiner, NY; operating at 100mTorr).

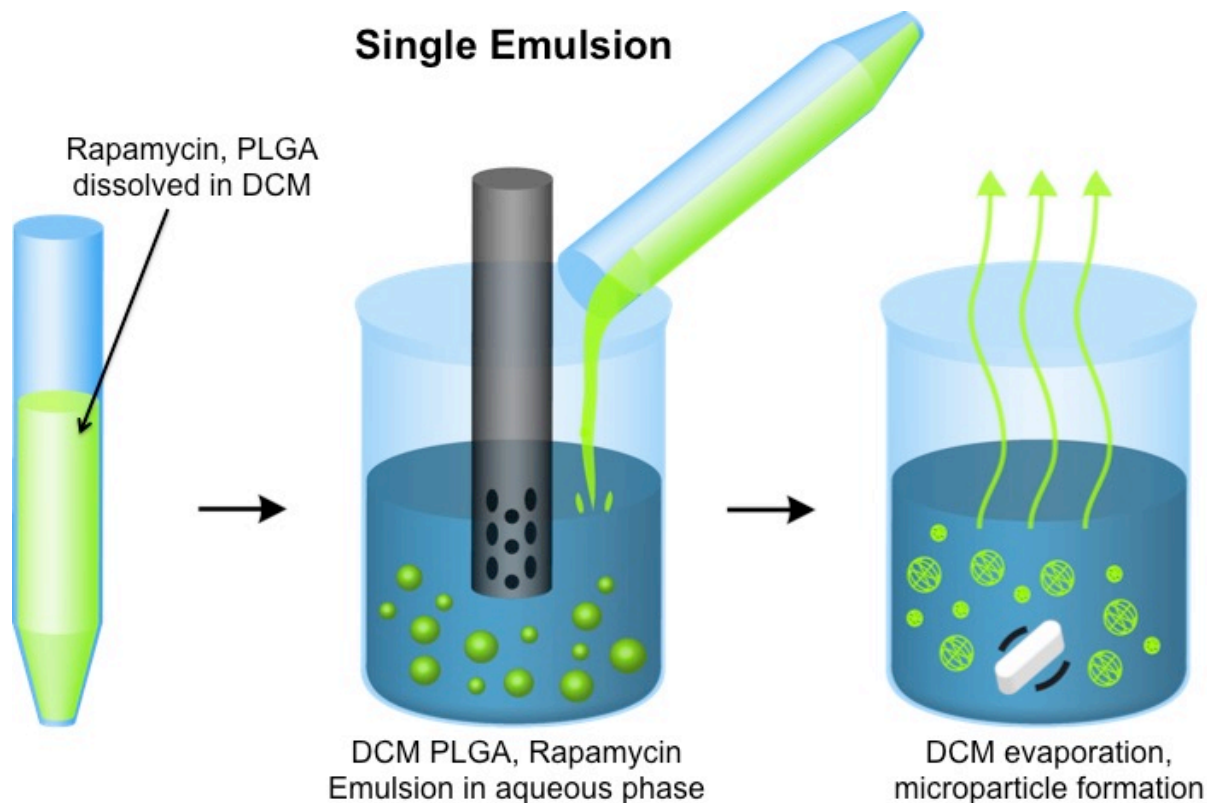


Figure 41: Single emulsion PLGA microspheres fabrication for rapamycin microspheres.

## 5.2.2 Characterization of Treg inducing microspheres formulations

Surface characterization of microspheres was conducted using scanning electron microscopy (JEOL JSM-6330F, Peabody, MA) and microsphere size distribution was determined by volume impedance measurements on a Beckman Coulter Counter (Multisizer-3, Beckman Coulter, Fullerton, CA). TGF- $\beta$ 1, and IL-2 and Rapamycin release from microspheres was determined by suspending 7-10 mg of microspheres in 1 mL of phosphate buffered saline (PBS) placed on an end-to-end rotator at 37°C. Release sampling was conducted at various time intervals by centrifuging microspheres and removing the supernatant for TGF- $\beta$ 1, and IL-2 quantification using ELISA (R&D Systems, Minneapolis, MN), the amount of rapamycin was determined by

spectrophotometry absorbance at 278 nm, sampling of releasates is shown in Figure 8 Above. Microspheres were re-suspended with 1 mL of fresh PBS and returned to the rotator at 37°C.

### **5.2.3 Treg inducing microsphere administration in mice**

For mouse investigations microspheres were administered to 4 sites via 2% carboxy methyl cellulose (CMC) in PBS suspension. Specifically, 2-5  $\mu$ L of solution containing 25 mg/mL of particles were administered to the proximal side of the first molar, each inter-dental site, and distal to the third molar of the right maxilla of the mice, shown in Figure 9 below. Microspheres were injected into maxillary gingiva of mice using 27-28.5 gauged insulin syringes. For BALB/cJ mice inoculated with *Porphyromonas gingivalis*, microspheres were injected on days -1, 20, and 40 relative to the first bacterial inoculation, shown in Figure 11 above. Microspheres were injected in mice at a depth of approximately 100-300 microns within the maxillary gingival tissues. All microsphere injections in mice were performed under a stereomicroscope. Small amounts of the microsphere solution were observed to overflow into the oral cavity of the mice during injections.

### **5.2.4 Periodontal disease induction in mice**

For experiments using *Porphyromonas gingivalis* as a colonizing periodontopathogen in BALB/cJ mice periodontitis was induced as described<sup>97</sup>. Briefly, male BALB/cJ mice age 6-8 weeks were purchased from Jackson Laboratories. To reduce the commensal oral bacteria, the drinking water of mice was modified with 15 mL/L of Sulfatrim Pediatric Suspension (sulfamethoxazole and trimethoprim, 2 mg/mL wt/vol and 0.4 mg/mL wt/vol, Henry Schein) for 10 days. After 10 days of antibiotic water, the mice were given clean drinking water for 5 days to prevent any direct

microbicidal effects of the antibiotic solution on the colonization of the oral pathogen. Mice were then colonized 3 times during the first week at 2 day intervals with *Porphyromonas gingivalis* (*Pg*, ATCC 33277) grown under anaerobic conditions, as shown in Figure 11. Bacteria were plated on brucella blood agar supplemented with hemin and vitamin k1, on days of inoculation, *Pg* was suspended in brain heart infusion (BBL BHI, BD Biosciences, San Jose, CA) supplemented with 2% carboxymethylcellulose at  $1 \times 10^{11}$  CFU. Mice received 0.5 mL of the *Pg* BHI suspension orally administered with gavage feeding needle.

### 5.2.5 Bacteria cultures

Bacterium *Porphyromonas gingivalis* (*Pg*, ATCC 33277) were cultured from isolates according to ATCC instructions. Briefly, *Porphyromonas gingivalis* isolates were suspended in tryptic soy broth (TSB) supplemented with hemin, vitamin k1 and L-cystine and cultured anaerobically (anaerobic jar, Oxoid anaerojar 2.5 L with an Oxoid anaerogen 2.5 L anaerobic sachet) at 37°C. After 48 hours *Porphyromonas gingivalis* cultures were isolated from the broth with centrifugation at  $>6000g$ , 10 minutes. Cultures were concentrated with TSB and plated on brucella blood agar supplemented with hemin and vitamin k1 and cultured anaerobically (anaerobic jar, Oxoid anaerojar 2.5 L with an Oxoid anaerogen 2.5 L anaerobic sachet) at 37°C, or glycerol was added to TSB based cultures O.D. 660 ~ 0.6 ABS, and cryopreserved for future use. After 5-7 days *Pg* plated on brucella blood agar supplemented with hemin and vitamin k1 turned black (pigment) and cultures were collected with loop for mouse infection. *Pg* was suspended in brain heart infusion (BBL BHI, BD Biosciences, San Jose, CA) supplemented with 2% carboxymethylcellulose at  $1 \times 10^{11}$  CFU (approximately 1 plate of *Pg* for every 3 mice to be infected).

### 5.2.6 Assessment of periodontal disease induced bone loss in mice

To evaluate the extent of alveolar bone destruction, murine maxillary alveolar bone was quantified as described previously<sup>97, 167</sup>. Briefly, resected maxillae were mechanically defleshed and exposed to dispase or 3% hydrogen peroxide overnight to remove all soft tissue. Palatal and buccal faces of the molars were imaged using dissecting microscopes (Leica, Wetzlar, Germany or Olympus SZX10 with DP72 camera). Digitized images were analyzed using ImageJ (NIH) or ImageTool 2.0 (University of Texas Health Science Center, San Antonio, Texas, USA). The area between the cemento-enamel junction (CEJ) and the alveolar bone crest (ABC) was quantified using arbitrary units of area (AUA) or square micrometers. Alternatively, mice maxilla were resected and fixed with 10% formalin and stored in 70% ethanol (30% water). Fixed maxilla were scanned by SCANCO vivaCT 40 micro-computed tomography (microCT) system (Switzerland). 3D images were reconstructed with SCANCO software at the same threshold across all the samples. Each scan was reoriented with DataViewer (GE Healthcare, London, ON). The images were reoriented by the planes adjusted to the cemento-enamel junction (CEJ), bucco-lingual center of the roots, and parallel to the root canal in the center of distal root. To assess the vertical bone reduction, the distance between CEJ and alveolar bone crest (ABC) was measured at the distal face and buccal face of the fourth premolar and the first molar after microCT image reorientation. Along the buccal face of the tooth, the ABC-CEJ distance was measured at 24 sites along the M1 molar, 10 sites along the M2 molar and 4 sites on the M3 molar.

### 5.2.7 Statistical analyses

All data was confirmed to portray a normal distribution (determined by Shapiro-Wilk test) and further analyzed using one-way ANOVA followed by Bonferroni's or Tukey-HSD *post-hoc* test to compare differences between multiple groups. Student's unpaired *t* test was used for all other statistical analyses. Differences were considered significant when  $P < 0.05$ . Statistics were performed using GraphPad Prism or JMP Pro 10 software.

## 5.3 RESULTS

### 5.3.1 Characterization of Treg inducing PLGA microspheres

First, three sets PLGA microspheres were fabricated for the release of factors, that when combined, have been shown to locally induce regulatory T cells *in vitro*<sup>51</sup>. Three microsphere systems composed of TGF- $\beta$ , IL-2, and Rapamycin encapsulated in PLGA were fabricated to extend the release of Treg inducing factors locally, Figure 42. All three microsphere formulations showed similar surface morphology observed in the scanning electron micrograph, Figure 42. Notably, IL-2 microspheres, fabricated with 10 mmol positive osmolality exhibited a slight increase in surface porosity to help accelerate the release of the cytokine from the PLGA microspheres, Figure 42, left. Interestingly, incorporation of 5 kDa PEG co-block 20 kDa PLGA with standard 50:50 12 kDa PLGA resulted in an amorphous surface pattern (as opposed to the smooth surface of standard PLGA microspheres) in the formulation encapsulating TGF- $\beta$ , Figure 42, middle. The abnormal surface morphology of the TGF- $\beta$  microspheres is thought to be a result of the

incorporation of PEG co-block polymer, which is significantly more hydrophilic than PLGA. Ultimately, this difference in hydrophobicity likely leads to non-uniform emulsions during the fabrication process and DCM evaporation, leading to the amorphous surface appearance, Figure 42 middle. However, the addition of PEG-co-block-PLGA polymer is believed to facilitate the release of TGF- $\beta$ , a relatively large and difficult protein to release from PLGA microspheres. Rapamycin PLGA microspheres appeared to have a smooth surface morphology in the scanning electron micrographs, Figure 42 right, typical of single emulsion fabrication procedures.

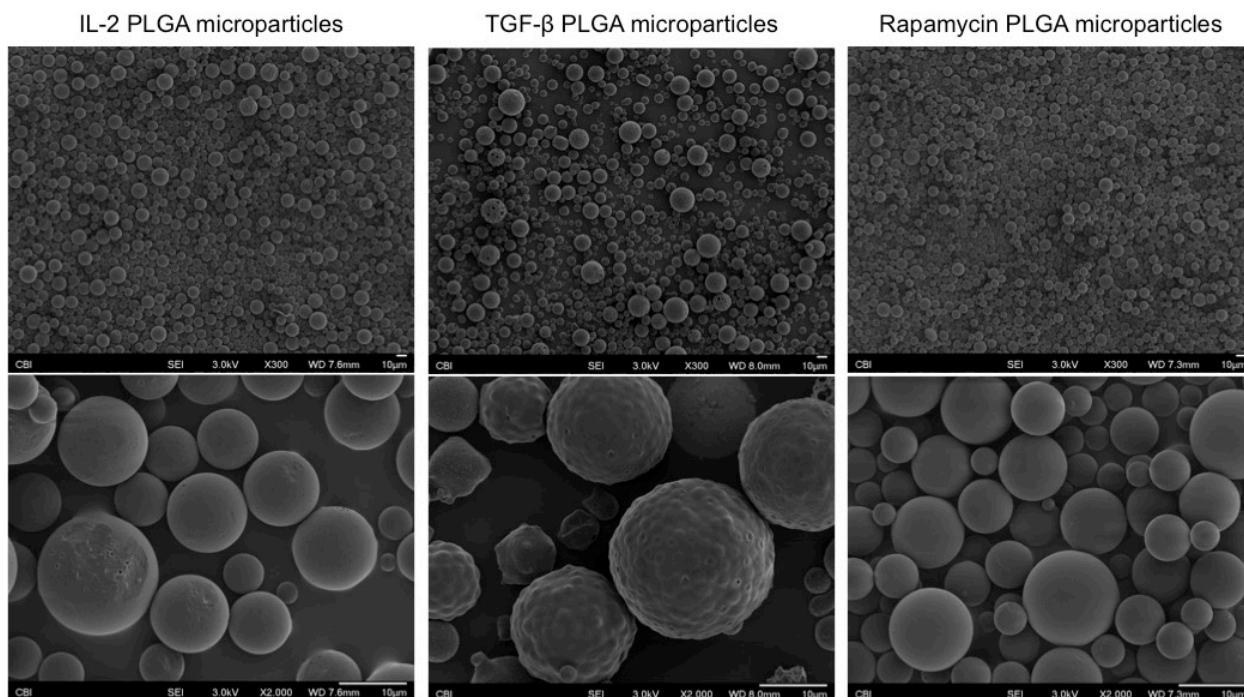


**Figure 42: Surface morphology of Treg inducing microspheres. Three batches of microspheres encapsulating TGF- $\beta$ , IL-2, and Rapamycin were fabricated for in situ Treg induction. Images are representative scanning electron micrographs of each microsphere formulation. Top magnification 300x, scale bar 10  $\mu$ m, bottom magnification 2000x, scale bar 10  $\mu$ m.**

### 5.3.2 Controlled release of TGF- $\beta$ , IL-2, and Rapamycin from PLGA microspheres

Three PLGA microspheres were fabricated encapsulating TGF- $\beta$ , IL-2, and Rapamycin respectively, using standard double and single emulsion fabrication processes. All three microspheres showed the ability to extend the release of TGF- $\beta$ , IL-2, and Rapamycin between 30 and 60 days, Figure 43. Interestingly, IL-2 microspheres exhibited a significant amount of initial burst release, with near 60% of the encapsulated payload releasing in the first 2 days, Figure 43 Left. IL-2 PLGA microsphere porosity is believed to attribute to the significant amount of burst release, as significant PLGA degradation is not required for IL-2 to elute from the PLGA microspheres. Notably, IL-2 release from PLGA microspheres is notoriously difficult<sup>214</sup>, indeed others have resorted to surface adsorption of IL-2 onto PLGA microspheres to bypass controlled release via encapsulation all together<sup>214</sup>.

TGF- $\beta$  release from PLGA microspheres was observed over a 60 day period, Figure 43, middle. Interestingly, TGF- $\beta$  microspheres incorporated 15% of a PLGA-PEG co-block polymer, which appears to significantly alter the surface morphology of the microspheres compared to those composed of purely of PLGA, Figure 42. While some initial burst was observed in the TGF- $\beta$  microspheres, Figure 43 middle, the overall release of TGF- $\beta$  was relatively constant (linear release profile) over the entire 60 day period. It can be noted that there appears to be a slight increase in release rate of TGF- $\beta$  around day 35, likely due to the secondary burst phase as the 12 kDa PLGA degrades to a critical release rate for TGF- $\beta$ , Figure 43 middle.

Rapamycin encapsulated in PLGA microspheres was controllably released for a period of 30 days, Figure 43 right. Rapamycin is orders of magnitude smaller than TGF- $\beta$ , and IL-2, with rapamycin molecular weight consisting of 914 Da. Rapamycin is relatively insoluble in water and therefore, PLGA microspheres encapsulating rapamycin were fabricated using a single

emulsion technique. As typical of single emulsion release profiles, rapamycin controlled release microspheres displayed very little initial burst. Single emulsion microsphere fabrication ultimately lacks any inner porosity, whereas, double emulsion microsphere fabrication inherently leads to the formation of stable inner occlusions that trap water soluble release agents. Interestingly, the release rate of rapamycin from PLGA microspheres increased rapidly at around day 9, as the polymer degraded sufficiently for the release of the small molecule, Figure 43 right. Notably, rapamycin being a small molecule, is less likely to have any interactions (ionic) with the negatively charged PLGA, therefore release is largely a product of particle degradation, as opposed to desorption, which can play a major role in PLGA microsphere release of proteins<sup>172</sup>.

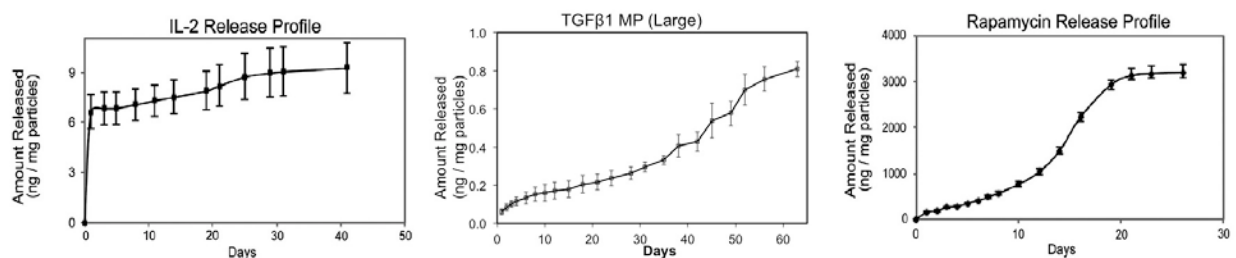


**Figure 43: Release of TGF- $\beta$ , IL-2, and rapamycin from PLGA microspheres for the local induction of Tregs. T TGF- $\beta$ , and IL-2 PLGA microspheres fabricated using a double emulsion technique. Rapamycin microspheres fabricated using a single emulsion fabrication protocol. Cumulative release of TGF- $\beta$ , IL-2 and rapamycin shown as measured in phosphate buffered saline (PBS).**

### **5.3.3 Treg inducing microspheres prevent alveolar bone loss in experimental murine periodontitis**

Next, the ability of TGF- $\beta$ , IL-2, and rapamycin Treg inducing microsphere combination was tested in its ability to prevent alveolar bone loss in the experimental mouse model for periodontal disease. Mice were infected with *Porphyromonas gingivalis* and treated with microspheres according to the schedule shown in Figure 11. Mice were treated with the combination of Treg-inducing factors TGF- $\beta$ , IL-2, and rapamycin from PLGA microspheres, or IL-2 microspheres alone, rapamycin microspheres alone and TGF- $\beta$  microspheres alone, Blank unloaded PLGA microspheres and infected, but Untreated mice served as negative controls, age matched mice served as positive controls. Alveolar bone loss was quantified in resected mouse maxilla 60 days after initial bacteria inoculation using microCT. The linear distance between the alveolar bone crest (ABC) and cementoamel junction (CEJ) was measured at 38 sites along each mouse maxilla. The summation of each linear CEJ-ABC measurement for a given maxilla represented a single overall value of bone loss for each mouse. The mice receiving all three factors, TGF- $\beta$ , IL-2, and rapamycin microspheres displayed statistically significant reductions in alveolar bone loss compared to blank microsphere treated and untreated mice, Figure 44. Furthermore, mice receiving all three TGF- $\beta$ , IL-2, and rapamycin microspheres showed alveolar bone loss comparable to age matched controls, Figure 44, and age matched control mice also showed significantly reduced bone loss compared to blank microsphere treated controls and untreated mice, Figure 44. The only other treatment group to show any significant reduction in bone loss were the mice receiving IL-2 microspheres alone, which showed a statistically significant reduction in bone loss compared to untreated control mice. Neither rapamycin nor TGF- $\beta$  microsphere treatments alone resulted in significant alveolar bone loss reductions.

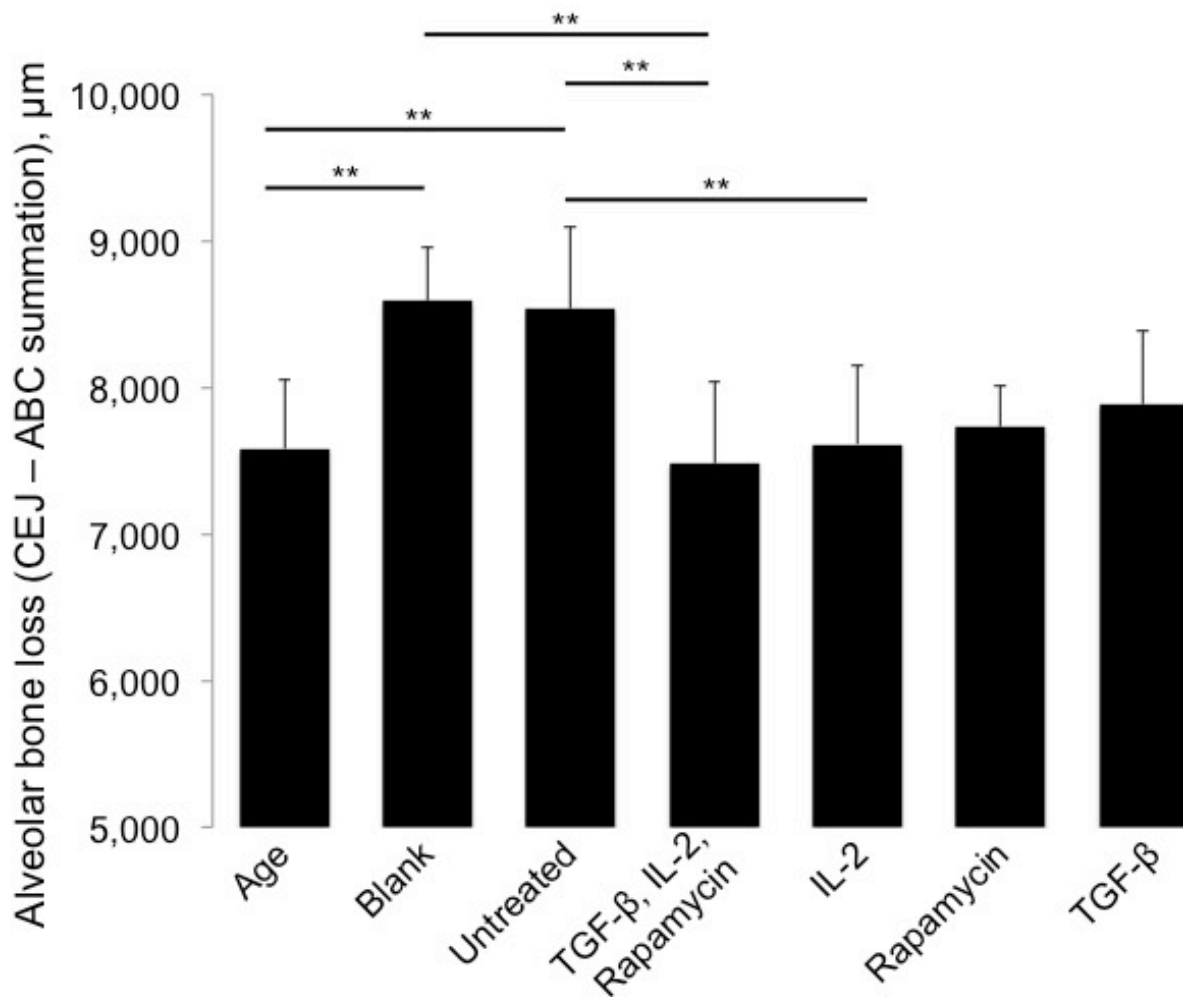


Figure 44: TGF- $\beta$ , IL-2, and rapamycin Treg inducing microspheres prevent alveolar bone loss in an experimental model for periodontal disease. BALB/cJ mice colonized with *Porphyromonas gingivalis* treated with Treg inducing microspheres injected in the maxillary gingiva at days -1, 20, 40 showed significant reduction in alveolar bone loss 60 days after initial colonization. Uninfected mice age matched control mice, infected Untreated, and blank microsphere treated mice served as controls. Alveolar bone loss was quantified by the summation of 38 linear cemento enamel junction (CEJ) to alveolar bone crest (ABC) measurements using microCT scans of resected maxilla. \*\* $P < 0.05$  determined by ANOVA followed by Tukey HSD post hoc multiple comparison test.

## 5.4 DISCUSSION

Microspheres capable of locally inducing regulatory T cells at the site of injection were fabricated using three PLGA microspheres formulations releasing TGF- $\beta$ , IL-2, and rapamycin, respectively. The microspheres exhibited similar surface morphology and overall particle size, as seen by scanning electron micrograph, Figure 42. Furthermore, the three PLGA microsphere formulations were capable of extending the release of the TGF- $\beta$ , IL-2, and rapamycin for over a period of 30 days *in vitro*, Figure 43. Aside from recruitment (as seen with CCL22 microspheres), regulatory T cells populations are naturally bolstered by the combination TGF- $\beta$ , IL-2, and rapamycin secreted from PLGA microspheres<sup>51</sup>. In fact, we previously showed that only the combination of all three factors, TGF- $\beta$ , IL-2, and rapamycin, was capable of robustly converting naïve T cells into regulatory T cells<sup>51</sup>. Therefore, we set out to see if local induction of Tregs in the periodontium may prevent alveolar bone loss in mice, as opposed to our previous work that showed Treg recruitment reduced alveolar bone resorption<sup>45</sup>.

Indeed, the combination of the three Treg inducing microspheres formulations releasing TGF- $\beta$ , IL-2, and rapamycin significantly reduced alveolar bone loss in mice, Figure 44. The microsphere-based combination therapy of TGF- $\beta$ , rapamycin and IL-2 is indeed more complex than the single factor delivery of CCL22 from microspheres. Therefore, to elucidate the therapeutic mechanism of the Treg inducing microspheres, we will need to investigate the role that each microsphere-released factor (separately) plays in periodontal disease amelioration in mice independently (according the time schedule shown Figure 11). Alone, TGF- $\beta$  microspheres may lead to some disease amelioration given that TGF- $\beta$  is a well-known anabolic anti-inflammatory cytokine that can promote bone regeneration<sup>215</sup>. However, it is possible that the presence of TGF- $\beta$  alone, in inflammatory environments, may actually induce the expansion of inflammatory TH17

cells<sup>216</sup>, potentially leading to increased inflammatory bone resorption. In fact our data suggests this may be the case, as TGF- $\beta$  alone microspheres showed the most amount of bone loss of all our therapeutic treatment groups, Figure 44. Rapamycin is small chemical species that functions as and intracellular mTOR inhibitor that ultimately blocks the receptor signal transduction mechanisms of inflammatory cytokines, suppressing the activation of conventional T and B cells while promoting regulatory T cell proliferation<sup>217</sup>. Furthermore, we have shown that rapamycin releasing microspheres, alone, are capable of generating suppressive or tolerogenic dendritic cells that may direct anti-inflammatory immune responses<sup>218</sup>. Therefore, it is possible that mice receiving only rapamycin releasing microspheres may exhibit an increase in the presence of Tregs and amelioration of periodontal disease outcomes. However, we did not expect them to perform as well as the microsphere combination given that: 1) the rapamycin dose delivered from the microspheres is significantly lower than typical immunosuppressive doses, and 2) in our hands we only observed robust Treg induction with all three factors in vitro<sup>51</sup>. And indeed the rapamycin alone microspheres displayed the second most bone loss of mice receiving therapeutic microspheres, Figure 44. IL-2 is a cytokine that originally has found clinical use as inflammatory mediator to treat cancers<sup>219, 220</sup>, however, IL-2 also plays an important role in the induction of regulatory T cells leading to immune tolerance<sup>221</sup>. Therefore, in the context of periodontal disease, we speculated that IL-2 releasing microspheres, alone, may actually promote inflammation and tissue destruction. However, IL-2 alone microspheres led to a statistically significant reduction in alveolar bone loss compared to untreated controls, Figure 44. This data suggest that IL-2 may be helping to promote immune tolerance at the given dose and delivery system, which has been supported by recent reports using IL-2 alone for the treatment of graft versus host disease<sup>222</sup>.

Regardless, future studies will be necessary to elucidate the full mechanism of TGF- $\beta$ , IL-2, and rapamycin combination microsphere treatments. Our current data suggests that this combination Treg inducing therapy may provide a robust alternative to the recruitment of Tregs (CCL22 microspheres) and may be particularly effective in patients that have impaired natural Treg populations. Therefore, we believe that these combination microspheres, although harder to translate (3 factors vs 1) may provide the most robust adjunct therapy for periodontal disease by harnessing endogenous regulators of damaging inflammation.

## **6.0 FUTURE WORK**

### **6.1 DEVELOPING CCL22 RELEASING MICROSPHERES FOR CLINICAL USE**

With the ultimate goal of developing a novel approach to treat the exacerbated inflammatory conditions seen in periodontal disease, as opposed to preventing the build-up of ever-present bacterial plaques, Treg-recruiting CCL22 microspheres offer an attractive alternative therapeutic strategy. In summary, administration of CCL22 releasing microspheres generated reduced alveolar bone loss both in mice and in the most clinically relevant dog model for periodontal disease. Furthermore, CCL22 microspheres were shown to function by preferentially recruiting endogenous anti-inflammatory regulatory T cells to the placement site, where they reduced the levels of inflammatory mediators responsible for tissue destruction in periodontal disease. While the data presented within this document provides very strong evidence toward the mechanism of action and efficacy of CCL22 microspheres in both rodent and large animal models for periodontitis, the Food and Drug Administration (FDA) tightly regulates any therapeutic prior to clinical use and an overview of the required testing is described below.

#### **6.1.1 Navigating FDA regulation for the development of CCL22 microspheres**

CCL22 microspheres will likely be regulated by the FDA, categorizing the product as a therapeutic biologic (CCL22 being a protein agent) regulated within the FDA's Center for Drug Evaluation (CDER). Because the therapeutic is designed for treatment of periodontal disease the FDA's Division of Dermatology and Dental Products (DDDP) under CDER will oversee the development

of the Investigational New Drug (IND) Biologic License Application (BLA) for CCL22 releasing microspheres. Ultimately, a FDA IND application will need to be prepared and approved by the FDA prior to clinical trials of CCL22 release PLGA microspheres. The major components and activities required to complete an IND for CCL22 releasing microspheres are listed below.

#### **6.1.1.1 IND Chemistry, Manufacturing and Control for CCL22 releasing microspheres**

One of the major components of the FDA application for new drug applications (NDA) is the Chemistry, Manufacturing and Control (CMC), which is a major component of the IND application. Within the CMC component the manufacturing of recombinant human CCL22 requires the most documentation and planning. Recombinant human CCL22 has to be manufactured using methods that both provide economically feasible yields (like *E. coli* based expression systems) and prevent the addition of trace toxic components (like bacteriophages). The manufacturing of human CCL22 will need to be conducted using suitable *E. coli* strains and CCL22 expression vectors. CCL22 protein produced by such recombinant techniques will need to be highly purified and characterized with each production batch to show consistency. Ultimately, characterization of the encapsulation and release of active rhCCL22 from PLGA microspheres will require further in depth characterization. Ideally, these manufacturing procedures will need to be conducted using Good Manufacturing Practice (GMP), however, University run investigator clinical trials may be able to utilize non-GMP products with appropriate guidance and approval.

#### **6.1.1.2 IND Toxicology and Pharmacology of CCL22 releasing microspheres**

Once manufacturing of rhCCL22 microspheres is complete, the FDA IND application requires extensive pharmacology and toxicology studies typically performed in at least two relevant animal

models. Generally, these studies are performed by Contract Research Organizations (CROs) following Good Laboratory Practices (GLP). These studies would investigate the effects of CCL22 microspheres administered by several routes on common metabolic markers in the blood and tissues of animals. Ultimately, pharmacology and toxicology studies are designed to elucidate the safety parameters and dosing associated with CCL22 microspheres and help guide initial dose testing in human clinical trials.

#### **6.1.1.3 IND Clinical Protocol design for CCL22 releasing microspheres**

The final major component of the FDA IND application is comprised of a clinical protocol that will be followed for testing the CCL22 microspheres in humans. This section of the IND focuses on defining the testing parameters for clinical trials, such as: dosing, number of patients, dose escalation studies, administration route, clinical monitoring program, and patient entrance criteria (indication). Ultimately, the clinical protocol portion of an IND application defines all aspects of the clinical trial and must be approved prior to human use of CCL22 releasing microspheres.

## **6.2 FUTURE INVESTIGATIONS USING TREG-INDUCING MICROPARTICLE FORMULATIONS**

As alternative strategy to recruiting endogenous regulatory T cells (CCL22 microspheres), several microparticle formulations were developed and described within capable of inducing the generation of regulatory T cells from naïve precursors at the site of microsphere placement. Above, the data suggested that Treg-inducing formulations (both VIP and IL-2, TFG- $\beta$  and rapamycin microsphere formulations) were able to prevent alveolar bone loss in mice (the primary disease

outcome), however, the cellular and molecular mechanisms of the Treg-inducing formulations was not fully characterized.

### **6.2.1 Future work for Vasoactive Intestinal Peptide (VIP) releasing microspheres**

Chapter 4 shows that microspheres can encapsulate and release VIP, a factor known to both recruit and induce regulatory T cells, ultimately led to a reduction in alveolar bone loss in a mouse model for periodontal disease. Interestingly, VIP has been shown to contribute therapeutic benefit harnessing Tregs both by inducing the local expression of CCL22 (leading to Treg recruitment) and directly inducing the differentiation of naïve T cells into FOXP3+ regulatory T cells<sup>135, 136, 142</sup>. To understand how the VIP microspheres are reducing periodontal disease symptoms in mice, further investigations will need to investigate populations of regulatory T cells within the periodontium of treated mice. Similar to the work described in the CCL22 microsphere mechanistic studies (Chapter 2), investigations into the cytokine, chemokine and growth factor profiles in the periodontium of mice may help to elucidate their therapeutic mechanisms after VIP microsphere treatment. Specifically, understanding how important VIP is for the induction of regulatory T cells may help to determine which mechanism of VIP is working to reduce alveolar bone loss in mice. *In vitro* testing of VIP effects T cells under activating media may help suggest how robust VIP Treg induction is with respect to previous work showing Treg induction using IL-2, TFG- $\beta$  and rapamycin microsphere formulations<sup>51</sup>.

## 6.2.2 Future work for TFG- $\beta$ and rapamycin microsphere formulations

Chapter 5 shows that Treg-inducing formulations composed of IL-2, TFG- $\beta$  and rapamycin releasing microspheres greatly reduced the primary outcome of murine periodontitis, by reducing alveolar bone resorption. However, the mechanism by which IL-2, TFG- $\beta$  and rapamycin microspheres ameliorate disease symptoms is not fully characterized. Future investigations will need to monitor Treg presence in the periodontium after treatment with Treg-inducing IL-2, TFG- $\beta$  and rapamycin microspheres. The microparticle-based combination therapy of TGF- $\beta$ , rapamycin and IL-2 is indeed more complex than the single factor delivery of CCL22 from microparticles (Chapters 2-3). Therefore, to elucidate the therapeutic mechanism of the Treg inducing microparticles, it will be crucial to investigate the role that each microparticle-released factor (separately) plays in periodontal disease amelioration in mice independently. Alone, TFG- $\beta$  microparticles may lead to some disease amelioration given that TGF- $\beta$  is a well-known anabolic anti-inflammatory cytokine that can promote bone regeneration<sup>215</sup>. However, it is possible that the presence of TGF- $\beta$  alone, in inflammatory environments, may actually induce the expansion of inflammatory TH17 cells<sup>216</sup>, potentially leading to increased inflammatory bone resorption. Rapamycin is small chemical species that functions as an intracellular mTOR inhibitor that ultimately blocks the receptor signal transduction mechanisms of inflammatory cytokines, suppressing the activation of conventional T and B cells while promoting regulatory T cell proliferation<sup>217</sup>. Furthermore, we have shown that rapamycin releasing microparticles, alone, are capable of generating suppressive or tolerogenic dendritic cells that may direct anti-inflammatory immune responses<sup>218</sup>. Therefore, it is possible that mice receiving only rapamycin releasing microparticles may exhibit an increase in the presence of Tregs and amelioration of periodontal disease outcomes. However, rapamycin microparticles alone are not expected to perform as well

as the microparticle combination given that: 1) the rapamycin dose delivered from the microparticles is significantly lower than typical immunosuppressive doses, and 2) in our hands we only observed robust Treg induction with all three factors *in vitro*<sup>51</sup>. IL-2 is a cytokine that originally has found clinical use as inflammatory mediator to treat cancers<sup>219, 220</sup>, however, IL-2 also plays an important role in the induction of regulatory T cells leading to immune tolerance<sup>221</sup>. Therefore, in the context of periodontal disease, we speculate that IL-2 releasing microparticles, alone, may actually promote inflammation and tissue destruction. Regardless, exploration of the outcomes of each microparticle formulation alone, and in dual combinations (e.g. IL-2 + Rapamycin) may provide insights into the mechanisms of the combination therapy.

## BIBLIOGRAPHY

1. Rakoff-Nahoum, S., Paglino, J., Eslami-Varzaneh, F., Edberg, S. & Medzhitov, R. Recognition of commensal microflora by toll-like receptors is required for intestinal homeostasis. *Cell* **118**, 229-241 (2004).
2. Barabino, S., Chen, Y., Chauhan, S. & Dana, R. Ocular surface immunity: homeostatic mechanisms and their disruption in dry eye disease. *Progress in retinal and eye research* **31**, 271-285 (2012).
3. Alfieri, K.A., Forsberg, J.A. & Potter, B.K. Blast injuries and heterotopic ossification. *Bone & Joint Research* **1**, 174-179 (2012).
4. Perl, M. et al. The pattern of preformed cytokines in tissues frequently affected by blunt trauma. *Shock (Augusta, Ga.)* **19**, 299-304 (2003).
5. Natoli, R.M. & Athanasiou, K.A. Traumatic loading of articular cartilage: Mechanical and biological responses and post-injury treatment. *Biorheology* **46**, 451-485 (2009).
6. Morelli, A.E. & Thomson, A.W. Tolerogenic dendritic cells and the quest for transplant tolerance. *Nat Rev Immunol* **7**, 610-621 (2007).
7. Dinarello, C.A. Anti-inflammatory Agents: Present and Future. *Cell* **140**, 935-950 (2010).
8. Neurath, M.F. Cytokines in inflammatory bowel disease. *Nat Rev Immunol* **14**, 329-342 (2014).
9. Sandborn, W.J. et al. Ustekinumab Induction and Maintenance Therapy in Refractory Crohn's Disease. *New England Journal of Medicine* **367**, 1519-1528 (2012).
10. Herrlinger, K.R. et al. Randomized, Double Blind Controlled Trial of Subcutaneous Recombinant Human Interleukin-11 Versus Prednisolone in Active Crohn's Disease. *Am J Gastroenterol* **101**, 793-797 (2006).
11. Jackson, W.M., Nesti, L.J. & Tuan, R.S. Concise review: clinical translation of wound healing therapies based on mesenchymal stem cells. *Stem cells translational medicine* **1**, 44-50 (2012).
12. Tang, Q. & Bluestone, J.A. The Foxp3<sup>+</sup> regulatory T cell: A jack of all trades, master of regulation. *Nature Immunology* **9**, 239-244 (2008).
13. Vignali, D.A.A., Collison, L.W. & Workman, C.J. How regulatory T cells work. *Nature Reviews Immunology* **8**, 523-532 (2008).

14. Wang, S., Qu, X. & Zhao, R.C. Clinical applications of mesenchymal stem cells. *Journal of hematology & oncology* **5**, 19 (2012).
15. Riley, J.L., June, C.H. & Blazar, B.R. Human T Regulatory Cell Therapy: Take a Billion or So and Call Me in the Morning. *Immunity* **30**, 656-665 (2009).
16. Le Blanc, K. & Mougiakakos, D. Multipotent mesenchymal stromal cells and the innate immune system. *Nat Rev Immunol* **12**, 383-U317 (2012).
17. Yagi, H. et al. Mesenchymal stem cells: Mechanisms of immunomodulation and homing. *Cell transplantation* **19**, 667-679 (2010).
18. Joyce, N. et al. Mesenchymal stem cells for the treatment of neurodegenerative disease. *Regenerative Medicine* **5**, 933-946 (2010).
19. Prockop, D.J. "Stemness" does not explain the repair of many tissues by mesenchymal stem/multipotent stromal cells (MSCs). *Clinical pharmacology and therapeutics* **82**, 241-243 (2007).
20. Salem, H.K. & Thiemermann, C. Mesenchymal Stromal Cells: Current Understanding and Clinical Status. *Stem cells* **28**, 585-596 (2010).
21. Iso, Y. et al. Multipotent human stromal cells improve cardiac function after myocardial infarction in mice without long-term engraftment. *Biochemical and biophysical research communications* **354**, 700-706 (2007).
22. Fukuda, K. & Yuasa, S. Stem cells as a source of regenerative cardiomyocytes. *Circulation research* **98**, 1002-1013 (2006).
23. Mougiakakos, D. et al. The impact of inflammatory licensing on heme oxygenase-1-mediated induction of regulatory T cells by human mesenchymal stem cells. *Blood* **117**, 4826-4835 (2011).
24. Meirelles Lda, S., Fontes, A.M., Covas, D.T. & Caplan, A.I. Mechanisms involved in the therapeutic properties of mesenchymal stem cells. *Cytokine & growth factor reviews* **20**, 419-427 (2009).
25. Reinders, M.E.J., Rabelink, T.J. & de Fijter, J.W. The role of mesenchymal stromal cells in chronic transplant rejection after solid organ transplantation. *Current opinion in organ transplantation* **18**, 44-50 (2013).
26. Pileggi, A., Xu, X., Tan, J. & Ricordi, C. Mesenchymal stromal (stem) cells to improve solid organ transplant outcome: lessons from the initial clinical trials. *Current opinion in organ transplantation* **18**, 672-681 (2013).
27. Tsai, S. et al. Reversal of autoimmunity by boosting memory-like autoregulatory T cells. *Immunity* **32**, 568-580 (2010).

28. Brunstein, C.G. et al. Infusion of ex vivo expanded T regulatory cells in adults transplanted with umbilical cord blood: safety profile and detection kinetics. *Blood* **117**, 1061-1070 (2011).
29. Blazar, B.R., Murphy, W.J. & Abedi, M. Advances in graft-versus-host disease biology and therapy. *Nat Rev Immunol* **12**, 443-458 (2012).
30. Martelli, M.F. et al. HLA-haploidentical transplantation with regulatory and conventional T cell adoptive immunotherapy prevents acute leukemia relapse. *Blood* (2014).
31. Di Ianni, M. et al. Tregs prevent GVHD and promote immune reconstitution in HLA-haploidentical transplantation. *Blood* **117**, 3921-3928 (2011).
32. Diano, S. et al. Peroxisome proliferation-associated control of reactive oxygen species sets melanocortin tone and feeding in diet-induced obesity. *Nat Med* **17**, 1121-1127 (2011).
33. Giordano, A., Galderisi, U. & Marino, I.R. From the laboratory bench to the patient's bedside: an update on clinical trials with mesenchymal stem cells. *J Cell Physiol* **211**, 27-35 (2007).
34. Hall, B.M., Tran, G. & Hodgkinson, S.J. Alloantigen specific T regulatory cells in transplant tolerance. *International immunopharmacology* **9**, 570-574 (2009).
35. Tan, X. et al. CD154 blockade modulates the ratio of Treg to Th1 cells and prolongs the survival of allogeneic corneal grafts in mice. *Experimental and therapeutic medicine* **7**, 827-834 (2014).
36. Muller, Y.D., Ehrchiou, D., Golshayan, D., Buhler, L.H. & Seebach, J.D. Potential of T-regulatory cells to protect xenografts. *Current opinion in organ transplantation* **17**, 155-161 (2012).
37. O'Shea, J.J. & Paul, W.E. Mechanisms underlying lineage commitment and plasticity of helper CD4+ T cells. *Science* **327**, 1098-1102 (2010).
38. Knoepfler, P.S. Deconstructing stem cell tumorigenicity: a roadmap to safe regenerative medicine. *Stem cells* **27**, 1050-1056 (2009).
39. Lewis, J.S., Roy, K. & Keselowsky, B.G. Materials that harness and modulate the immune system. *MRS Bulletin* **39**, 25-34 (2014).
40. Moon, J.J., Huang, B. & Irvine, D.J. Engineering nano- and microparticles to tune immunity. *Adv Mater* **24**, 3724-3746 (2012).
41. Mora-Solano, C. & Collier, J.H. Engaging adaptive immunity with biomaterials. *Journal of materials chemistry. B, Materials for biology and medicine* **2**, 2409-2421 (2014).
42. Ulerly, B.D., Nair, L.S. & Laurencin, C.T. Biomedical Applications of Biodegradable Polymers. *Journal of polymer science. Part B, Polymer physics* **49**, 832-864 (2011).

43. Mailloux, A.W. & Young, M.R.I. NK-dependent increases in CCL22 secretion selectively recruits regulatory T cells to the tumor microenvironment. *Journal of Immunology* **182**, 2753-2765 (2009).
44. Curiel, T.J. et al. Specific recruitment of regulatory T cells in ovarian carcinoma fosters immune privilege and predicts reduced survival. *Nat Med* **10**, 942-949 (2004).
45. Glowacki, A.J. et al. Prevention of inflammation-mediated bone loss in murine and canine periodontal disease via recruitment of regulatory lymphocytes. *Proc Natl Acad Sci U S A* **110**, 18525-18530 (2013).
46. Jhunjunwala, S. et al. Bioinspired controlled release of CCL22 recruits regulatory T cells in vivo. *Adv Mater* **24**, 4735-4738 (2012).
47. Montane, J. et al. Prevention of murine autoimmune diabetes by CCL22-mediated Treg recruitment to the pancreatic islets. *The Journal of clinical investigation* **121**, 3024-3028 (2011).
48. Park, J. et al. Modulation of CD4+ T Lymphocyte Lineage Outcomes with Targeted, Nanoparticle-Mediated Cytokine Delivery. *Molecular Pharmaceutics* **8**, 143-152 (2010).
49. Dong, H. et al. Immuno-isolation of pancreatic islet allografts using pegylated nanotherapy leads to long-term normoglycemia in full MHC mismatch recipient mice. *PLoS One* **7**, e50265 (2012).
50. Phillips, B. et al. A microsphere-based vaccine prevents and reverses new-onset autoimmune diabetes. *Diabetes* **57**, 1544-1555 (2008).
51. Jhunjunwala, S. et al. Controlled release formulations of IL-2, TGF-beta1 and rapamycin for the induction of regulatory T cells. *J Control Release* **159**, 78-84 (2012).
52. Dresner-Pollak, R., Gelb, N., Rachmilewitz, D., Karmeli, F. & Weinreb, M. Interleukin 10-deficient mice develop osteopenia, decreased bone formation, and mechanical fragility of long bones. *Gastroenterology* **127**, 792-801 (2004).
53. Janssens, K., ten Dijke, P., Janssens, S. & Van Hul, W. Transforming growth factor-beta1 to the bone. *Endocr Rev* **26**, 743-774 (2005).
54. Kanaan, R.A. & Kanaan, L.A. Transforming growth factor  $\beta$ 1, bone connection. *Medical Science Monitor* **12** (2006).
55. Li, M.O., Wan, Y.Y., Sanjabi, S., Robertson, A.K. & Flavell, R.A. Transforming growth factor-beta regulation of immune responses. *Annu Rev Immunol* **24**, 99-146 (2006).
56. Igotz, R.A., Endo, T. & Massague, J. Regulation of fibronectin and type I collagen mRNA levels by transforming growth factor-beta. *J Biol Chem* **262**, 6443-6446 (1987).

57. Matsuda, N., Lin, W.L., Kumar, N.M., Cho, M.I. & Genco, R.J. Mitogenic, chemotactic, and synthetic responses of rat periodontal ligament fibroblastic cells to polypeptide growth factors in vitro. *Journal of Periodontology* **63**, 515-525 (1992).
58. Gandolfo, M.T. et al. Foxp3+ regulatory T cells participate in repair of ischemic acute kidney injury. *Kidney international* **76**, 717-729 (2009).
59. Glowacki, A.J. et al. Strategies to Direct the Enrichment, Expansion, and Recruitment of Regulatory Cells for the Treatment of Disease. *Annals of biomedical engineering* (2014).
60. Chen, F.-M., An, Y., Zhang, R. & Zhang, M. New insights into and novel applications of release technology for periodontal reconstructive therapies. *Journal of controlled release* **149**, 92-110 (2011).
61. Ponte, A.L. et al. The in vitro migration capacity of human bone marrow mesenchymal stem cells: comparison of chemokine and growth factor chemotactic activities. *Stem cells* **25**, 1737-1745 (2007).
62. Bleul, C.C., Fuhlbrigge, R.C., Casasnovas, J.M., Aiuti, A. & Springer, T.A. A highly efficacious lymphocyte chemoattractant, stromal cell-derived factor 1 (SDF-1). *The Journal of experimental medicine* **184**, 1101-1109 (1996).
63. Phipps, M.C., Xu, Y. & Bellis, S.L. Delivery of platelet-derived growth factor as a chemotactic factor for mesenchymal stem cells by bone-mimetic electrospun scaffolds. *PloS one* **7**, e40831 (2012).
64. Discher, D.E., Moonery, D.J. & Zandstra, P.W. Growth Factors, Matrices, and Forces Combine and Control Stem Cells. *Science* **324**, 1673-1677 (2009).
65. Song, G. et al. The homing of bone marrow MSCs to non-osseous sites for ectopic bone formation induced by osteoinductive calcium phosphate. *Biomaterials* **34**, 2167-2176 (2013).
66. Santoro, M., Tataru, A.M. & Mikos, A.G. Gelatin carriers for drug and cell delivery in tissue engineering. *Journal of controlled release* **doi: 10.10** (2014).
67. Lam, M.K. et al. Comparison of 3 biodegradable polymer and durable polymer-based drug-eluting stents in all-comers (BIO-RESORT): rationale and study design of the randomized TWENTE III multicenter trial. *American heart journal* **167**, 445-451 (2014).
68. Nair, L.S. & Laurencin, C.T. Polymers as biomaterials for tissue engineering and controlled drug delivery. *Advances in biochemical engineering/biotechnology* **102**, 47-90 (2006).
69. Lee, S.H., Moon, J.J. & West, J.L. Three-dimensional micropatterning of bioactive hydrogels via two-photon laser scanning photolithography for guided 3D cell migration. *Biomaterials* **29**, 2962-2968 (2008).

70. Huebsch, N. & Mooney, D.J. Inspiration and application in the evolution of biomaterials. *Nature* **462**, 426-432 (2009).
71. Kearney, C.J. & Mooney, D.J. Macroscale delivery systems for molecular and cellular payloads. *Nature materials* **12**, 1004-1017 (2013).
72. He, X., Ma, J. & Jabbari, E. Migration of marrow stromal cells in response to sustained release of stromal-derived factor-1alpha from poly(lactide ethylene oxide fumarate) hydrogels. *International journal of pharmaceutics* **390**, 107-116 (2010).
73. Gonçalves, R.M., Antunes, J.C. & Barbosa, M.A. Mesenchymal stem cell recruitment by stromal derived factor-1-delivery systems based on chitosan/poly( $\gamma$ -glutamic acid) polyelectrolyte complexes. *European cells & materials* **23**, 249-260; discussion 260-241 (2012).
74. Cross, D. & Wang, C. Stromal-Derived Factor-1 Alpha-Loaded PLGA Microspheres for Stem Cell Recruitment. *Pharmaceutical Research* **28**, 2477-2489 (2011).
75. Jin, Q. et al. Nanofibrous scaffolds incorporating PDGF-BB microspheres induce chemokine expression and tissue neogenesis in vivo. *PloS one* **3**, e1729 (2008).
76. Rothstein, S.N., Federspiel, W.J. & Little, S.R. A unified mathematical model for the prediction of controlled release from surface and bulk eroding polymer matrices. *Biomaterials* **30**, 1657-1664 (2009).
77. Rothstein, S.N., Kay, J.E., Schopfer, F.J., Freeman, B.A. & Little, S.R. A retrospective mathematical analysis of controlled release design and experimentation. *Molecular pharmaceutics* **9**, 3003-3011 (2012).
78. Bian, L. et al. Enhanced MSC chondrogenesis following delivery of TGF- $\beta$ 3 from alginate microspheres within hyaluronic acid hydrogels in vitro and in vivo. *Biomaterials* **32**, 6425-6434 (2011).
79. Lai, H.-J. et al. Tailored design of electrospun composite nanofibers with staged release of multiple angiogenic growth factors for chronic wound healing. *Acta biomaterialia* (2014).
80. Davies, N.H., Schmidt, C., Bezuidenhout, D. & Zilla, P. Sustaining neovascularization of a scaffold through staged release of vascular endothelial growth factor-A and platelet-derived growth factor-BB. *Tissue engineering. Part A* **18**, 26-34 (2012).
81. Chang, P.-C. et al. Sequential platelet-derived growth factor-simvastatin release promotes dentoalveolar regeneration. *Tissue engineering. Part A* **20**, 356-364 (2014).
82. Lehner, R., Wang, X., Wolf, M. & Hunziker, P. Designing switchable nanosystems for medical application. *Journal of controlled release* **161**, 307-316 (2012).
83. Siegel, R.A. Stimuli Sensitive Polymers and Self Regulated Drug Delivery Systems: A Very Partial Review. *Journal of controlled release* (2014).

84. Eke, P.I. et al. Prevalence of periodontitis in adults in the United States: 2009 and 2010. *J Dent Res* **91**, 914-920 (2012).
85. Seymour, G.J., Ford, P.J., Cullinan, M.P., Leishman, S. & Yamazaki, K. Relationship between periodontal infections and systemic disease. *Clin Microbiol Infect* **13 Suppl 4**, 3-10 (2007).
86. Fisher, M.A. et al. Periodontal disease and other nontraditional risk factors for CKD. *Am J Kidney Dis* **51**, 45-52 (2008).
87. Boggess, K.A., Beck, J.D., Murtha, A.P., Moss, K. & Offenbacher, S. Maternal periodontal disease in early pregnancy and risk for a small-for-gestational-age infant. *Am J Obstet Gynecol* **194**, 1316-1322 (2006).
88. Backes, J.M., Howard, P.A. & Moriarty, P.M. Role of C-reactive protein in cardiovascular disease. *Ann Pharmacother* **38**, 110-118 (2004).
89. Offenbacher, S. & Beck, J.D. A perspective on the potential cardioprotective benefits of periodontal therapy. *Am Heart J* **149**, 950-954 (2005).
90. Williams, R.C. et al. Treatment of periodontitis by local administration of minocycline microspheres: A controlled trial. *Journal of Periodontology* **72**, 1535-1544 (2001).
91. Magnusson, I. & Walker, C.B. Refractory periodontitis or recurrence of disease. *J Clin Periodontol* **23**, 289-292 (1996).
92. Baker, P.J. The role of immune responses in bone loss during periodontal disease. *Microbes and Infection* **2**, 1181-1192 (2000).
93. Graves, D.T., Fine, D., Teng, Y.T., Van Dyke, T.E. & Hajishengallis, G. The use of rodent models to investigate host-bacteria interactions related to periodontal diseases. *J Clin Periodontol* **35**, 89-105 (2008).
94. Garlet, G.P. et al. The essential role of IFN-gamma in the control of lethal *Aggregatibacter actinomycetemcomitans* infection in mice. *Microbes Infect* **10**, 489-496 (2008).
95. Garlet, G.P. et al. The dual role of p55 tumour necrosis factor- $\alpha$  receptor in *Actinobacillus actinomycetemcomitans*-induced experimental periodontitis: Host protection and tissue destruction. *Clinical and Experimental Immunology* **147**, 128-138 (2007).
96. Silva, T.A. et al. Macrophages and mast cells control the neutrophil migration induced by dentin proteins. *Journal of Dental Research* **84**, 79-83 (2005).
97. Yu, J.J. et al. An essential role for IL-17 in preventing pathogen-initiated bone destruction: Recruitment of neutrophils to inflamed bone requires IL-17 receptor-dependent signals. *Blood* **109**, 3794-3802 (2007).

98. Garlet, G.P., Avila-Campos, M.J., Milanezi, C.M., Ferreira, B.R. & Silva, J.S. Actinobacillus actinomycetemcomitans-induced periodontal disease in mice: Patterns of cytokine, chemokine, and chemokine receptor expression and leukocyte migration. *Microbes and Infection* **7**, 738-747 (2005).
99. Garlet, G.P., Martins Jr, W., Ferreira, B.R., Milanezi, C.M. & Silva, J.S. Patterns of chemokines and chemokine receptors expression in different forms of human periodontal disease. *Journal of Periodontal Research* **38**, 210-217 (2003).
100. Garlet, G.P. et al. Cytokine pattern determines the progression of experimental periodontal disease induced by Actinobacillus actinomycetemcomitans through the modulation of MMPs, RANKL, and their physiological inhibitors. *Oral Microbiology and Immunology* **21**, 12-20 (2006).
101. Eke, P.I. & Genco, R.J. CDC periodontal disease surveillance project: Background, objectives, and progress report. *Journal of Periodontology* **78**, 1366-1371 (2007).
102. Khalili, J. Periodontal disease: an overview for medical practitioners. *Likars'ka sprava / Ministerstvo okhorony zdorov'ia Ukraïny*, 10-21 (2008).
103. Fisher, M.A. et al. Periodontal Disease and Other Nontraditional Risk Factors for CKD. *American Journal of Kidney Diseases* **51**, 45-52 (2008).
104. Seymour, G.J., Ford, P.J., Cullinan, M.P., Leishman, S. & Yamazaki, K. Relationship between periodontal infections and systemic disease. *Clinical Microbiology and Infection* **13**, 3-10 (2007).
105. Boggess, K.A., Beck, J.D., Murtha, A.P., Moss, K. & Offenbacher, S. Maternal periodontal disease in early pregnancy and risk for a small-for-gestational-age infant. *American Journal of Obstetrics and Gynecology* **194**, 1316-1322 (2006).
106. Jensen, G.L. Inflammation as the Key Interface of the Medical and Nutrition Universes: A Provocative Examination of the Future of Clinical Nutrition and Medicine. *Journal of Parenteral and Enteral Nutrition* **30**, 453-463 (2006).
107. Beck, J., Garcia, R., Heiss, G., Vokonas, P.S. & Offenbacher, S. Periodontal disease and cardiovascular disease. *J Periodontol* **67**, 1123-1137 (1996).
108. Backes, J.M., Howard, P.A. & Moriarty, P.M. Role of C-Reactive Protein in Cardiovascular Disease. *Annals of Pharmacotherapy* **38**, 110-118 (2004).
109. Offenbacher, S. & Beck, J.D. A perspective on the potential cardioprotective benefits of periodontal therapy. *American Heart Journal* **149**, 950-954 (2005).
110. Smith, R.A., M'ikanatha N, M. & Read, A.F. Antibiotic Resistance: A Primer and Call to Action. *Health communication*, 1-6 (2014).

111. Hu, J., Van den Steen, P.E., Sang, Q.X. & Opdenakker, G. Matrix metalloproteinase inhibitors as therapy for inflammatory and vascular diseases. *Nature reviews. Drug discovery* **6**, 480-498 (2007).
112. Thomas, J.G., Metheny, R.J., Karakiozis, J.M., Wetzel, J.M. & Crout, R.J. Long-term sub-antimicrobial doxycycline (Periostat) as adjunctive management in adult periodontitis: effects on subgingival bacterial population dynamics. *Adv Dent Res* **12**, 32-39 (1998).
113. Greenstein, G. Clinical significance of bacterial resistance to tetracyclines in the treatment of periodontal diseases. *J Periodontol* **66**, 925-932 (1995).
114. Roberts, A.P. & Mullany, P. Oral biofilms: a reservoir of transferable, bacterial, antimicrobial resistance. *Expert Rev Anti Infect Ther* **8**, 1441-1450 (2010).
115. Garlet, G.P. et al. The dual role of p55 tumour necrosis factor-alpha receptor in Actinobacillus actinomycetemcomitans-induced experimental periodontitis: host protection and tissue destruction. *Clin Exp Immunol* **147**, 128-138 (2007).
116. Silva, T.A. et al. Macrophages and mast cells control the neutrophil migration induced by dentin proteins. *J Dent Res* **84**, 79-83 (2005).
117. Gerard, C. & Rollins, B.J. Chemokines and disease. *Nat Immunol* **2**, 108-115 (2001).
118. Luther, S.A. & Cyster, J.G. Chemokines as regulators of T cell differentiation. *Nat Immunol* **2**, 102-107 (2001).
119. Garlet, G.P., Martins, W., Jr., Ferreira, B.R., Milanezi, C.M. & Silva, J.S. Patterns of chemokines and chemokine receptors expression in different forms of human periodontal disease. *J Periodontal Res* **38**, 210-217 (2003).
120. Graves, D.T., Oates, T. & Garlet, G.P. Review of osteoimmunology and the host response in endodontic and periodontal lesions. *Journal of oral microbiology* **3** (2011).
121. Kramer, J.M. & Gaffen, S.L. Interleukin-17: a new paradigm in inflammation, autoimmunity, and therapy. *J Periodontol* **78**, 1083-1093 (2007).
122. Gilroy, D.W., Lawrence, T., Perretti, M. & Rossi, A.G. Inflammatory resolution: new opportunities for drug discovery. *Nature reviews. Drug discovery* **3**, 401-416 (2004).
123. Hasturk, H. et al. Resolvin E1 regulates inflammation at the cellular and tissue level and restores tissue homeostasis in vivo. *J Immunol* **179**, 7021-7029 (2007).
124. Gurgel, B.C. et al. Selective COX-2 inhibitor reduces bone healing in bone defects. *Brazilian oral research* **19**, 312-316 (2005).
125. Ribeiro, F.V. et al. Selective cyclooxygenase-2 inhibitor may impair bone healing around titanium implants in rats. *Journal of Periodontology* **77**, 1731-1735 (2006).

126. Simon, A.M., Manigrasso, M.B. & O'Connor, J.P. Cyclo-oxygenase 2 function is essential for bone fracture healing. *Journal of Bone and Mineral Research* **17**, 963-976 (2002).
127. Vuolteenaho, K., Moilanen, T. & Moilanen, E. Non-steroidal anti-inflammatory drugs, cyclooxygenase-2 and the bone healing process. *Basic and Clinical Pharmacology and Toxicology* **102**, 10-14 (2008).
128. Zhang, X., Kohli, M., Zhou, Q., Graves, D.T. & Amar, S. Short- and long-term effects of IL-1 and TNF antagonists on periodontal wound healing. *Journal of Immunology* **173**, 3514-3523 (2004).
129. Cardoso, C.R. et al. Characterization of CD4+CD25+ natural regulatory T cells in the inflammatory infiltrate of human chronic periodontitis. *Journal of Leukocyte Biology* **84**, 311-318 (2008).
130. Jiao, Z. et al. Accumulation of FoxP3-expressing CD4+CD25+ T cells with distinct chemokine receptors in synovial fluid of patients with active rheumatoid arthritis. *Scandinavian Journal of Rheumatology* **36**, 428-433 (2007).
131. Sather, B.D. et al. Altering the distribution of Foxp3+ regulatory T cells results in tissue-specific inflammatory disease. *Journal of Experimental Medicine* **204**, 1335-1347 (2007).
132. Rabinovich, G.A., Gabilovich, D. & Sotomayor, E.M. in *Annual Review of Immunology*, Vol. 25 267-296 (2007).
133. Rothstein, S.N., Federspiel, W.J., and Little, S.R. A simple model framework for the prediction of controlled release from bulk eroding polymer matrices. *Journal of Materials Chemistry* **18**, 1873-1880 (2008).
134. Rothstein, S.N., Federspiel, W. J., Little, S. R. A unified mathematical model for the prediction of controlled release from surface and bulk eroding polymer matrices. *Biomaterials* (2009).
135. Delgado, M., Gonzalez-Rey, E. & Ganea, D. VIP/PACAP preferentially attract Th2 effectors through differential regulation of chemokine production by dendritic cells. *FASEB Journal* **18**, 1453-1455 (2004).
136. Delgado, M. & Ganea, D. Anti-inflammatory neuropeptides: A new class of endogenous immunoregulatory agents. *Brain, Behavior, and Immunity* **22**, 1146-1151 (2008).
137. Ganea, D., Gonzalez-Rey, E. & Delgado, M. A novel mechanism for immunosuppression: From neuropeptides to regulatory T cells. *Journal of Neuroimmune Pharmacology* **1**, 400-409 (2006).
138. Fernandez-Martin, A., Gonzalez-Rey, E., Chorny, A., Ganea, D. & Delgado, M. Vasoactive intestinal peptide induces regulatory T cells during experimental autoimmune encephalomyelitis. *European journal of immunology* **36**, 318-326 (2006).

139. Gonzalez-Rey, E., Fernandez-Martin, A., Chorny, A. & Delgado, M. Vasoactive intestinal peptide induces CD4<sup>+</sup>,CD25<sup>+</sup> T regulatory cells with therapeutic effect in collagen-induced arthritis. *Arthritis and rheumatism* **54**, 864-876 (2006).
140. Pozo, D. et al. Tuning immune tolerance with vasoactive intestinal peptide: a new therapeutic approach for immune disorders. *Peptides* **28**, 1833-1846 (2007).
141. Lundberg, P. & Lerner, U.H. Expression and regulatory role of receptors for vasoactive intestinal peptide in bone cells. *Microscopy Research and Technique* **58**, 98-103 (2002).
142. Delgado, M. Generating tolerogenic dendritic cells with neuropeptides. *Human Immunology* **70**, 300-307 (2009).
143. Gonzalez-Rey, E., Anderson, P. & Delgado, M. Emerging roles of vasoactive intestinal peptide: A new approach for autoimmune therapy. *Annals of the Rheumatic Diseases* **66** (2007).
144. Webster, K.E. et al. In vivo expansion of T reg cells with IL-2-mAb complexes: induction of resistance to EAE and long-term acceptance of islet allografts without immunosuppression. *The Journal of experimental medicine* **206**, 751-760 (2009).
145. Beyersdorf, N. et al. Selective targeting of regulatory T cells with CD28 superagonists allows effective therapy of experimental autoimmune encephalomyelitis. *The Journal of experimental medicine* **202**, 445-455 (2005).
146. Deal watch: Boosting TRegs to target autoimmune disease. *Nature reviews. Drug discovery* **10**, 566 (2011).
147. Suntharalingam, G. et al. Cytokine storm in a phase 1 trial of the anti-CD28 monoclonal antibody TGN1412. *The New England journal of medicine* **355**, 1018-1028 (2006).
148. Cobbold, S.P. et al. Infectious tolerance via the consumption of essential amino acids and mTOR signaling. *Proc Natl Acad Sci U S A* **106**, 12055-12060 (2009).
149. Haxhinasto, S., Mathis, D. & Benoist, C. The AKT-mTOR axis regulates de novo differentiation of CD4<sup>+</sup>Foxp3<sup>+</sup> cells. *The Journal of experimental medicine* **205**, 565-574 (2008).
150. Kopf, H., de la Rosa, G.M., Howard, O.M. & Chen, X. Rapamycin inhibits differentiation of Th17 cells and promotes generation of FoxP3<sup>+</sup> T regulatory cells. *International immunopharmacology* **7**, 1819-1824 (2007).
151. Shive, M.S. & Anderson, J.M. Biodegradation and biocompatibility of PLA and PLGA microspheres. *Adv Drug Deliv Rev* **28**, 5-24 (1997).
152. Little, S.R. et al. Poly-beta amino ester-containing microparticles enhance the activity of nonviral genetic vaccines. *Proc Natl Acad Sci U S A* **101**, 9534-9539 (2004).

153. Rothstein, S.N., Federspiel, W.J. & Little, S.R. A unified mathematical model for the prediction of controlled release from surface and bulk eroding polymer matrices. *Biomaterials* **30**, 1657-1664 (2009).
154. Zhang, N. et al. Regulatory T Cells Sequentially Migrate from Inflamed Tissues to Draining Lymph Nodes to Suppress the Alloimmune Response. *Immunity* **30**, 458-469 (2009).
155. Claudino, M. et al. The broad effects of the functional IL-10 promoter-592 polymorphism: Modulation of IL-10, TIMP-3, and OPG expression and their association with periodontal disease outcome. *Journal of Leukocyte Biology* **84**, 1565-1573 (2008).
156. Garlet, G.P., Cardoso, C.R., Campanelli, A.P., Martins Jr, W. & Silva, J.S. Expression of suppressors of cytokine signaling in diseased periodontal tissues: A stop signal for disease progression? *Journal of Periodontal Research* **41**, 580-584 (2006).
157. Abe, T. et al. Osteoblast differentiation is impaired in SOCS-1-deficient mice. *J Bone Miner Metab* **24**, 283-290 (2006).
158. Lorentzon, M., Greenhalgh, C.J., Mohan, S., Alexander, W.S. & Ohlsson, C. Reduced bone mineral density in SOCS-2-deficient mice. *Pediatr Res* **57**, 223-226 (2005).
159. Ouyang, X. et al. SOCS-2 interferes with myotube formation and potentiates osteoblast differentiation through upregulation of JunB in C2C12 cells. *J Cell Physiol* **207**, 428-436 (2006).
160. Ernst, C.W.O. et al. Diminished forkhead box P3/CD25 double-positive T regulatory cells are associated with the increased nuclear factor-kB ligand (RANKL+) T cells in bone resorption lesion of periodontal disease. *Clinical and Experimental Immunology* **148**, 271-280 (2007).
161. Janssens, K., Ten Dijke, P., Janssens, S. & Van Hul, W. Transforming growth factor- $\beta$ 1 to the bone. *Endocrine Reviews* **26**, 743-774 (2005).
162. Garlet, G.P. Destructive and protective roles of cytokines in periodontitis: a re-appraisal from host defense and tissue destruction viewpoints. *J Dent Res* **89**, 1349-1363 (2010).
163. Birkedal-Hansen, H. et al. Matrix metalloproteinases: a review. *Crit Rev Oral Biol Med* **4**, 197-250 (1993).
164. Taubman, M.A., Valverde, P., Han, X. & Kawai, T. Immune response: the key to bone resorption in periodontal disease. *J Periodontol* **76**, 2033-2041 (2005).
165. Dutzan, N., Gamonal, J., Silva, A., Sanz, M. & Vernal, R. Over-expression of forkhead box P3 and its association with receptor activator of nuclear factor- $\kappa$ B ligand, interleukin (IL) -17, IL-10 and transforming growth factor- $\beta$  during the progression of chronic periodontitis. *Journal of Clinical Periodontology* **36**, 396-403 (2009).

166. Okui, T. et al. Characterization of CD4+ FOXP3+ T-cell clones established from chronic inflammatory lesions. *Oral Microbiol Immunol* **23**, 49-54 (2008).
167. Garlet, G.P. et al. Regulatory T cells attenuate experimental periodontitis progression in mice. *J Clin Periodontol* **37**, 591-600 (2010).
168. Rothstein, S.N. & Little, S.R. A "tool box" for rational design of degradable controlled release formulations. *Journal of Materials Chemistry* **21**, 29-39 (2011).
169. Baker, P.J., Dixon, M. & Roopenian, D.C. Genetic control of susceptibility to Porphyromonas gingivalis-induced alveolar bone loss in mice. *Infection and Immunity* **68**, 5864-5868 (2000).
170. Sharma, G. et al. Polymer particle shape independently influences binding and internalization by macrophages. *J Control Release* **147**, 408-412 (2010).
171. Wang, J., Wang, B.M. & Schwendeman, S.P. Characterization of the initial burst release of a model peptide from poly(d,l-lactide-co-glycolide) microspheres. *Journal of Controlled Release* **82**, 289-307 (2002).
172. Balmert, S.C. et al. Positive Charge of "Sticky" Peptides and Proteins Impedes Release From Negatively Charged PLGA Matrices. *Journal of materials chemistry. B, Materials for biology and medicine* **3**, 4723-4734 (2015).
173. Lopez, N.J. Occurrence of Actinobacillus actinomycetemcomitans, Porphyromonas gingivalis, and Prevotella intermedia in progressive adult periodontitis. *J Periodontol* **71**, 948-954 (2000).
174. Petit, M.D., van Steenberg, T.J., Timmerman, M.F., de Graaff, J. & van der Velden, U. Prevalence of periodontitis and suspected periodontal pathogens in families of adult periodontitis patients. *J Clin Periodontol* **21**, 76-85 (1994).
175. Savitt, E.D. & Kent, R.L. Distribution of Actinobacillus actinomycetemcomitans and Porphyromonas gingivalis by subject age. *J Periodontol* **62**, 490-494 (1991).
176. XIE Xiang-yang, YANG Yang, ZHANG Hui, LI Zhi-ping, LI Ying, YANG Zhen-bo, C.X.-s.M.X.-g. An in vitro accelerated approach based on in vivo release to assess thymopentin release from PLGA microspheres. *JIPR* **41**, 672-679 (2014).
177. Kohm, A.P., Williams, J.S. & Miller, S.D. Cutting edge: ligation of the glucocorticoid-induced TNF receptor enhances autoreactive CD4+ T cell activation and experimental autoimmune encephalomyelitis. *J Immunol* **172**, 4686-4690 (2004).
178. Belkaid, Y. & Rouse, B.T. Natural regulatory T cells in infectious disease. *Nature Immunology* **6**, 353-360 (2005).

179. Wikesjo, U.M. et al. Periodontal repair in dogs: effect of recombinant human transforming growth factor-beta1 on guided tissue regeneration. *J Clin Periodontol* **25**, 475-481 (1998).
180. Huber, S. et al. Th17 cells express interleukin-10 receptor and are controlled by Foxp3(-) and Foxp3+ regulatory CD4+ T cells in an interleukin-10-dependent manner. *Immunity* **34**, 554-565 (2011).
181. Sojka, D.K. & Fowell, D.J. Regulatory T cells inhibit acute IFN-gamma synthesis without blocking T-helper cell type 1 (Th1) differentiation via a compartmentalized requirement for IL-10. *Proc Natl Acad Sci U S A* **108**, 18336-18341 (2011).
182. Garlet, G.P. et al. The essential role of IFN- $\gamma$  in the control of lethal *Aggregatibacter actinomycetemcomitans* infection in mice. *Microbes and Infection* **10**, 489-496 (2008).
183. Eskan, M.A. et al. The leukocyte integrin antagonist Del-1 inhibits IL-17-mediated inflammatory bone loss. *Nat Immunol* **13**, 465-473 (2012).
184. Graves, D.T. & Cochran, D. The contribution of interleukin-1 and tumor necrosis factor to periodontal tissue destruction. *J Periodontol* **74**, 391-401 (2003).
185. Kawai, T. et al. Requirement of B7 costimulation for Th1-mediated inflammatory bone resorption in experimental periodontal disease. *J Immunol* **164**, 2102-2109 (2000).
186. Ratajczak, M.Z. & Kim, C. The use of chemokine receptor agonists in stem cell mobilization. *Expert opinion on biological therapy* **12**, 287-297 (2012).
187. Toupadakis, C.A. et al. Long-term administration of AMD3100, an antagonist of SDF-1/CXCR4 signaling, alters fracture repair. *Journal of orthopaedic research : official publication of the Orthopaedic Research Society* (2012).
188. Sordi, V. Mesenchymal stem cell homing capacity. *Transplantation* **87**, S42-45 (2009).
189. Struillou, X., Boutigny, H., Soueidan, A. & Layrolle, P. Experimental animal models in periodontology: a review. *Open Dent J* **4**, 37-47 (2010).
190. Weinberg, M.A. & Bral, M. Laboratory animal models in periodontology. *J Clin Periodontol* **26**, 335-340 (1999).
191. Fine, D.H., Kaplan, J.B., Kachlany, S.C. & Schreiner, H.C. How we got attached to *Actinobacillus actinomycetemcomitans*: A model for infectious diseases. *Periodontology 2000* **42**, 114-157 (2006).
192. Holt, S.C. & Ebersole, J.L. *Porphyromonas gingivalis*, *Treponema denticola*, and *Tannerella forsythia*: the "red complex", a prototype polybacterial pathogenic consortium in periodontitis. *Periodontology 2000* **38**, 72-122 (2005).

193. Hajishengallis, G. Aging and its Impact on Innate Immunity and Inflammation: Implications for Periodontitis. *Journal of oral biosciences / JAOB, Japanese Association for Oral Biology* **56**, 30-37 (2014).
194. Rogers, J.E. et al. A p38 mitogen-activated protein kinase inhibitor arrests active alveolar bone loss in a rat periodontitis model. *J Periodontol* **78**, 1992-1998 (2007).
195. Rossa, C., Jr., Liu, M., Patil, C. & Kirkwood, K.L. MKK3/6-p38 MAPK negatively regulates murine MMP-13 gene expression induced by IL-1beta and TNF-alpha in immortalized periodontal ligament fibroblasts. *Matrix Biol* **24**, 478-488 (2005).
196. Sartori, R., Li, F. & Kirkwood, K.L. MAP kinase phosphatase-1 protects against inflammatory bone loss. *J Dent Res* **88**, 1125-1130 (2009).
197. Caton, J., Mota, L., Gandini, L. & Laskaris, B. Non-human primate models for testing the efficacy and safety of periodontal regeneration procedures. *J Periodontol* **65**, 1143-1150 (1994).
198. Shin, J. et al. DEL-1 restrains osteoclastogenesis and inhibits inflammatory bone loss in nonhuman primates. *Science translational medicine* **7**, 307ra155 (2015).
199. Martuscelli, G., Fiorellini, J.P., Crohin, C.C. & Howell, T.H. The effect of interleukin-11 on the progression of ligature-induced periodontal disease in the beagle dog. *J Periodontol* **71**, 573-578 (2000).
200. Kornman, K.S., Siegrist, B., Soskolne, W.A. & Nuki, K. The predominant cultivable subgingival flora of beagle dogs following ligature placement and metronidazole therapy. *J Periodontol Res* **16**, 251-258 (1981).
201. Pellegrini, G., Seol, Y.J., Gruber, R. & Giannobile, W.V. Pre-clinical models for oral and periodontal reconstructive therapies. *J Dent Res* **88**, 1065-1076 (2009).
202. Kaldahl, W.B., Kalkwarf, K.L., Patil, K.D., Molvar, M.P. & Dyer, J.K. Long-term evaluation of periodontal therapy: I. Response to 4 therapeutic modalities. *J Periodontol* **67**, 93-102 (1996).
203. Anderson, J.M. & Shive, M.S. Biodegradation and biocompatibility of PLA and PLGA microspheres. *Advanced Drug Delivery Reviews* **28**, 5-24 (1997).
204. June, C.H. & Blazar, B.R. Clinical application of expanded CD4+25+ cells. *Seminars in immunology* **18**, 78-88 (2006).
205. Delgado, M., Abad, C., Martinez, C., Leceta, J. & Gomariz, R.P. Vasoactive intestinal peptide prevents experimental arthritis by downregulating both autoimmune and inflammatory components of the disease. *Nature Medicine* **7**, 563-568 (2001).
206. Wernig, K. et al. Depot formulation of vasoactive intestinal peptide by protamine-based biodegradable nanoparticles. *J Control Release* **130**, 192-198 (2008).

207. Misaka, S. et al. Inhalable powder formulation of a stabilized vasoactive intestinal peptide (VIP) derivative: anti-inflammatory effect in experimental asthmatic rats. *Peptides* **31**, 72-78 (2010).
208. Ardavin, C. Origin, precursors and differentiation of mouse dendritic cells. *Nat Rev Immunol* **3**, 582-591 (2003).
209. Zou, W. Regulatory T cells, tumour immunity and immunotherapy. *Nat Rev Immunol* **6**, 295-307 (2006).
210. Cardoso, C.R. et al. Characterization of CD4+CD25+ natural regulatory T cells in the inflammatory infiltrate of human chronic periodontitis. *J Leukoc Biol* (2008).
211. Kanaan, R.A. & Kanaan, L.A. Transforming growth factor beta1, bone connection. *Med Sci Monit* **12**, RA164-169 (2006).
212. Sakaguchi, S. Naturally arising Foxp3-expressing CD25+CD4+ regulatory T cells in immunological tolerance to self and non-self. *Nat Immunol* **6**, 345-352 (2005).
213. Sugiyama, H. et al. Dysfunctional blood and target tissue CD4+CD25high regulatory T cells in psoriasis: mechanism underlying unrestrained pathogenic effector T cell proliferation. *J Immunol* **174**, 164-173 (2005).
214. Steenblock, E.R., Fadel, T., Labowsky, M., Pober, J.S. & Fahmy, T.M. An artificial antigen-presenting cell with paracrine delivery of IL-2 impacts the magnitude and direction of the T cell response. *J Biol Chem* **286**, 34883-34892 (2011).
215. Beck, L.S. et al. TGF-beta 1 induces bone closure of skull defects: temporal dynamics of bone formation in defects exposed to rhTGF-beta 1. *Journal of bone and mineral research : the official journal of the American Society for Bone and Mineral Research* **8**, 753-761 (1993).
216. Veldhoen, M., Hocking, R.J., Atkins, C.J., Locksley, R.M. & Stockinger, B. TGF $\beta$  in the Context of an Inflammatory Cytokine Milieu Supports De Novo Differentiation of IL-17-Producing T Cells. *Immunity* **24**, 179-189 (2006).
217. Thomson, A.W., Turnquist, H.R. & Raimondi, G. Immunoregulatory Functions of mTOR Inhibition. *Nature reviews. Immunology* **9**, 324-337 (2009).
218. Jhunjhunwala, S., Raimondi, G., Thomson, A.W. & Little, S.R. Delivery of rapamycin to dendritic cells using degradable microparticles. *Journal of Controlled Release* **133**, 191-197 (2009).
219. Blattman, J.N. & Greenberg, P.D. Cancer Immunotherapy: A Treatment for the Masses. *Science* **305**, 200-205 (2004).
220. Coussens, L.M. & Werb, Z. Inflammation and cancer. *Nature* **420**, 860-867 (2002).

221. Sakaguchi, S., Yamaguchi, T., Nomura, T. & Ono, M. Regulatory T Cells and Immune Tolerance. *Cell* **133**, 775-787 (2008).
222. Matsuoka, K. et al. Low-dose interleukin-2 therapy restores regulatory T cell homeostasis in patients with chronic graft-versus-host disease. *Science translational medicine* **5**, 179ra143 (2013).